

INCORPORATION OF WASTE AND POZZOLANIC MATERIALS AS
PARTIAL REPLACEMENT FOR THE DEVELOPMENT OF SUSTAINABLE
CONCRETE

A THESIS SUBMITTED TO
THE BOARD OF CAMPUS GRADUATE SCHOOL OF
MIDDLE EAST TECHNICAL UNIVERSITY NORTHERN CYPRUS CAMPUS

BY

ALI HAMZA

IN PARTIAL FULFILLMENT OF THE REQUIREMENTS
FOR
THE DEGREE OF MASTER OF SCIENCE
IN
SUSTAINABLE ENVIRONMENT AND ENERGY SYSTEMS PROGRAM

JANUARY 2018

Approval of the Board of Graduate Programs

Prof. Dr. Gürkan Karakaş

Chairperson

I certify that this thesis satisfies all the requirements as a thesis for the degree of Master of Science.

Assist. Prof. Dr. Carter Mandrik

Program Coordinator

This is to certify that we have read the thesis and that in our opinion it is fully adequate, in scope and quality, as a thesis for the degree of Master of Science.

Assist. Prof. Dr. Ceren İnce

Supervisor

Examining Committee Members:

Assist. Prof Dr. Ceren İnce	Civil Engineering METU NCC	_____
Assoc. Prof. Dr. Volkan Esat	Mechanical Engineering METU NCC	_____
Assist. Prof. Dr. Ertuğ Aydın	Civil Engineering European University of Lefke	_____

I hereby declare that all information in this document has been obtained and presented in accordance with academic rules and ethical conduct. I also declare that, as required by these rules and conduct, I have fully cited and referenced all material and results that are not original to this work.

Name, Last Name: Ali Hamza

Signature: _____

ABSTRACT

Incorporation of waste and pozzolanic materials as partial replacement for the development of sustainable concrete

Hamza, Ali

MSc. Sustainable Environment and Energy Systems

Supervisor: Assist. Prof. Dr. Ceren İnce

January 2018, 137 pages

Excessive production of cement due to modern construction practices frames cement as a leading pollutant of releasing significant amounts of CO₂ in the atmosphere. The thesis begins with the examination of the alternative binding materials used as partial replacement to cement. Supplementary cementitious material, silica fume, is used as partial replacement to Portland cement whereas, waste materials, marble dust and crushed bricks, are used as partial replacement to the fine aggregates in this thesis. The study investigates the long-term mechanical properties and durability characteristics of pozzolanic concrete incorporated with waste materials. The main parameters studied in this thesis are compressive strength, water permeability, resistance to sulfate and freeze and thaw attack as well as porosity. The development of the complex chemical reactions within the cement matrix such as cement hydration and pozzolanic reaction are examined using Scanning Electron Microscope. Material characterization is carried out using X-ray fluorescence and particle size distribution. The results suggested that it is not only possible to reduce the consumption of Portland cement and natural resources up to 40% using pozzolans and waste materials but also enhances the mechanical properties of concrete at long term. The use of waste materials in combination with pozzolans showed a dramatic decrease in water permeability and porosity as well as improved the resistance against external sulfate attack and action of freeze and thaw significantly.

Keywords: Silica fume, marble dust, crushed bricks, mechanical properties, durability characteristics

ÖZ

Sürdürülebilir beton gelişimi için atık ve pozzolanik malzelerin kısmi takviye olarak katılması

Hamza, Ali

Yüksek Lisans, Sürdürülebilir Çevre ve Enerji Sistemleri

Tez Yöneticisi: Yrd. Doç. Dr. Ceren İnce

Ocak 2018, 137 sayfa

Modern yapı uygulamaları nedeniyle çimentonun aşırı miktarda üretilmesi, atmosfere önemli miktarda CO₂ salınımı dolayısı ile çimentoyu öncü bir kirletici madde olarak tanımlamaktadır. Tez, çimentoya kısmi takviye malzemesi olarak kullanılan alternatif bağlayıcı maddelerin incelenmesiyle başlar. Tamamlayıcı çimento malzemesi, silika dumanı, Portland çimentosuna kısmen takviye olarak kullanılırken, atık maddeler, mermer tozu ve öğütülüşüm tuğla, bu tezdeki ince agregaların yerine kısmen takviye olarak kullanılmıştır. Çalışma, puzolanik betona atık maddeler katılarak uzun süreli mekanik özelliklerini ve dayanıklılık özelliklerini araştırmaktadır. Bu tezde çalışılan ana parametreler basınç dayanımı, su geçirgenliği, sülfat ve donma çözünmeye karşı direnç ve gözenekliliktir. Çimento hidrasyonu ve puzolanik reaksiyonlar gibi çimento matrisi içindeki kompleks kimyasal reaksiyonların gelişimi Taramalı Elektron Mikroskopu tarafından incelenmiştir. Malzeme karakterizasyonu, X-ışını flüoresan ve parçacık boyutu dağılımı kullanılarak gerçekleştirildi. Sonuçlar, sadece puzolanlar ve atık maddeler kullanarak Portland çimentosu ve doğal kaynakların tüketimini %40'a düşürmekle kalmayıp uzun vadede betonun mekanik özelliklerini de arttırdığını gösterdi. Atıkların puzolanlarla birlikte kullanımı, su geçirgenliğinde ve gözeneklilikte belirgin bir düşüş sağladığı gibi sülfat atağa ve dondurma ve çözülmeye karşı direnci önemli ölçüde artırdı.

Anahtar Kelimeler: Silika dumanı, mermer tozu, öğütülmüş tuğla, mekanik özellikler, durabilite.

DEDICATION

To my beloved family

For their unconditional support, trust and encouragement

ACKNOWLEDGEMENTS

I believe that writing this thesis has had a significant impact on me. I would like to pay my special thankfulness, warmth and appreciation to the people as well as the institutions/companies who made my thesis successful and assisted me at every point to cherish my goal.

Firstly, I offer my heartiest gratitude to my thesis advisor Assist. Prof. Dr. Ceren İnce of the Civil Engineering Department at Middle East Technical University Northern Cyprus Campus, who has supported and guided me throughout the completion of my thesis with her patience, skill and knowledge. Her constant encouragement made it possible for me to achieve this goal in a successful way. She consistently allowed this research to be my own work, but steered me in the right direction with constructive suggestions and ideas. Without her deep knowledge and incredible commitment, my accomplishments would have been greatly diminished. I am deeply indebted to her and it was a privilege to be her student

Besides my thesis advisor, I would like to offer my special thanks to the rest of my thesis committee: Assist. Prof. Dr. Ertuğ Aydın and Assoc. Prof. Dr. Volkan Esat for their insightful comments and encouragement, which incited me to widen my research from various perspectives. Moreover, I would also like to offer my special gratitude to Assist. Prof. Dr. Shahram Derogar for his valuable advices and suggestions, which encouraged me to develop my research in the best possible way. I am also deeply grateful to Mr. Abdullah Önal for his undoubted support and immense help at the Materials Laboratory, Middle East Technical University Northern Cyprus Campus.

Special thanks to the Middle East Technical University, Northern Cyprus Campus and Middle East Technical University, Ankara Campus for funding a scientific research project (FEN-16-YG-11), which helped me to pursue advanced testing techniques at Central Laboratory, Middle East Technical University, Ankara Campus.

I would like to offer my special thanks to Assist. Prof. Dr. Bertuğ Akıntuğ who always gave me insightful comments and suggestions, which have always enlightened me to look at my research from various perspectives. I am also grateful to him for providing me the opportunity to be a part of Civil Engineering Department as a teaching assistant; profound academic experience along with such financial support made it possible to conduct this research with peace of mind.

I would also like to thank Cyprus Environmental Enterprises Ltd., Mr. Arsen Ancı, Director of Izmer Enterprises Ltd. and Mr. Necat from Gürdağ Madencilik Ltd. for material supply of silica fume, marble dust and crushed bricks necessary for the experimental work of this thesis.

I would like to thank all the student assistants for their great support and contribution at the Materials Laboratory, Middle East Technical University Northern Cyprus Campus. Student assistants especially Abdallah Wahib, Ece Öztürk, Emre Yıldırım, Gamze Akbulut, Kevin Mithia and Tolga Tüylüoğlu; provided immense help and support throughout the experimental work of this thesis.

Besides the technical assistance, I would also like to acknowledge and thank all the graduate students and my sincere friends especially Ceren Yağmur Öztürk, Alina Calateru, Ahmad Rasheed, Ahmet Faruk, Berkay Koyuncu, Pelin Güven, Anil Berkin, Ege Gülen, Burcu Esen, Huriye Özdemir, Derya Nereli, Esra Fügen Paşaoğluları, Koray Gürkaya, Arman Malekloo, Fahad Haneef, Kamran Maharramov, Mohammad Abujubbeh, Pradeep Jayaweera, Hana Kasht, Shahab Miri, Akif Cem Özkardeş, Obaidullah Mohiuddin, Madina Obaidullah, Bushra Fatima, Muhammad Saleh Rashid, Tariq Rahim, Sana Khan, Zakria Qadir, Haroon Rasheed and many others who made my stay and experience at Middle East Technical University, Northern Cyprus Campus enjoyable and memorable.

Lastly, I must express my very profound gratitude to my family for providing me with unfailing support and continuous encouragement throughout my years of study and through the process of researching and writing this thesis. This accomplishment would not have been possible without them.

TABLE OF CONTENTS

ABSTRACT	v
ÖZ.....	vi
DEDICATION	vii
ACKNOWLEDGEMENTS	viii
TABLE OF CONTENTS	x
LIST OF TABLES	xiii
LIST OF FIGURES	xiv
1. INTRODUCTION.....	1
1.1 Sustainable assessment of Portland cement.....	1
1.2 Objective and scope	2
2. LITERATURE REVIEW	4
2.1 Introduction.....	4
2.2 Portland Cement	4
2.2.1 General definition	4
2.2.2 Manufacturing of Portland cement	4
2.2.3 Components of Portland cement	5
2.2.4 Hydration reaction of Portland cement	6
2.3 Supplementary Cementitious Materials (SCMs).....	9
2.3.1 General definition	9
2.3.2 Classification and types of supplementary cementitious materials (SCMs)	9
2.3.3 Pozzolanic reaction of supplementary cementitious materials (SCMs).....	10
2.3.4 Significance of supplementary cementitious materials (SCMs)	11
2.3.5 Sustainability of using supplementary cementitious materials (SCMs)	13
2.4 Mechanical properties of concrete.....	15
2.4.1 Strength	15
2.5 Durability characteristics of concrete	16
2.5.1 Water permeability.....	16
2.5.2 Porosity	16

2.5.3 External sulfate attack.....	17
2.5.4 Freezing and thawing.....	17
2.6 Influence of SCMs on mechanical properties of concrete	18
2.7 Influence of SCMs on durability characteristics of concrete	20
2.8 Waste materials	22
2.8.1 Influence of waste materials on the properties of concrete	23
3. METHODOLOGY	31
3.1 Introduction	31
3.2 Materials used	32
3.2.1 Portland cement	32
3.2.2 Supplementary cementitious materials (SCMs)	33
3.2.3 Waste materials.....	34
3.2.4 Fine aggregates	36
3.2.5 Coarse aggregates	38
3.2.6 Water.....	39
3.3 Concrete mix design.....	39
3.4 Experimental procedures.....	47
3.4.1 Determination of Slump	47
3.4.2 Determination of Compressive Strength Test	48
3.4.3 Determination of Water Penetration Depth	49
3.4.4 Determination of Porosity by Mercury Intrusion Porosimetry.....	50
3.4.5 Determination of Resistance to External Sulfate Attacks.....	50
3.4.6 Determination of Resistance to Freeze and Thaw Cycles	51
3.4.7 Scanning Electron Microscopy (SEM).....	52
3.4.8 X-Ray Florescence (XRF)	53
3.4.9 Particle Size Distribution (PSD).....	54
4. MECHANICAL PROPERTIES AND DURABILITY CHARACTERISTICS OF CONCRETE INCORPORATED WITH SILICA FUME AND MARBLE DUST ..	55
4.1 Introduction	55
4.2 Characterization of raw materials	55
4.3 Fresh properties	58
4.3.1 Water content.....	58

4.4 Mechanical properties.....	59
4.4.1 Compressive strength.....	59
4.5 Durability.....	63
4.5.1 Water permeability.....	63
4.5.2 External sulfate attack.....	67
4.5.3 Freeze and thaw resistance.....	74
4.5.4 Porosity.....	81
4.6 Conclusions.....	85
5. MECHANICAL PROPERTIES AND DURABILITY CHARACTERISTICS OF CONCRETE INCORPORATED WITH SILICA FUME AND CRUSHED BRICKS	87
5.1 Introduction.....	87
5.2 Characterization of raw materials.....	87
5.3 Fresh properties.....	90
5.3.1 Water content.....	90
5.4 Mechanical properties.....	91
5.4.1 Compressive strength.....	91
5.5 Durability.....	93
5.5.1 Water permeability.....	93
5.5.2 External sulfate attack.....	96
5.5.3 Freeze and thaw resistance.....	100
5.5.4 Porosity.....	104
5.6 Conclusions.....	107
6. CONCLUSIONS AND RECOMMENDATIONS	109
6.1 Conclusions.....	109
6.2 Recommendations.....	112
REFERENCES	113

LIST OF TABLES

Table 2.1. Approximate composition limits of oxides in Portland cement.....	6
Table 2.2. Major compounds present in Portland cement.....	6
Table 3.1. Chemical composition of Portland cement.	32
Table 3.2. Chemical composition of silica fume.	33
Table 3.3. Chemical composition of marble dust.	34
Table 3.4. Chemical composition of crushed bricks.....	35
Table 3.5. Chemical composition of fine aggregates.....	36
Table 3.6. Gradation sieve sizes of fine aggregates.....	37
Table 3.7. Gradation sieve sizes of coarse aggregates.....	39
Table 3.8. Determined concrete combinations.....	46
Table 3.9. Water content of determined concrete combinations.....	47
Table 4.1. Elemental oxide composition of Portland cement, silica fume, marble dust and fine aggregates determined by X-ray fluorescence spectroscopy.	56
Table 4.2. Porosity measurements of concrete incorporated with silica fume and marble dust under normal curing conditions.	81
Table 4.3. Porosity measurements of concrete incorporated with silica fume and marble dust under sulfate solution.	82
Table 4.4. Porosity measurements of concrete incorporated with silica fume and marble dust under action of freeze and thaw.	84
Table 5.1. Elemental oxide composition of Portland cement, silica fume, crushed bricks and fine aggregates determined by X-ray fluorescence spectroscopy.	88
Table 5.2. Porosity measurements of concrete incorporated with silica fume and crushed bricks under normal curing conditions.	104
Table 5.3. Porosity measurements of concrete incorporated with silica fume and crushed bricks under sulfate solution.....	105
Table 5.4. Porosity measurements of concrete incorporated with silica fume and crushed bricks under action of freeze and thaw.	106

LIST OF FIGURES

Figure 3.1. Particle size distribution of Portland cement.	32
Figure 3.2. Particle size distribution of silica fume.....	33
Figure 3.3. Particle size distribution of marble dust.....	34
Figure 3.4. Particle size distribution of crushed bricks.	35
Figure 3.5. Particle size distribution of fine aggregates.	36
Figure 3.6. Gradation curve of fine aggregates.	37
Figure 3.7. Gradation curve of coarse aggregates.	38
Figure 3.8. Concrete mixer.....	42
Figure 3.9. Slump measurement taken on fresh concrete.....	43
Figure 3.10. Vibrators providing compaction to half-filled concrete mold.	43
Figure 3.11. Vibrators providing compaction to fully-filled concrete mold.	44
Figure 3.12. Molding of concrete.	44
Figure 3.13. Curing condition.	45
Figure 3.14. Determination of slump.	48
Figure 3.15. Compressive strength testing equipment for concrete samples.	49
Figure 3.16. Water permeability testing equipment.	50
Figure 3.17. External sulfate attack curing condition.	51
Figure 3.18. Freeze and thaw cabinet.	52
Figure 3.19. Scanning electron microscope.	53
Figure 3.20. XRF Apparatus.	54
Figure 4.1. Particle size distribution of Portland cement, silica fume, marble dust and fine aggregates.	57
Figure 4.2. Slump (mm) and water/binder ratios for all the mix proportions of concrete incorporated with silica fume and marble dust. Water/binder ratio plotted in a secondary axis.	58
Figure 4.3. Compressive strength of silica fume – concrete incorporated with marble dust.	59
Figure 4.4. Concrete control at 28 days.....	60
Figure 4.5. Concrete control at 1 year.	61
Figure 4.6. Concrete containing 20% SF at 28 days.	61

Figure 4.7. Concrete containing 20% SF at 1 year.	62
Figure 4.8. Water penetration depth of concrete incorporated with 20% SF and with 10 and 20% MD. Mass of absorbed water through the application of pressurized water during the experiment, plotted in a secondary axis.....	64
Figure 4.9. Concrete containing 20% SF + 20% MD at 28 days.	65
Figure 4.10. Concrete containing 20% SF + 20% MD at 1 year.	66
Figure 4.11. Compressive strength loss of concrete subjected to sulfate attack versus immersed time. Expansion of concrete subjected to sulfate attack is plotted in a secondary axis.	68
Figure 4.12. Concrete control under sulfate attack at 28 days.	70
Figure 4.13. Concrete control under sulfate attack at 1 year.	71
Figure 4.14. Concrete containing 20% SF under sulfate attack at 28 days.....	71
Figure 4.15. Concrete containing 20% SF under sulfate attack at 1 year.....	72
Figure 4.16. Concrete containing 20% SF + 20% MD under sulfate attack at 28 days.	72
Figure 4.17. Concrete containing 20% SF + 20% MD under sulfate attack at 1 year.	73
Figure 4.18. Compressive strength loss of concrete subjected to freeze and thaw versus time. Mass loss of concrete subjected to freeze and thaw is plotted on in secondary axis.	75
Figure 4.19. Concrete control under freeze and thaw at 28 days.	77
Figure 4.20. Concrete control under freeze and thaw at 1 year.	77
Figure 4.21. Concrete containing 20% SF under freeze and thaw at 28 days.	78
Figure 4.22. Concrete containing 20% SF under freeze and thaw at 1 year.....	78
Figure 4.23. Concrete containing 20% SF + 20% MD under freeze and thaw at 28 days.	79
Figure 4.24. Concrete containing 20% SF + 20% MD freeze and thaw attack at 1 year.	79
Figure 5.1. Particle size distribution of Portland cement, silica fume, crushed bricks and fine aggregates.	89

Figure 5.2. Slump (mm) and water/binder ratios for all the mix proportions of concrete incorporated with silica fume and crushed bricks. Water/binder ratio plotted in a secondary axis.	90
Figure 5.3. Compressive strength of silica fume – concrete incorporated with crushed bricks.	91
Figure 5.4. Water penetration depth of concrete incorporated with 20% SF and with 10% CB and 20% CB. Mass of absorbed water through the application of pressurized water during the experiment, plotted in a secondary axis.	93
Figure 5.5. Concrete containing 20% SF + 20% CB at 28 days.	94
Figure 5.6. Concrete containing 20% SF + 20% CB at 1 year.	95
Figure 5.7. Compressive strength loss of concrete subjected to sulfate attack versus immersed time. Expansion of concrete subjected to sulfate attack is plotted in a secondary axis.	97
Figure 5.8. Concrete containing 20% SF + 20% CB under sulfate attack at 28 days.	99
Figure 5.9. Concrete containing 20% SF + 20% CB under sulfate attack at 1 year. .	99
Figure 5.10. Compressive strength loss of concrete subjected to freeze and thaw versus time. Mass loss of concrete subjected to freeze and thaw is plotted on in secondary axis.	101
Figure 5.11. Concrete containing 20% SF + 20% CB under freeze and thaw at 28 days.	102
Figure 5.12. Concrete containing 20% SF + 20% CB freeze and thaw attack at 1 year.	103

CHAPTER 1

INTRODUCTION

1.1 Sustainable assessment of Portland cement

Concrete is the most famous building material due to its admirable mechanical and physical properties. In recent years, annual manufacturing of concrete has scaled up to more than 10 billion tons. Since the world's population tends to grow, the manufacturing of concrete has been forecasted to reach around 18 billion tons annually by 2050 (Aprianti, 2017).

Concrete provides various benefits to construction industry. However, within the last 10 decades, concrete industry had a major negative effect on environment due to CO₂ emissions produced during the manufacturing processes of Portland cement. High amounts of raw materials obtained from natural/artificial resources are also required to produce substantial amount of concrete bringing an adverse impact to the environment annually. Moreover, cement industry contributes up to 7% of total CO₂ emissions generated worldwide. This notion has been generalized as “for each ton production of Portland cement, approximately one ton of CO₂ released in the atmosphere” (Malhotra, 2010).

Manufacturing of Portland cement is a “carbon and energy intensive process”. It has been recognized that 5 – 9% of total global anthropogenic carbon emissions (Shi, 2011; Harrison, 2013) and 2 – 3% of energy use (Juenger, 2011) is due to the manufacturing of Portland cement. In addition to that, fully replacement of Portland cement as a basic constituent for concrete manufacturing is inevitable. However, in recent years, “second generation” and “low carbon” cements have been developed which partially replace Portland cement for concrete manufacturing (Grist, 2015).

Apart from CO₂ emissions, during concrete manufacturing processes, various factors such as energy use, depletion of natural resources and construction and demolition waste (CDW) management are also becoming alarming issues of recent times. Due to the influence of these various factors associated with the manufacturing of concrete,

environmental degradation has increased exponentially. Hence, in recent years, the need of sustainable development in concrete manufacturing is emerging drastically to reduce the adverse impacts of concrete manufacture, especially on environment (Malhotra, 2010; Harrison, 2013; Grist, 2015).

In recent years, various types of alternative binding materials have been developed, however the conformability and compatibility towards mechanical properties and durability characteristics of concrete play a crucial role for the construction industry (Grist, 2015). The sustainable assessment of using alternative binding materials as well as alternative filler materials is also mandatory for the development of sustainable concrete. Hence, sustainable assessment of concrete can be determined by investigating the mechanical properties and durability characteristics of concrete.

1.2 Objective and scope

The objective of this thesis is to investigate the influence of supplementary cementitious materials (SCM) and waste materials on the mechanical properties and durability characteristics of concrete for the development of sustainable concrete. Silica fume is used as partial replacement material to Portland cement whereas marble dust and crushed bricks are used as partial replacement materials to fine aggregates for the production of sustainable concrete. Concrete mix design approach is adopted to produce concrete with various replacement levels of Portland cement and fine aggregates. Mechanical properties including compressive strength of concrete and durability characteristics such as water permeability, external sulfate attack, freezing and thawing and mercury intrusion porosimetry of concrete are investigated in this study. Microstructural analysis at 28 days and after 1 year are analyzed not only to gain an insight into the microstructural development of sustainable concrete but also to support the macro-structural properties and characteristics investigated in this thesis.

This thesis is composed of seven chapters. Chapter 1 contains summarized introductory information addressing the issues of extensive usage of Portland cement and natural resources for the manufacturing of concrete. In Chapter 2, a theoretical background along with literature review on Portland cement and Portland cement hydration reaction, supplementary cementitious materials (SCMs), pozzolanic reaction and its effect on Portland cement hydration are discussed. Most importantly,

significance and sustainable use of SCMs and waste materials in concrete are addressed. In addition to that, studies addressing the effects of using SCMs and waste materials on the mechanical properties and durability characteristics of concrete are reported. Chapter 3 contains the details of the constituents of concrete that are used to produce concrete in this thesis. Concrete mix design approach is introduced and formulated to produce various concrete combinations incorporating SCMs and waste materials. Chapter 4 addresses the experimental procedures associated for the determination of mechanical properties, durability characteristics and microstructural analyses adopted for this thesis. Chapter 5 and 6 give experimental results, interpretations and discussions on the influence of using SCMs and waste materials on the mechanical properties and durability characteristics of concrete. Major findings of the experimental study are summarized. Lastly, conclusions highlighted and suggestions for the future research work are addressed in Chapter 7.

CHAPTER 2

LITERATURE REVIEW

2.1 Introduction

In this chapter, theoretical background and literature review of the influence of Portland cement, supplementary cementitious materials (SCMs) and waste materials on the mechanical properties and durability characteristics of sustainable concrete are reported. Firstly, theoretical background of Portland cement including the hydration reaction of Portland cement is discussed. Thereafter, theoretical background, significances and sustainability of supplementary cementitious materials (SCMs) and waste materials are broadly discussed. Theoretical background of the mechanical properties and durability characteristics of concrete is investigated in this thesis are then highlighted. Lastly, the influence of SCMs and waste materials on the mechanical properties and durability characteristics of concrete are summarized.

2.2 Portland Cement

2.2.1 General definition

Portland cement is a binding material, which is produced by mixing calcareous, clayey materials and/or other silica-, alumina-, iron oxide- containing materials, known as Portland cement clinker. Portland cement clinker along with the small addition of gypsum content is burnt and ground at clinkering temperature. The finished product, called as Portland cement, is obtained in powdered form and possess grayish color (Neville, 1995).

2.2.2 Manufacturing of Portland cement

Manufacturing of Portland cement (Portland cement clinker) is performed primarily from the combination of calcareous materials such as limestone (CaCO_3) and clayey materials that mostly contain high silica and alumina content. Manufacturing process involves a series of processes. Firstly, grinding of these raw materials uniformly into a very fine powder state is obtained followed by mixing of raw materials in

predetermined/appropriate mixing proportions. Burning of raw materials in rotary kiln at a temperature of approximately 1400°C until the raw material sinters and partially fuses into small balls known as clinker comes afterwards. However, when raw materials move down the kiln, progressively increasing temperature inside the kiln allows various chemical reactions take place. Firstly, water is evaporated completely and CO₂ is released from limestone (CaCO₃). Moreover, clayey minerals containing silica and alumina also start to decompose. As the decomposition process continues, materials start to melt and compound formation takes place. As the temperature increases until 1400°C, the melted material containing compounds of calcium, silica and alumina recombine into flocs of various sizes by the process of agglomeration. The clinker is then cooled and gypsum content (3 – 6%) is added in order to prevent quick setting of Portland cement. Grinding process is followed then, which makes Portland cement clinker into fine powdered state (Neville, 1995).

2.2.3 Components of Portland cement

2.2.3.1 Oxides composition of Portland cement

Raw materials of Portland cement mainly consist of lime, silica, alumina and iron oxide. These -compounds interact together during the process of cement manufacture; therefore, the major oxides present in Portland cement are calcium oxide (CaO), silica (SiO₂), alumina (Al₂O₃) and iron oxide (Fe₂O₃) respectively. Shortened notation, used by cement chemists describes each oxide by one letter (Neville, 1995).

- Calcium oxide (CaO) – C
- Silica (SiO₂) – S
- Alumina (Al₂O₃) – A
- Iron oxide (Fe₂O₃) – F
- Water (H₂O) – H

In addition to major oxides, Portland cement does contain insignificant proportions of minor oxides as well. These are mainly magnesia (MgO), alkalis (Na₂O and K₂O) and sulfuric anhydride (SO₃). All the oxides are obtained during the burning process of raw materials inside the kiln except sulfuric anhydride that comes from the presence

of gypsum in Portland cement. Approximate composition limits of oxides in Portland cement is illustrated in Table 2.1 (Neville, 1995).

Table 2.1. Approximate composition limits of oxides in Portland cement.

Oxide	Content, per cent
CaO	60 – 67
SiO ₂	17 – 25
Al ₂ O ₃	3 – 8
Fe ₂ O ₃	0.5 – 6
MgO	0.1 – 4
Alkalis	0.2 – 1.3
SO ₃	1 – 3

2.2.3.2 Major compounds of Portland cement

The major compounds present in Portland cement are illustrated in Table 2.2 (Neville, 1995).

Table 2.2. Major compounds present in Portland cement.

Name of Compound	Oxide Composition	Abbreviation
Tri-calcium silicate	3CaO.SiO ₂	C ₃ S
Di-calcium silicate	2CaO.SiO ₂	C ₂ S
Tri-calcium aluminate	3CaO.Al ₂ O ₃	C ₃ A
Tetra-calcium alumino-ferrite	4CaO.Al ₂ O ₃ .Fe ₂ O ₃	C ₄ AF

These four major compounds are produced as the result of the chemical reactions among the major oxides of Portland cement. Therefore, these four major compounds establish Portland cement approximately up to 90%. The remaining 10% are the minor oxides. The amounts of these minor oxides are often limited in the standards due to their damaging effects on the durability of cement paste (Neville, 1995).

2.2.4 Hydration reaction of Portland cement

Hydration, simply called as the chemical reaction that occurs when cement is mixed with water. Hydration of Portland cement is referred as complex process since

hydration process of cement not only involves the reactions of distinct compounds with water but also the interfaces among them. In other words, each compound present in the cement is assumed to react with water independently. Therefore, each compound produces different products following hydration of Portland cement. Hydration of Portland cement constitutes a group of coincident and sequential reactions (Bapat, 2012).

When Portland cement reacts with water, the production of portlandite crystal known as calcium hydroxide (CH) and amorphous calcium silicate hydrate gel (C-S-H) is observed. The main hydration reaction of Portland cement is illustrated below (Neville, 1995):

Cement + Water \rightarrow Calcium Silicate Hydrate (Gel) and Calcium Hydroxide (Crystal);

Individually, hydration reaction of major compounds of Portland cement are shown below (Neville, 1995):

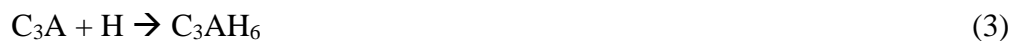
- Chemical reaction between C₃S and water:



- Chemical reaction between C₂S and water:



- Chemical reaction between C₃A and water:



- Chemical reaction between C₄AF and water:

The chemical reaction between C₄AF and water is similar to the chemical reaction between C₃A and water. Furthermore, the products of chemical reaction between C₄AF do not contribute significantly to the strength gain of concrete. However, it reacts with gypsum to form calcium sulfo-ferrite. Calcium sulfo-ferrite may accelerate the hydration reaction of silicates.

In addition to these reactions of major compounds of Portland cement with water, various major factors such as chemical composition, fineness, particle size distribution, specific surface area, selected water/binder ratio and curing temperature do affect the hydration reaction of Portland cement (Neville, 1995).

From the reactions, it is evident that hydrated Portland cement paste contains nearly 70% C-S-H, 20% CH and 10% minor compounds such as sulfo-aluminates and other secondary phases (Bapat, 2012). C_3S and C_2S are the main products and contributors for the strength development of cement paste during an ongoing hydration reaction of cement. C_3S gives a faster rate of reaction, which results in heat of hydration during the process of hydration of cement. Hence, C_3S contributes to early strength development of cement paste. However, C_2S involves a slower rate of hydration, therefore has low heat of hydration and hardens slowly. It further contributes in ultimate strength and provides greater resistance to chemical attacks in the service life of cement paste (Neville, 1995).

The presence of C_3A compound is detrimental, since it only contributes to strength development of Portland cement at early ages. The hydration of C_3A is quick, leading to the formation of crystalline alumino hydrates. The quick hydration of C_3A causes an abrupt stiffening of paste. This is termed as “flash set”. To overcome this issue, gypsum is added during the manufacture of cement to slow down the reaction between C_3A and water. In addition to that, if Portland cement contains high amounts of gypsum, excess gypsum reacts with water in the presence of C_3A that produces calcium-alumino-mono-sulfo-hydrate. If the reaction continues, calcium-alumino-tri-sulfate-hydrate, called as ettringite is formed. The formation of ettringite, rod-like crystals, causes great expansion in cement paste that further causes cracking. Therefore, it is desirable that C_3A content should have minimum availability for the reaction with gypsum content in Portland cement (Neville, 1995; Bapat, 2012).

Calcium hydroxide abbreviated as CH, which is produced due the hydration reaction between Portland cement and water affects the quality of the concrete in a negative manner. Microstructurally, cavities are formed throughout the cement paste since CH compounds are relatively soluble in water. Due to this solubility of CH compounds, the strength development tends to delay, resulting in low compressive strength and low durability characteristics (Toutanji, 2004; Bapat, 2012).

In addition to that, gel pores and capillary pores are formed as the hydration reaction of Portland cement continues to occur. Gel pores are formed in between the poorly crystallized hydrates of cementitious compounds (C-S-H), crystals of CH, minor compounds, residue of the water-filled spaces in the fresh paste and unhydrated

cement. The residual of water-filled spaces in the fresh paste of Portland cement are called capillary pores (Neville, 1995).

2.3 Supplementary Cementitious Materials (SCMs)

2.3.1 General definition

Supplementary Cementitious Materials (SCMs) are defined as those materials, occurring naturally or artificially, which possess either hydraulic or pozzolanic characteristics. A material possessing hydraulic properties can set and harden when mixed with water by forming cementitious products in a hydration reaction similar to Portland cement. However, various supplementary cementitious materials show “latent hydraulic” behavior, i.e. “it may exhibit hydraulic activity only in consequence of chemical reaction with some other compounds such as the products of hydration of Portland cement which co-exists in the mixture” (Neville, 1995). Thus, these materials required physical and/or chemical activation to begin and continue the hydration reaction (Snellings, 2012).

A material possessing pozzolanic properties, called as pozzolan is normally defined as, “a siliceous or siliceous and aluminous material, which in itself possesses little or no cementitious value but will, in finely divided form and in the presence of moisture, chemically react with calcium hydroxide to form compounds possessing cementitious properties” (ASTM, 2015; ASTM, 2017). Therefore, pozzolans show the capability of reacting in the presence of calcium hydroxide (lime) and water, which is assessed by the pozzolanic activity of the pozzolan.

2.3.2 Classification and types of supplementary cementitious materials (SCMs)

Supplementary Cementitious Materials (SCMs) are categorized in terms of origin, chemical and mineralogical composition. In terms of origin, SCMs are categorized as naturally occurring SCMs and artificially made SCMs. In terms of chemical composition, they are categorized as hydraulic, latent hydraulic binders and non-reactive/filler materials. Though hydraulic, latent hydraulic or pozzolanic activity of SCMs is influenced broadly by their physical and chemical properties rather than the origin of the SCMs, however classifications of SCMs according to their activity and/or their performance in concrete are partially available in the literature. Therefore,

classification of SCMs based on origin is mostly followed (Massazza, 2001; Snellings, 2012).

SCMs occurring in their natural form mostly require characterization of particle properties by sieving and grinding processes. Typical naturally occurring SCMs are volcanic ash, pyroclastic rocks, diatomaceous earth, pumice, clay and ceramic materials. Artificially occurring SCMs mostly go through modifications depending on the type of manufacturing or production processes. Artificial SCMs are produced on purpose, by thermal activation of clayey material to obtain metakaolin clay (MK), or as waste by-products from high temperature industrial processes such as ground granulated blast furnace slag (GGBS), fly ashes (FA) and silica fume (SF) respectively (Snellings, 2012).

2.3.3 Pozzolanic reaction of supplementary cementitious materials (SCMs)

Pozzolanic reaction initiates when finely divided pozzolanic particles react with calcium hydroxide in the presence of water. Chemical reaction, which takes place between the silica (from pozzolans) and calcium hydroxide (from the hydration reaction of Portland cement), contributes in further formation of calcium silicate hydrate (C-S-H) gel. Pozzolanic activity, which depends on the hydration reaction of Portland cement, is explained by the pozzolanic reaction equation shown below (Oner, 2007).

- Calcium Hydroxide (CH) + Silica (S) + Water (H) → Calcium silicate hydrate (C-S-H) gel

From the above equation, it can be seen that calcium hydroxide is formed by the hydration reaction of Portland cement and thus, used by the reactive silica of pozzolans to produce more C-S-H gels. Neville (1995) mentions that pozzolanic reaction is dependent on the hydration reaction of Portland cement. Furthermore, the rate of pozzolanic activity is slower in comparison with hydration of Portland cement.

In addition to that, basic criterion to classify SCMs as pozzolan is that if silica, alumina and iron oxide content present in their composition is less than 70%, the material cannot be classified as pozzolan. Therefore, irrespective of origin of SCMs, they can

be classified as pozzolan if they conform the requirement of 70% silica, alumina and iron oxide content present in their composition (ASTM, 2015).

Various important criteria and factors that affect the pozzolanic classification and activity of pozzolans are shown below (Massazza, 2001):

- Content of silica, alumina and iron oxide present
- Silica content of active phases in pozzolans
- Degree of amorphousness of pozzolanic microstructure
- Calcium hydroxide content/pozzolanic content ratio
- Specific area of pozzolanic particles
- Fineness of pozzolanic particles
- Water/binder ratio
- Temperature
- Curing time

2.3.4 Significance of supplementary cementitious materials (SCMs)

At a global perspective, 3.6 billion tons of cement were produced in 2011. It is also projected that by 2050, the production will reach up to 5.8 billion tons (Juenger, 2015). However, the annual global production of SCMs account around 1 billion and 360 million tons only (Malhotra, 2006).

At present, use of SCMs in concrete is often limited; only 5 – 20% replacement of Portland cement is often preferred in the literature due to many associated factors (Juenger, 2015). These associated factors may include economy, lack of research and improvements in mechanical properties and durability of concrete incorporated with these materials. Increased use of SCMs results in reduction of CO₂ emissions during concrete production; however, the use of high SCMs volume fractions in Portland cement cause performance loss, especially early strength development.

It has been mentioned in Section 2.2.2 that manufacturing of Portland cement is an energy intensive process due to considerably high emissions of greenhouse gases. The use of SCMs can result in the reduction of cement content in the concrete production. Van den Heede (2012) mentioned pozzolans as “avoided waste”. The reason of

consideration is due to the nature of these materials, as they allocate zero power generation for the production of these materials. Hence, from an environmental perspective they are more likely to be used for concrete production.

Advantages of pozzolanic concrete and sustainability aspects of using pozzolanic concrete are reported in the literature. Pozzolans, used as mineral admixtures with Portland cement improve strength and durability characteristics of concrete. Furthermore, natural and artificial occurrence of pozzolans as waste products; the application of pozzolans in concrete has been increased due to their environmental friendly nature, qualitative structural performance, enhanced durability characteristics and reduced energy utilization. Hence, the impact of CO₂ emissions is considerably low (Mehta, 1999).

Pozzolanic activity and hydration of Portland cement is explained in Section 2.2.4 and 2.3.3; however, the significance of pozzolanic activity is further reported in this section. SCMs addition in the cementitious matrix will induce the pozzolanic effect that will result in the unavailability of CH compounds in the structure of hardened paste. Additional C-S-H gels will produce in the cementitious matrix by the presence of SCMs. Thus, a denser structure of hardened paste is evident compared to the structure of hardened paste formed by Portland cement hydration only. Hence, strength development, durability characteristics and performance of concrete will improve significantly by the addition of pozzolans (Thomas, 1999; Shehata, 2002; Papadakis, 2002; Oner, 2005; Erdem, 2008; Wang, 2015).

Physical properties of pozzolans include particle size distribution and specific surface area whereas chemical properties include oxide composition and amorphous content respectively as mentioned previously in Section 2.3.3. To enhance the pozzolanic reactivity of pozzolans, particle size reduction of pozzolans up to nano-scale level is reported in the literature. Pozzolanic reactivity will not only accelerate the development of early strength, but also reduce the permeability. The bond formation between the particles of cement and pozzolans will show denser structure as fine particles of pozzolanic materials can fill the gaps between the particles of cement (Toutanji, 2004; Rößler, 2014).

In addition to that, various approaches to accelerate the pozzolanic reaction are reported in the literature. One of the approaches is to provide mechanical treatment by grinding the pozzolans. Another approach discusses accelerated curing process whereas some of them also mentioned chemical activation processes such as alkali and sulfate activation (Aimim, 1991; Paya, 1995; 1996; 1997). However, considering the durability of concrete, alkali-activated concrete may lead to alkali – silica reaction (Aigin, 1999) whereas sulfate activation may form ettringite, causing sulfate attack on the exposed surface of concrete. In addition, pozzolans may contain reactive silica particles. These reactive silica particles accumulate, corroding the bond that might form between silica and hydrated cement gel. To overcome this issue, it is suggested to use pozzolans such as silica fume. Silica fume, possessing higher surface area compared with other pozzolans such as fly ash or GGBS may reduce the accumulation of reactive silica particles. Silica fume, having 94% SiO₂ content has mentioned to be highly reactive than other pozzolans (Barbhuiya, 2009). Therefore, silica fume can be used as potential pozzolanic binder replacement for Portland cement compared with other pozzolanic materials.

The diversity of pozzolanic reaction is investigated in the literature. For instance, GGBS do possess hydraulic properties. However, the GGBS requires chemical activation by Ca(OH)₂ and gypsum, due to lower rate of reaction with water alone. In case of FA, the pozzolanic reaction is comparatively slow as FA may retard the hydration of cement. Hence, it is important to consider various types of pozzolanic materials, since different types of pozzolanic materials have different influence of the mechanical and durability properties of concrete. Hence, using a considerable addition of Ca(OH)₂ can further accelerate the pozzolanic reaction and enhance mechanical properties and durability characteristics of concrete, even after 91 days (Berry, 1990; Yu, 2015).

2.3.5 Sustainability of using supplementary cementitious materials (SCMs)

Optimization strategies have been mentioned in the literature to analyze the sustainability of concrete production. Hooton et al. (2014) emphasized on using aggregate gradation optimization strategies. They mentioned the use of admixtures and fillers may enable the reduction of Portland cement content during concrete production. Particle size distribution of binders such as cement, SCMs and fillers can

be optimized which may increase the use of SCM content, hence reducing the adverse influence on early age properties of concrete. Moreover, they also emphasized on the use of Portland-limestone cements (PLC) in order to reduce the clinker content of Portland cement. Hence, point-source reduction of CO₂ emissions can be possible during the manufacturing of Portland cement.

Zhang et al. (2012) discusses the use of gap-graded powder; mixture of various binders characterized to ensure the required particle size distribution. They also suggested that the use of SCMs that fine SCMs and fillers might occupy the fine fraction in the concrete mix whereas the coarse SCMs may occupy the coarser fraction to maintain the efficient use of these materials along with Portland cement. However, the quantity of replacement and influence of SCMs, especially on mechanical properties and durability characteristics of concrete requires information that is more evident. In addition to that, some standards restrict the idea of maximum replacement of Portland cement by SCMs. Hence, to achieve sustainability in concrete production, the concrete production should focus on long-term durability characteristics to achieve sustainable production of concrete.

Long et al. (2015) discusses the use of self-compacted concrete (SCC), due to its various advantages along with the use of SCMs. Reduction in construction cost and improvements in construction environment have made the SCC follow the direction of sustainably developed concrete. Moreover, they also mentioned that the environmental index, which includes CO₂ emissions index, energy index and resource index, has significantly decreased with the increasing replacement ratio of SCMs in the cementitious matrix. Hence, in terms of sustainable assessment of SCMs, the use of SCMs for the production of concrete is environmentally acceptable.

Gartner et al. (2015) discusses the use of alternative approaches to reduce CO₂ emissions associated with the manufacture of Portland-based cements. They mentioned the use of alternative fuels/raw materials such as municipal waste incinerator ash and pulverized waste concrete as potential partial replacement materials within the Portland cement clinker during the manufacturing process of Portland cement. Furthermore, they also emphasized on the use of low-carbon SCMs in order to replace Portland cement clinker during the manufacturing of Portland

cement. Hence, to reduce CO₂ emissions, SCMs are seen as one of the potential replacement material, which can be used instead of Portland cement.

Furthermore, pozzolans have been successfully used as replacement material to Portland cement up to 30% by mass, without affecting the mechanical properties and durability characteristics adversely (Al-Ani, 1989; Lam, 1998; Han, 2003). The cost of concrete production is relatively reduced as pozzolans are normally characterized as by-products of various industrial processes. However, the early strength of pozzolanic concrete is reduced. Rate of pozzolanic reaction is slower compared with cement hydration reaction. Hence, the significance of pozzolans is greatly seen in long-term ages (Malhotra, 2000).

2.4 Mechanical properties of concrete

2.4.1 Strength

Strength of concrete is considered the most significant property to investigate the quality of concrete. It shows the quality of the structure of the hydrated cementitious paste. Strength development has a significant relationship with the capillary pores present in the hydrated cementitious paste. The sum of the volumes of gel pores and capillary pores present in cementitious paste is inversely proportional to the volume of hydrated cementitious paste. Therefore, if the volume of capillary pores are less in the structure of hydrated cementitious paste, the strength development of hydrated cementitious paste (concrete) will be high and vice versa (Neville, 1995).

Strength of concrete is also dependable on factors such as water/binder ratio and degree of compaction. Water/binder ratio is inversely proportion to the strength of concrete, if the concrete is fully compacted. Optimum water/binder ratio is required to provide enough workability, since lower than optimum water/binder ratio will make the compaction of concrete difficult, thus affecting the strength of concrete. In addition to that, high water/binder ratio will cause the loss of bond between the cementitious paste and filler particles such as coarse aggregates, causing segregation in concrete once hardened. Degree of compaction also have a great effect; if the concrete is insufficiently compacted regardless of water/binder ratio, large air voids will be present on the surface of the concrete. The bond between the cementitious paste and

coarse aggregates will weaken, thus reducing the strength of concrete. Hence, strength of concrete results from the strength of cementitious paste, bond between the cementitious paste and filler particles, strength of coarse aggregates, water/binder ratio and effective degree of compaction respectively (Neville, 1995; Kosmatka, 2011).

2.5 Durability characteristics of concrete

2.5.1 Water permeability

Permeability, in general is defined as the quality of a material that causes allowance of transport of particles through it. In concrete, permeability is referred as the transportation of fluids such as water, carbon dioxide and oxygen done under pressure inside the concrete. Permeability of concrete mainly depends on the structure of hydrated cement paste and the nature of pore system of concrete (Neville, 1995).

In case of water permeability, it can be defined as the flow of water through concrete under porous structure of concrete under differential pressure. It must be noted that permeability of concrete is not a simple function of determine the porousness of the structure of concrete. Water permeability depends on the size, distribution, shape and continuity of pores inside the pore system of hydrated cement paste of concrete. Furthermore, permeability of concrete is directly influenced by the capillary pores present in the hydrated cementitious paste of concrete (Neville, 1995; Kosmatka, 2011).

2.5.2 Porosity

Porosity is defined as “the measure of the proportion of the total volume of concrete occupied by pores” (Neville, 1995). Unlike permeability of concrete, porosity of concrete is referred to the porousness of structure of concrete. The relationship between porosity and permeability of hardened cementitious paste is qualitative, instead of quantitative. Porosity depends the availability of pores, irrespective of their nature, in the hardened concrete. Porosity can also be obtained by determining the absorption capacity of concrete (Neville, 1995).

2.5.3 External sulfate attack

Common sulfates such as sodium sulfate, potassium sulfate, magnesium sulfate and calcium sulfate are normally present in soil and/or in groundwater. For instance, when calcium sulfate chemically reacts with calcium aluminate hydrate (C_3A), calcium-alumino-tri-sulfate-hydrate, known as ettringite are formed (mentioned previously in Section 2.2.4). The formation of ettringite causes disruptive volume expansion of hardened concrete, which results in strength loss, decrease in modulus of elasticity and micro cracking of concrete (Neville, 1995; Kosmatka, 2011).

In addition to that, sulfate ions, for instance when calcium sulfate reacts with CH, which is hydration product of Portland cement, ettringite is formed on the surface of C_3A . By this reaction, further reaction between sulfate ions and C_3A is accelerated, causing more ettringite to form. Thus, expansion of volume as well as increase in porosity is observed. Hence, the consequences of sulfate attack include not only disruptive volume expansion of hardened concrete but also reduces the strength. Loss of strength is due to the loss of cohesion within the hydrated cementitious paste as well as with the aggregate particles respectively (Neville, 1995; Kosmatka, 2011).

2.5.4 Freezing and thawing

Mechanism of freezing and thawing is somehow natural. Pure water freezes at 0°C , however water available inside concrete is a solution of cementitious particles and filler particles, therefore, freezing point is lower. In addition to that, the size of pores, full of water do have an influence on freezing temperature. Smaller pores filled with water have lower freezing temperature and vice versa. Though gel pores and air voids are present in cementitious paste, freezing takes place in capillary pores (Neville, 1995).

Freezing is a gradual process, so when water freezes, unfrozen water in the capillary pores is subjected to hydraulic pressure due to the volume expansion of ice. The pressure exerted by the volume expansion of ice results in internal tensile stresses that may cause local failure of concrete. After that, on subsequent thawing, the volume expansion of ice caused additional space for water, which may be subsequently absorbed by water. If thawing is followed by re-freezing, further expansion will take

place, thus, repeated cycles of freezing and thawing will have a cumulative effect. This cumulative effect causes damage to concrete. Furthermore, repeated cycles of freezing and thawing causes progressive damage. Each cycle of freezing results the movement of water to various locations inside the cementitious paste where it can freeze. These locations develop as fine cracks when pressure by ice is exerted on them. Those cracks develop significantly during thawing when those locations will be filled with water. Thus, subsequent freezing will repeat the similar development of cracks, affecting the durability of concrete adversely (Neville, 1995; Kosmatka, 2011).

2.6 Influence of SCMs on mechanical properties of concrete

Elahi et al. (2010) discusses concrete mixes including various supplementary cementitious materials such as SF, FA and GGBS are used as binder replacement to Portland cement. It is mentioned that by replacing Portland cement with FA and GGBS in various proportions along with 7.5% use of SF in the mix, compressive strength is increased at all ages i.e. up to 91 days. However, a decrease in compressive strength is also likely to be seen at early ages when the SF content was increased from 7.5% to 15%. It may show a possibility to enhance the long-term compressive strength as binary and ternary mixes are used. However, early strength development is more likely to decrease in strength compared with Portland cement due to the slow rate of hydration and pozzolanic reactions.

Toutanji et al. (2004) discussed the effect of SCMs on strength development of concrete. They suggested that the addition of 8% of silica fume by mass could be considered as the optimum content that may produce the highest increase in compressive strength. However, they also mentioned that beyond 10% silica fume content, the compressive strength starts to decrease. As for GGBS, they reported slight increase in compressive strength by suggesting the optimum level of 30% replacement of Portland cement with GGBS. However, they also referred to curing time of concrete as their study was based on short-term study. They mentioned that the results might differ if the curing period was much longer. They also further indicated that long-term study is required to fully understand the influence and effects of SCMs in concrete production.

Yazıcı (2008) investigated the effects of silica fume and fly ash on mechanical properties of concrete. It is reported that concrete containing fly ash content without any influence of silica fume resulted in a reduction at both early and ultimate compressive strengths. However, concrete containing fly ash content with 10% silica fume content provided an enhancing affect in strength development compared with the previous scenario.

Mazloom et al. (2004) examined the short and long term mechanical properties of concrete containing different replacement levels of silica fume (SF) as a binder. They have replaced Portland cement with silica fume at the percentages of 0%, 6%, 10% and 15% respectively. It was mentioned that as the replacement level of SF increased, workability decreased. Furthermore, to maintain a required slump (100 ± 10 mm), higher SF replacement level require higher dosage of superplasticizers. Compressive strength is reported to increase with the increase of SF content within 28 days of curing time. However, after 90 days of curing time, no change in compressive strength is observed.

Nazari and Riahi (2011) suggested the use of nano – silica fume in cement and/or concrete production to enhance the mechanical properties. It is reported that by an addition of 4% of nano – silica fume in the concrete mixture by mass of cement may enhance the compressive strength of concrete by 70%. Furthermore, Li et al. discussed that compressive strength is enhanced by 14% and 18% at 28 days by the addition of nano – silica fume of 3% and 5% mass of cement content (Li, 2004). Similarly, Yu (2014) reported that mechanical properties are also enhanced with the addition of nano – silica fume. However, a further increase from 4% silica content to 5% silica content, a decrease in mechanical properties is reported at 28 days. On the other hand, Ltifi et al. (2011) reported a decrease in compressive strength of concrete incorporated with 3% nano – silica content in comparison with plain concrete. Hence, these differences in compressive strength are dependable on the heterogeneity of pozzolanic characteristics of the material itself.

Duan et al. (2013) mentioned that by the addition of metakaolin (MK), there is a gradual increase in compressive strength at early ages, lowering the content of calcium hydroxide (CH). However, Siddique et al. (2011) mentioned that concrete incorporated with 5 – 15% MK showed only minimal increase in compressive strength at 56 and 84

days respectively. Therefore, optimum amount of SCMs replacement level requires further certainty to assess mechanical properties of concrete.

2.7 Influence of SCMs on durability characteristics of concrete

Durability of normal strength concrete has been investigated in the literature; however, the influence of pozzolans on durability characteristics requires further investigation. Various methods such as resistance to air, water and other ions such as sulfates and chlorides penetration are mentioned as few of the simple approaches to determine durability of concrete. The penetration of these aggressive ions as well as water affect the physical and chemical processes of concrete deterioration, therefore it is important to determine the durability characteristics of concrete by these necessary measures (Mehta, 2006).

In addition to that, it is evident in the literature that by using SCMs in concrete, rheological and durability properties do enhance substantially. Miura et al. investigated the effect of SCMs on workability and suggested that 30% fly ash content replacement for Portland cement may enhance rheological properties. Furthermore, reduction of cement content in concrete mixture is also an advantage of using SCMs (Miura, 1993). Though such practice provides economic and environmental benefits, it has also become the means of reducing heat of hydration and durability characteristics of concrete. Moreover, it is also mentioned that occurrence of creep and shrinkage is also reduced by using SCMs in concrete (Chang, 2004).

In addition to that, water demand also plays a crucial part when SCMs are used in the concrete manufacturing. Water demand is likely to increase when pozzolans are used due to the reduced particle size distribution and high specific surface area (Walker, 2011). However, if the amount of water is higher, excess water may enhance the porosity of concrete (Neville, 1995). Therefore, it is crucial to choose optimum water/binder ratio so that durability characteristics as well as mechanical properties are not compromised.

Elahi et al. (2010) investigated durability characteristics such as air permeability, sorptivity and chloride diffusion of concrete mixes incorporated with SF, FA and GGBS as binder replacement to Portland cement respectively. For air permeability,

the use of SF did not significantly improve the air permeability. However, in the presence of FA up to 40% replaced by Portland cement, air permeability has greatly decreased compared with Portland cement at early ages. Moreover, in case of sorptivity, an overall decrease is likely to be investigated. 50% GGBS replacement along with addition of SF improved the water absorption compared with Portland cement concrete. Furthermore, all mixes are also reported to show approximately three times greater resistance against chloride diffusion compared with Portland cement concrete. SF is mentioned to be the best among all the mixes improving the resistance against chloride diffusion.

Yu et al. (2015) conducted a study on water permeability and porosity on concrete incorporated with FA and GGBS. They concluded that water/binder ratio is crucial for understanding water permeability and porosity, especially in case of pozzolans-binders. They suggested that if the amount of water is considerably less, the added water is likely to absorb by the pozzolanic binders. This may limit the production of cement hydration products, causing high water permeable and porous concrete. However, due to increase in capillary pores by excessive amount of water present in the concrete mixture, high water permeability is likely to observe. Hence, they further suggested that decision of choosing an optimum water content is required, at which the water permeability and porosity of pozzolanic concrete may reduce. They also compared water permeability of FA and GGBS concrete mixtures and concluded that water permeability of FA concrete mixture is comparatively higher than GGBS concrete mixture.

Van et al. (2011) suggested that the addition of silica fume in concrete mixture might enhance the workability without providing any adverse effect to the performance of concrete. Instead, higher performance is likely to observe compared with Portland cement concrete. Optimal replacement of silica fume was mentioned in the range of 10% - 20% for the workability of concrete. However, Aldahdooh (2013) concluded that silica fume decreased the workability of concrete. Hence, difference of conclusions might be due the difference in the characteristics of raw materials.

Yu et al. (2014) discusses the incorporation of nano – silica fume in concrete to assess porosity. They concluded that an increase of water content in concrete mixture might be due to the addition of nano – silica fume. Furthermore, they reported that porosity

decreases first, then a slight increase is observed until an optimum porosity value is reached with the addition of nano – silica fume. They also suggested that by the addition of nano – silica fume, early pozzolanic reaction which takes place to help the hydration reaction of cement; further contributing in the development of microstructure of concrete at early ages.

Mazloom et al. (2004) reported that the influence of silica fume in concrete might reduce porosity and permeability of concrete without compromising the required strength of concrete. Similarly, Siddique et al. (2011) reported that improvement in the pore microstructure of concrete due to decrease in the initial surface absorption and sorption of concrete by the addition of MK.

Liu et al. (2003) investigated the resistance against freezing and thawing on concrete incorporated with ultra-fine pozzolanic particles. They mentioned that the durability coefficient of concrete incorporated with ultra-fine pozzolanic particles was greater than or equal to 100 after 600 freeze and thaw cycles. They further reported that mass loss was insignificant after 600 freeze and thaw cycles conforming that durability characteristics have enhanced by the addition of pozzolanic material.

2.8 Waste materials

Waste materials, disposed from agriculture and industry, are less valuable and often ignored; however, they might offer a prospect for recycling processes (Aprianti, 2017). In general, waste materials have investigated based on their properties, value and efficiency, especially for their use in cement and concrete manufacturing researchers (Belaidi, 2012; Sharma, 2015; Aprianti, 2017). Waste materials containing Si and Al content are suggested to be used in cement and concrete manufacturing. This may be due to their elemental properties and chemical coherence with hydration process of cement. Moreover, the use of these waste materials containing Si and Al content may contribute to increase compressive strength and significantly reduce permeability and porosity of concrete (Belaidi, 2012; Rodrigues, 2015). Moreover, improvement against reactive ions such as sulfate and chloride attacks is also suggested. Reduction in segregation and resistance to freeze and thaw reactions improved the strength and durability characteristics of concrete. As the recyclability of concrete will increase by

utilizing waste materials, the economic burden of procuring required materials for cement and concrete manufacturing will significantly reduce.

The most important parameter for the assessment of concrete is its compressive strength. However, the critical parameter of assessing concrete performance is its durability. Economy does influence, as the production cost of concrete is required to be estimated. From an environmental perspective, using waste materials is also vital which can reduce the environmental degradation due to these waste materials. If all these factors are critically incorporated during the production of concrete, then the production of sustainable concrete is inevitable (Toutanji, 2004).

In the past, limited number of studies suggested the utilization of supplementary cementitious materials (SCMs) and waste materials as a substitution to Portland cement. Materialistic properties that reduce heat liberation provide critical resistance against chemical attacks and reduction in porosity were found. Hence, the possibility of enhancing durability of concrete is mentioned by the addition of waste materials. (Tagnit, 2003; Ghrici, 2006; Ghrici, 2007). However, absence of long-term investigations that may additionally explore the impact of supplementary cementitious materials with the influence of pozzolanic and/or inert waste materials within the concrete mixture.

2.8.1 Influence of waste materials on the properties of concrete

2.8.1.1 Marble Dust

Various studies have found in the literature on the performance of concrete incorporated with marble dust; however, they have categorized based on their addition in concrete mixture. Studies have shown that marble dust has been used as an additive in the production of Portland cement (Aruntas, 2010; Gesoglu, 2012), as an admixture replacing Portland cement (Alyamac and Ince, 2009; Turker, 2007; Ergun, 2011; Aliabdo, 2014) and even as a filler material replacing fine aggregates and coarse aggregates (Wu, 2001; Binici, 2007; Corinaldesi, 2010; Demirel, 2010; Hebhoub, 2011) in the concrete mixture.

2.9.1.1.1 Marble dust as an additive

Aruntas et al. (2010) investigated the influence of Portland cement and marble dust as binary blends of self-compacting concrete. According to their results, fresh properties of concrete are enhanced by the use of marble dust. Increase in slump flow is reported by the addition of marble dust, thus increasing the workability of concrete. Moreover, Ghrici et al. (2007) investigated the effect of limestone fillers and natural pozzolans addition to assess the mechanical properties and resistance against chemical attacks of cementitious mortars. Mortar prisms are produced replacing Portland cement by 20% limestone filler and 30% natural pozzolans. They reported that mechanical properties improved at early age as well as at long term i.e. 90 days. They suggested that the use of ternary blends of cementitious materials might be the reason of enhanced mechanical properties, especially at early ages. Furthermore, they also investigated the resistance against sulfate, chloride ion and acid attacks. They reported that the resistance against reactive chemical ions also improved.

Menendez et al. (2003) suggested that by the use of Portland cement with the incorporation of GGBS and marble dust provide economic and environmental advantage by reducing CO₂ emissions. However, the study is limited to mechanical properties only, suggesting that ternary mixes may enhance the early and long-term compressive strengths. Therefore, Gesoglu (2012) concluded that a comprehensive investigation is essential to understand the true effectiveness of marble dust with binary and ternary cementitious blends on fresh and hardened properties of concrete.

2.8.1.1.2 Marble dust as a binder replacement

Mohamadien (2012) determined the effect of marble dust along with silica fume as a partial replacement of Portland cement at various proportions. The partial replacement levels of marble dust and silica fume are set to 0%, 5%, 10%, 15%, 20%, 30%, 40% and 50% by weight of cement and are mixed with a separate manner. Mechanical properties were investigated at 7 days as well as at 28 days. It is reported that concrete mixture incorporated with 15% replacement ratio for marble dust as well as for silica fume show maximum compressive strength values compared with other replacement ratios. The increase in compressive strength at 15% silica fume content concrete was 31.4% and 48.3% at 7 and 28 days respectively. Likewise, the increase in compressive

strength at 15% marble dust content concrete was 22.7% and 27.8% at 7 and 28 days respectively.

Aliabdo et al. (2014) refers to replacement of cement by marble dust content mentions that by using marble dust up to 15% as the binder replacement may show similar mechanical properties compared with Portland cement concrete. Furthermore, they also reported that when 10% of cement content is replaced by marble dust, the values of splitting tensile strength test are the highest. However, Ergun et al. (2011) mentioned a decrease in flexural strength of concrete in case of high replacement levels of cement by marble dust. They also reported that by replacing 5% cement content with marble dust content along with the addition of superplasticizer, the compressive strength of concrete may be optimized compared to the Portland cement concrete. They also mentioned that due to the addition of filler material in concrete mixture, water demand to maintain the level of workability of concrete may increase. Therefore, it might be possible that the positive effects of filler materials to enhance mechanical properties of concrete is less likely to be seen. Turker et al. (2007) mentioned that compressive strength has drastically decreased for all curing periods when marble dust is used as a replacement material for Portland cement. They suggested that this decrease might have caused due to the dilution of cement hydration compounds i.e. C_2S and C_3S that resulted in longer setting times compared with Portland cement concrete. Therefore, the strength development has altered due to unavailability of these compounds.

2.8.1.1.3 Marble dust as a filler replacement

Corinaldesi et al. (2010) discussed the characterization of marble dust for mortar and concrete. They concluded that high degree of fineness of marble dust caused the effective cohesiveness in concrete. Moreover, in the presence of super-plasticizing admixture, along with 10% replacement of fine aggregates by marble dust, maximum compressive strength of concrete was achieved compared to other concrete mixtures. However, the workability level of concrete incorporated with marble dust was the same compared to the Portland cement concrete. Hence, an early rise in compressive strength might link to the filler effect of marble dust.

Omar et al. (2012) discussed the influence of limestone waste as partial replacement material for sand with the addition of marble dust to assess the mechanical properties of concrete. They mentioned that by the use of 50% limestone waste material content, 12% increase in compressive strength of the concrete is reported at 28 days. Furthermore, by the addition of marble dust along with 50% limestone waste material content, a 7% increase in compressive strength is reported. However, by increasing the percentage replacement of limestone waste material i.e. more than 50%, the rate of strength gain started to decrease. Furthermore, using 15% marble dust content, the compressive strength enhanced significantly.

Binici (2007) and Hebhouh (2011) discussed the effect of marble dust when replaced with fine aggregates. They mentioned that replacing fine aggregates with marble dust reduces the slump value as the replacement level increases. Natural aggregates have higher water absorption ratio compared to marble dust. Therefore, the reduction in slump value may be due to this reason. Furthermore, bulk density of the concrete did not change with the incremental addition of marble dust. Moreover, Hebhouh et al. (2011) suggested that by replacing fine aggregates up to 75% with marble dust might lead to an increase in compressive strength. Binici et al. (2007) discussed the resistance against sulfate attack. Incremental addition of marble dust improved the resistance against sulfate attack. Binici et al. (2008) also mentioned that by the addition of marble dust with granite waste aggregates might influence the performance of concrete by improving the mechanical properties, workability and the resistance against chemical attacks.

Demirel (2010) investigated the feasibility of using marble dust in comparison with fine aggregates that pass through a 0.25 mm sieve. The effects of marble dust have been studied to investigate the mechanical properties of the concrete. Concrete mixtures are prepared by replacing fine aggregates with marble dust with the proportions of 0, 25, 50 and 100% by weight on concrete. Several conclusions were reported. By the increase in the unit weight of concrete, the amount of marble dust incorporated in concrete also increases. The compressive strength has increased with an increase in marble dust content. After 28 days, the increase in compressive strength is reported to be 10% for the concrete mixture incorporated with 100% marble dust. However, after 90 days, the increase in the compressive strength in the similar type of

concrete mixture is reported to be 5% only. Hence, it is suggested that with an increase in curing time, the contribution of marble dust in strength development may decrease. In addition to that, highest percentage replacement i.e. 100% marble dust concrete mixture possesses maximum compressive strength in comparison with all other addition of marble proportions at all curing ages. Moreover, the porosity of concrete incorporated with marble dust decreased with an increased content of marble dust. Lastly, sorptivity has also shown a decreasing trend with an increase in marble dust content. Similar findings have already been discussed by Topcu (2009). Furthermore, the sorptivity coefficient of concrete incorporated with marble dust decreased slightly with an increase in compressive strength. Hence, filler effect of marble dust on the hydration reaction of cement particles caused the reduction of porosity and sorptivity, as well as enhancing the durability characteristics of concrete.

2.8.1.2 Crushed Bricks

One of the alternatives is to reuse the crushed bricks by incorporating them in the production of concrete. It is mentioned in the literature that the recycling of crushed bricks in the production of concrete is economically viable. Furthermore, it is suggested as a sustainable approach to utilize waste materials in the production of concrete (Milicevic, 2015). In the literature, crushed bricks are used either replacing coarse aggregates and/or replacing fine aggregates in the concrete mixture.

2.8.1.2.1 Crushed bricks as coarse aggregates

Akhtaruzzaman and Hasnat (1983) focused on the use of crushed bricks as 100% coarse aggregates replacement in the production of concrete. The aim of this study is to determine the influence of crushed bricks to assess the physical and mechanical properties of concrete. They reported that normal compressive strength ranged in between 14 MPa and 35 MPa. Furthermore, the unit weight of concrete incorporated with crushed bricks is 17% less than the concrete incorporated with natural coarse aggregates. Hence, they suggested that it might be possible to achieve concrete with appropriate strength using crushed bricks as a replacement to coarse aggregates.

Mansur et al. (1999) discussed the suitability of crushed bricks to use as a replacement material of coarse aggregate for concrete. Physical properties of concrete incorporated

with crushed bricks in comparison with the normal concrete incorporated with natural coarse aggregates were investigated. They concluded that by the replacing natural coarse aggregates with crushed bricks, higher compressive and tensile stresses are likely to be observed compared to conventional concrete. However, significant loss in modulus of elasticity and workability of fresh concrete incorporated with crushed bricks is also observed.

Similarly, Khalaf and Devenny (1999) also investigated the use of crushed brick as a replacement material of coarse aggregates in concrete. They compared the compressive strength of concrete incorporated with crushed bricks and concrete incorporated with granite aggregates. They concluded that using crushed bricks might enhance the compressive strength compared with compressive strength of concrete containing granite aggregates.

Furthermore, Khalaf (2006) mentioned that the use of crushed bricks as a replacement of granite aggregates in concrete production, a decrease in compressive strength is observed. However, it is also mentioned that compressive strength also depends on the nature of crushed bricks. If the crushed bricks used have higher density, it is likely to see higher compressive strength. However, the decrease in compressive strength is also influenced with the high water absorption property of crushed bricks. Corriea (2006) and Adamson (2015) also discuss similar issues of high water absorption. Hence, more investigation is required to study the fresh and hardened properties of concrete incorporated with crushed bricks.

2.8.1.2.2 Crushed bricks as fine aggregates

Cachim (2009) mentioned that crushed bricks might show properties to be used as filler replacement material. However, to overcome any strength reduction, 15% replacement content of crushed brick is suggested. Poon and Chan (2007) investigated that by the addition of 20% fine crushed bricks as a replacement to aggregates decreased the compressive strength by 18%. Debeib and Kenai (2008) also reported that mechanical properties reduced by 40% when coarse, fine or both fine and coarse aggregates are replaced by crushed bricks.

Khatib (2005) discussed the use of crushed bricks as a replacement to fine aggregates. It is concluded that replacing fine aggregates by 50% crushed bricks content, no reduction in compressive strength is observed. However, after 50% replacement fraction, 10% decrease in compressive strength is reported. Bektas (2009) mentioned about the improvement of resistance against freeze and thaw when crushed bricks are used as a partial replacement material of fine aggregates in concrete under the action of air entrainment. Permeability of concrete containing crushed bricks is likely to decrease due to discontinuity of pores present between crushed bricks particles and cement paste. However, high porosity values are reported in the literature and mostly associated with the physical characteristics of crushed bricks (Adamson, 2015).

2.8.1.3 Other waste materials

Various waste materials are used as supplementary cementitious materials as well as filler replacements during the production of concrete. For instance, rice husk ash (RHA) are the natural coverings formed on rice grains during their growth. RHA is abundantly available in rice-producing countries and therefore, it is denoted as an agricultural solid waste material. One of the reasons RHA is used as a supplementary cementitious material is due to its fineness. RHA is a very fine material containing 85 – 90% amorphous silica and the average particle size of RHA ranges from 5 to 10 μm respectively (Sensale, 2010). Furthermore, the use of RHA as a supplementary cementitious material for the production of high strength concrete was discovered within the middle of 19th century (Raman, 2011).

In addition to that, several other waste materials such as tire-rubber particles, plastic waste and iron waste had used as a filler replacement during the production of concrete. Tire-rubber particles were mostly used to develop waste tire fiber modified concrete. Khaloo (2008) reports the mechanical properties of concrete containing a high volume of tire-rubber particles. Maximum replacement of fine aggregates and coarse aggregates was up to 100% by tire-rubber particles. The results showed that an increase in tire-rubber particles replacement levels decreased the unit weight of concrete compared with control concrete. Furthermore, replacement of fine and coarse aggregates with tire-rubber particles reduced the ultimate strength significantly. However, ductility of concrete incorporated with tire-rubber particles increased in

comparison with control concrete. The failure of tire-rubber concrete did not occur instantly and crack openings were smaller compared with control concrete.

Ismail (2008) studied the use of plastic waste in concrete mixture as fine aggregates replacement. Plastic waste that was obtained in this study contained 80% polyethylene and 20% polystyrene respectively. Maximum replacement of fine aggregates by plastic waste was 20% respectively. Results show that with an increase of plastic waste replacement, the flexure strength as well as compressive strength of all concrete mixes containing plastic waste decreased below the values of control concrete. Concrete containing 20% plastic waste replacement as fine aggregates had the lowest flexural strength at 28 days in comparison with all other concrete mixes.

Moreover, Ismail (2007) also studied the reuse of iron waste as a partial replacement of fine aggregates in concrete. The iron waste used had the maximum particle size of 4.75mm. Maximum replacement of fine aggregates by iron waste was 20% respectively. The results show that flexural strength of concrete containing iron waste enhanced by increasing the replacement levels of iron waste. Concrete containing 20% iron waste replacement as fine aggregates showed 27.86% increase in flexural strength compared with control concrete at 28 days. Similarly, compressive strength of concrete containing 20% iron waste replacement as fine aggregates showed an increase of 17.40% at 28 days.

CHAPTER 3

METHODOLOGY

3.1 Introduction

This chapter summarizes the methodology used in the thesis. Firstly, the materials used in the experimental work of the thesis, are introduced. All the materials used were locally procured. Identification of each material used, along with its chemical composition and particle size distribution has been done at Central Laboratory at METU Ankara using X-ray fluorescence (XRF) and particle size distribution techniques. Moreover, concrete mix design calculations for producing concrete along with gradation curves of aggregates are reported. Mix design details, determined concrete combinations and curing conditions examined in this thesis are summarized briefly. In addition to that, the experimental procedures conducted in the experimental work of the thesis are also summarized. Experiments are mainly carried out at the Materials Laboratory of METU NCC to study the mechanical properties and durability characteristics of concrete. In addition to that, advance techniques such as Scanning Electron Microscopy (SEM), particle size distribution, chemical analysis, X-ray fluorescence (XRF) and porosity are conducted at the Central Laboratory at METU Ankara funded by the Scientific Research Project (FEN-16-YG-11). This part of the chapter begins with the experimental procedures of the fresh properties of cementitious mortars and concrete. Experimental procedures to determine mechanical properties and durability characteristics are then reported. Advanced experimental techniques such as SEM, XRF, particle size distribution, chemical analysis and porosity are then summarized briefly.

3.2 Materials used

3.2.1 Portland cement

Portland cement, manufactured by Adana Cimento Ltd., having the design strength of 32.5 MPa in compliance with ASTM (2016e1). Portland cement is used as a binding material for the production of concrete. The specific gravity of Portland cement, provided by the manufacturer, is 3.15. Chemical composition along with particle size distribution has been found at Central Laboratory, METU Ankara.

3.2.1.1 Chemical Composition

Chemical composition of Portland cement is given in Table 3.1.

Table 3.1. Chemical composition of Portland cement.

Component	wt.%
CaO	43.8
SiO ₂	30.2
Al ₂ O ₃	11.4
Fe ₂ O ₃	5.11
SO ₃	3.29
MgO	2.61
K ₂ O	1.34

3.2.1.2 Particle Size Distribution

Particle size distribution of Portland cement is given in Figure 3.1.

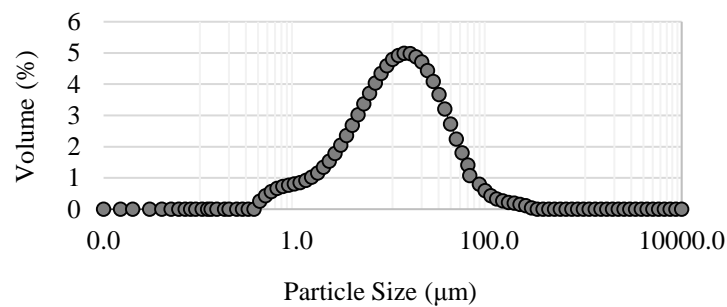


Figure 3.1. Particle size distribution of Portland cement.

3.2.2 Supplementary cementitious materials (SCMs)

3.2.2.1 Silica fume

Silica fume (SF) is a pozzolanic supplementary cementitious material, which is produced as by-product during the smelting process in the production of silicon metal and ferrosilicon alloys. In this thesis, silica fume is used as a binder replacement to Portland cement and is manufactured by Cyprus Environmental Enterprises Ltd. (CEE) in compliance with ASTM (2015). Chemical composition along with particle size distribution has been found at Central Laboratory, METU Ankara.

3.2.2.1.1 Chemical Composition

Chemical composition of silica fume is shown in Table 3.2.

Table 3.2. Chemical composition of silica fume.

Component	wt.%
SiO ₂	93.3
Fe ₂ O ₃	1.82
CaO	1.25
K ₂ O	1.21
MgO	0.891
Al ₂ O ₃	0.733
SO ₃	0.218

3.2.2.1.2 Particle Size Distribution

Particle size distribution of silica fume is shown in Figure 3.2.

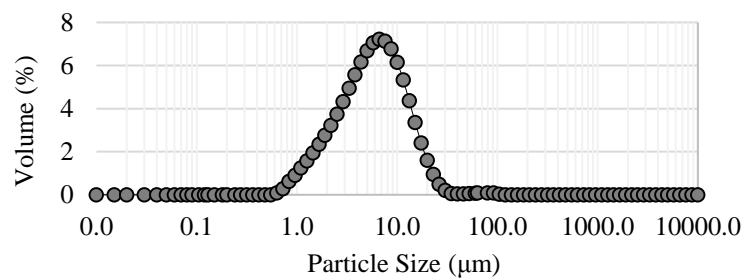


Figure 3.2. Particle size distribution of silica fume.

3.2.3 Waste materials

3.2.3.1 Marble dust

Marble Dust is used in this thesis as a filler replacement material to fine aggregates. Marble dust is obtained from Izmer Ltd. Chemical composition along with particle size distribution has been found at Central Laboratory, METU Ankara.

3.2.3.1.1 Chemical Composition

Chemical composition of marble dust is shown in Table 3.3.

Table 3.3. Chemical composition of marble dust.

Component	wt.%
CaO	64.5
SiO ₂	23.4
Al ₂ O ₃	4.32
Fe ₂ O ₃	2.83
MgO	1.73
K ₂ O	1.04
SO ₃	0.471

3.2.3.1.2 Particle Size Distribution

Particle size distribution of marble dust is shown in Figure 3.3.

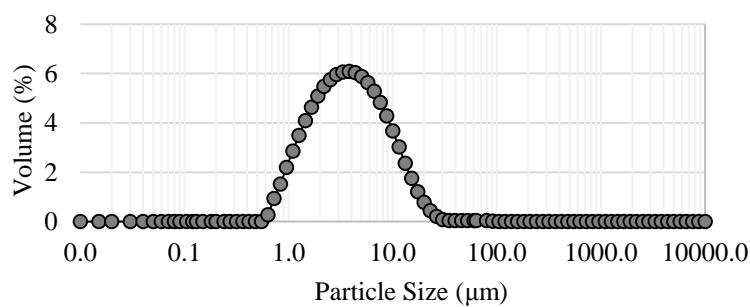


Figure 3.3. Particle size distribution of marble dust.

3.2.3.2 Crushed bricks

Crushed bricks are used in this thesis as a filler replacement material to fine aggregates. Crushed bricks are obtained from Gurdag Madencilik Ltd. Chemical composition along with particle size distribution has been found at Central Laboratory, METU Ankara.

3.2.3.2.1 Chemical Composition

Chemical composition of crushed bricks is shown in Table 3.4.

Table 3.4. Chemical composition of crushed bricks.

Component	wt.%
SiO ₂	41
CaO	21.6
Al ₂ O ₃	13.4
Fe ₂ O ₃	10.2
MgO	6.03
SO ₃	3.02
K ₂ O	1.91

3.2.3.2.2 Particle Size Distribution

Particle size distribution of crushed bricks is shown in Figure 3.4.

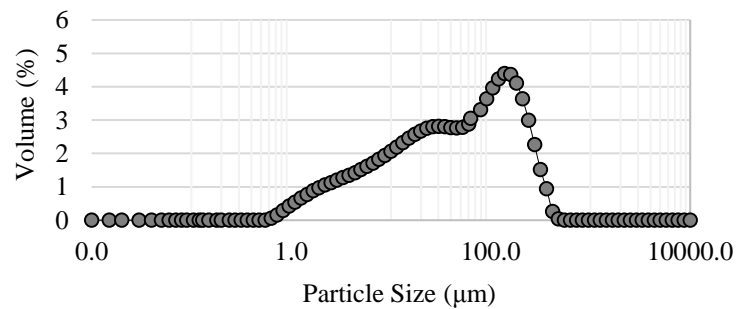


Figure 3.4. Particle size distribution of crushed bricks.

3.2.4 Fine aggregates

Locally available fine aggregates are used in this thesis. Average fine aggregates density was 1.65 g/cm^3 . Following the sieve analysis, the particle size distribution of fine aggregates was smaller than 4 mm and greater than 0.125 mm respectively. Specific gravity of fine aggregates found experimentally was 2.62 conforming ASTM (2015). Hence, specific gravity of fine aggregates obtained experimentally is used for concrete mix design calculations reported in Section 3.8. Furthermore, chemical composition along with particle size distribution has been found at Central Laboratory, METU Ankara.

3.2.4.1 Chemical Composition

Chemical composition of fine aggregates is shown in Table 3.5.

Table 3.5. Chemical composition of fine aggregates.

Component	wt.%
SiO ₂	91.9
Al ₂ O ₃	3.91
K ₂ O	1.31
CaO	0.463
TiO ₂	0.832
Fe ₂ O ₃	0.659

3.2.4.2 Particle Size Distribution

Particle size distribution of fine aggregates is shown in Figure 3.5.

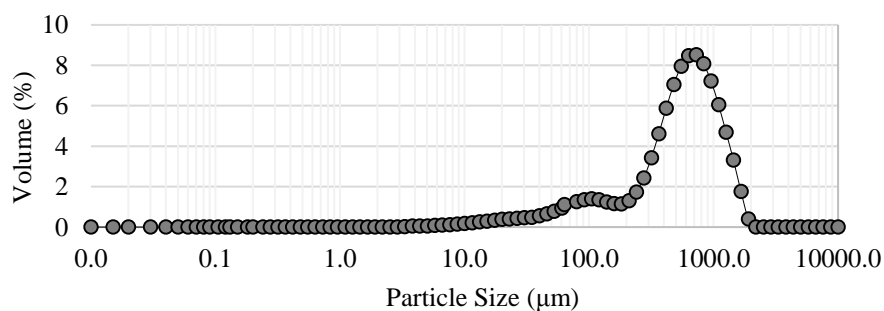


Figure 3.5. Particle size distribution of fine aggregates.

3.2.4.3 Gradation Curve

Gradation curve of fine aggregates as well as percentage retained on each sieve is shown in Figure 3.6 and Table 3.6 respectively. ASTM C33 (2016) provides upper and lower boundary limits of gradation curve, showed by the dotted lines in Figure 3.6. Figure 3.6 shows that the gradation curve is within the upper and lower boundary limits of ASTM C33 (2016). Hence, fine aggregates are suitable to be used for concrete mix design calculations. Gradation curve of fine aggregates is found at Materials Laboratory, METU NCC.

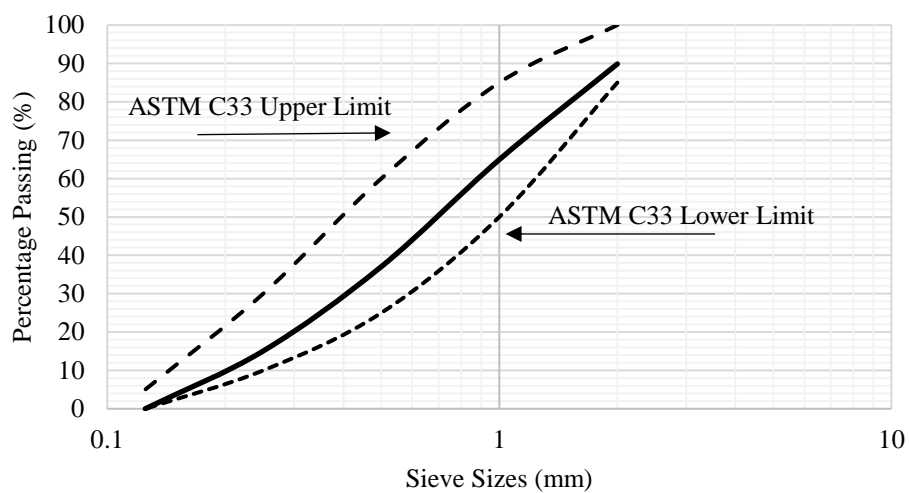


Figure 3.6. Gradation curve of fine aggregates.

Table 3.6. Gradation sieve sizes of fine aggregates.

Sieve sizes (mm)	Percentage retained (%)	Cumulative percentage passing (%)
4 mm	0	100
2 mm	10	90
1 mm	25	65
0.5 mm	28	37
0.25 mm	22	15
0.125 mm	15	0

3.2.5 Coarse aggregates

Locally available coarse aggregates are used in this thesis. Following the sieve analysis, the particle size distribution of fine aggregates were smaller than 32 mm and greater than 4 mm respectively. Specific gravity of coarse aggregates found experimentally was 2.68 conforming ASTM (2015). Hence, specific gravity of coarse aggregates obtained experimentally is used for concrete mix design calculations reported in Section 3.8.

3.2.5.1 Gradation Curve

Gradation curve of coarse aggregates as well as percentage retained on each sieve is shown in Figure 3.7 and Table 3.7 respectively. ASTM C33 (2016) provides upper and lower boundary limits of gradation curve, showed by the dotted lines in Figure 3.7. Figure 3.7 shows that the gradation curve is within the upper and lower boundary limits of ASTM C33 (2016). Hence, coarse aggregates are suitable to be used for concrete mix design calculations. Gradation curve of coarse aggregates is found at Materials Laboratory, METU NCC.

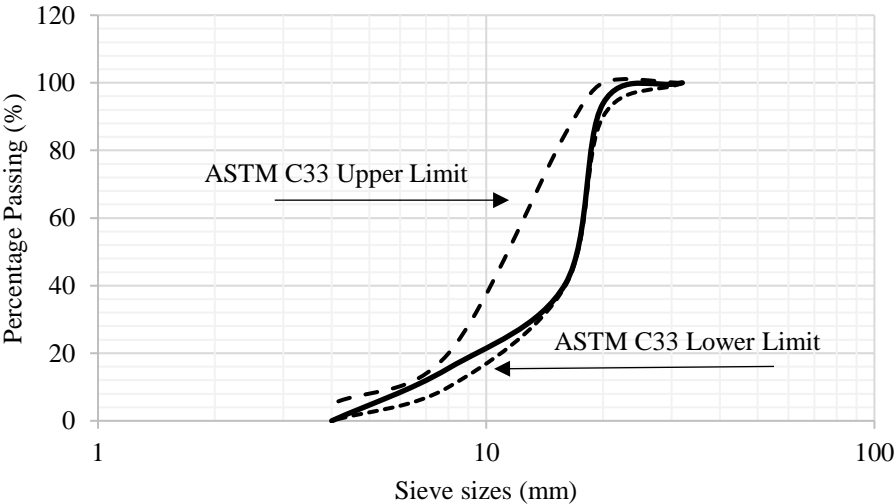


Figure 3.7. Gradation curve of coarse aggregates.

Table 3.7. Gradation sieve sizes of coarse aggregates.

Sieve sizes (mm)	Percentage retained (%)	Cumulative percentage passing (%)
32 mm	0	100
20 mm	5	95
16 mm	55	40
8 mm	25	15
4 mm	15	0

3.2.6 Water

Quantity and quality of water are essential since water in the mix has a direct influence with the strength of cementitious materials such as mortars and concrete. In this thesis, the mixing water used for the production of concrete as well as for curing are in compliance with ASTM C94 (2017) and ASTM C1602 (2012) respectively.

3.3 Concrete mix design

Concrete mix design is the process of determining required characteristics of concrete. Characteristics of concrete, which are necessary to include, are summarized as follows (ACI, 2009).

- Fresh concrete properties.
- Mechanical properties of hardened concrete.
- Durability characteristics of hardened concrete.
- Limits on specific proportions/constituents and additives/admixtures.

Proportioning of the concrete mixture discusses the determination of required quantities of concrete constituents to attain the specified properties of concrete. Therefore, to ensure properly proportioned concrete mix, considerations such as acceptable workability of freshly mixed concrete and uniform appearance of the hardened concrete should be monitored.

Mix proportions of concrete mix are specified, designed and proportionated by actual calculations and considerations reported by ACI Recommended Practice 211.1 (ACI,

2009). Concrete mix design procedure provides approximation of the proportions to be used; however, sequential steps must be followed. The steps are summarized as follows (ACI, 2009):

- Determination of parameters such as aggregates properties, maximum aggregate size, slump value, water and air content, water/binder ratio, additives and admixtures.
- Determination of cement content, fine and coarse aggregate content and adjustments in moisture content.
- Calculation and adjustments for batch weight of concrete.

In this thesis, concrete mix design is prepared under required material information and choice of slump. Slump value is assumed to 75 – 100 mm, whereas the maximum aggregate size used in the concrete mix design was selected as 25 mm. Both of these considerations were taken from ACI Recommended Practice 211.1 (ACI, 2009). The slump value is kept constant, to provide required workability of concrete. Hence, determination the water and air contents required for the concrete mix design are taken from the tables provided in ACI Recommended Practice 211.1 (ACI, 2009) i.e. approximate amounts of mixing water and air content requirements for concrete. Water content is decided to be 193 kg/m³ whereas entrapped air content is kept 1.5% respectively. In addition to that, ACI Recommended Practice 211.1 (ACI, 2009) also provides a relationship between water/binder ratio and compressive strength of concrete. Hence, water/binder ratio can be selected as well for the required compressive strength of concrete. In this thesis, water/binder ratio, selected from the table, is 0.54 for 30 MPa compressive strength of concrete at 28 days. Hence, determination of cement content is found by dividing water content by water/binder ratio (ACI, 2009).

- Cement content = $193/0.54 = 359 \text{ kg/m}^3$

Coarse aggregate content is determined after the determination of cement content. Fineness modulus of fine aggregate has already been found experimentally by sieve analysis and gradation curve. The fineness modulus of fine aggregate found is 2.60. Volume of coarse aggregates per unit volume of concrete is also provided in ACI Recommended Practice 211.1 (ACI, 2009) i.e. volume of dry-rodded coarse aggregate per unit volume of concrete. Hence, the volume of dry-rodded coarse aggregate per

unit volume of concrete is found to be 0.69m^3 , which was determined by comparing the maximum size of coarse aggregate value and fineness modulus of fine aggregates. Unit weight of coarse aggregates, mentioned in ACI Recommended Practice 211.1 (ACI, 2009), is 1600 kg/m^3 . Hence, dry weight of coarse aggregate can be determined by multiplying the volume of dry-rodded coarse aggregate per unit volume of concrete with the unit weight of coarse aggregates, as shown below (ACI, 2009).

- Dry weight of coarse aggregates = $0.69 \times 1600 = 1104\text{ kg/m}^3$

Absorption capacity of coarse aggregates is also found experimentally and the value is 0.5%. Therefore, the saturated surface dry (SSD) weight of coarse aggregate can be obtained by multiplying the dry weight of coarse aggregates with the absorption capacity of coarse aggregates, as shown below (ACI, 2009).

- SSD weight of coarse aggregates = $(1104 \times 0.005) + 1104 = 1110\text{ kg/m}^3$

Fine aggregate content is determined after the determination of coarse aggregate. The volume of fine aggregate per cubic meter of concrete is found by subtracting the cumulative volume of water, cement, coarse aggregates in SSD condition and entrapped air content in unit cubic meter of concrete by unit cubic meter respectively. The volume of water, cement and coarse aggregates are found by dividing their weights by their specific gravities, as shown below (ACI, 2009).

- Water = $(0.193/1) = 0.193\text{ m}^3$
- Cement = $(0.358/3.15) = 0.114\text{ m}^3$
- Coarse aggregate (SSD) = $(1.110/2.68) = 0.414\text{ m}^3$
- Air content = $(0.015/1) = 0.015\text{ m}^3$

The cumulative volume of water, cement, coarse aggregates and air content is 0.736 m^3 . Considering that these calculations are based on 1 m^3 of concrete, volume of fine aggregates can be determined, as shown below (ACI, 2009)

- Volume of fine aggregate (SSD) = $1 - 0.736 = 0.264\text{ m}^3$

Similarly, the weight of fine aggregate in SSD condition can be found by multiplying the volume of fine aggregates with the bulk specific gravity of fine aggregates, as shown below (ACI, 2009).

- SSD weight of fine aggregates = $(0.264 \times 2.62) / 1000 = 692\text{ kg/m}^3$

Hence, the concrete constituents required to produce unit cubic meter of concrete are shown below (ACI, 2009).

- Water = 193 kg/m³
- Cement = 358 kg/m³
- Coarse aggregates = 1110 kg/m³
- Fine aggregates = 692 kg/m³

Portland cement control concrete specimens are made using this concrete mix proportions. However, silica fume is used as binder replacement to Portland cement, whereas marble dust and crushed bricks are used as filler replacement to fine aggregates, therefore, adjustments in mixing proportions are done with respect to the replacement level of each concrete constituent respectively. Coarse aggregates are not replaced by any material; therefore, volume of coarse aggregates remains same for any replacement done by binders and/or fillers.

In this thesis, the mixing procedure of concrete follows ASTM C192/C192M -16a (ASTM, 2016a). A concrete mixer is used to produce concrete. Figure 3.8 shows the concrete mixer that is used for the mixing procedure of concrete.



Figure 3.8. Concrete mixer.

Slump apparatus is also used to measure the slump before molding the concrete inside the cubic molds. Figure 3.9 shows the measurement of slump taken after the mixing procedure of concrete.



Figure 3.9. Slump measurement taken on fresh concrete.

Vibrators, as shown in Figure 3.10 and Figure 3.11, are also used to provide sufficient compaction of concrete, which is placed inside concrete molds of size 150 mm by 150 mm by 150 mm. Concrete is poured into molds in two stages. Firstly, half of the concrete mold is filled and vibration is applied. Afterwards, the remaining half is filled until the top surface of concrete mold and sufficient vibration is applied to remove excessive air bubbles on the surface of the concrete.



Figure 3.10. Vibrators providing compaction to half-filled concrete mold.



Figure 3.11. Vibrators providing compaction to fully filled concrete mold.

Molding of concrete inside the cubic concrete molds, as shown in Figure 3.12, is done manually with the help of scoops and blunted trowels.

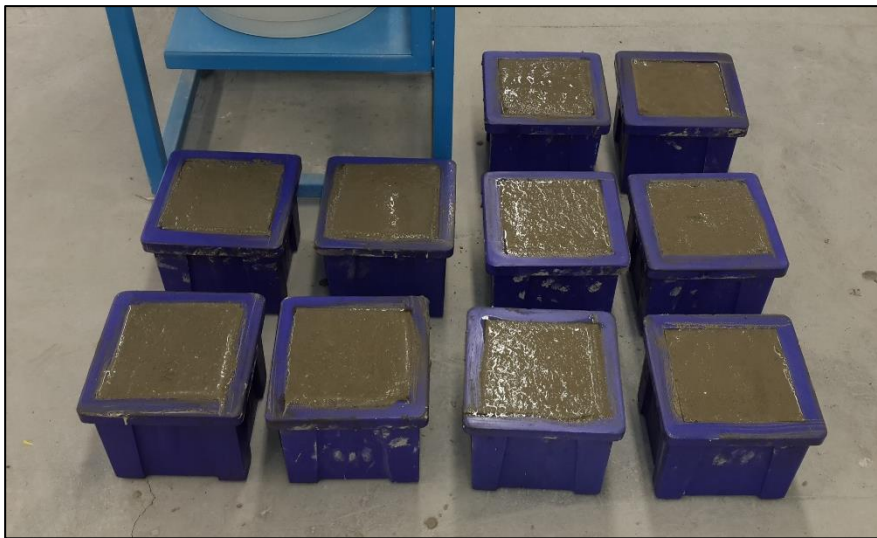


Figure 3.12. Molding of concrete.

Fresh concrete, molded inside the cubic concrete molds, is allowed to set and hardened in first 24 hours. After 24 hours, concrete specimens are demolded from the cubic concrete molds and are marked with their designated specimen name/date/number respectively. Afterwards, the concrete specimens are placed to the specified/planned curing conditions.

Various types of curing conditions are prepared for the experimental work in this thesis. Normal curing tank that has the temperature maintained at room temperature is shown in Figure 3.13. Furthermore, in Figure 3.13, it can be seen that all the concrete specimens are marked with their designated specimen name/date/number respectively, before placing them in their respective curing conditions.



Figure 3.13. Curing condition.

To study sulfate attack exposure, concrete specimens were cured under sulfate solution as a curing condition. Furthermore, to study the resistance to freeze and thaw cycles of concrete, freeze and thaw cabinet is used. Sodium sulfate solution is used for sulfate solution curing whereas freeze and thaw cabinet having the temperature range between 30°C and -30°C is used. Detailed procedures for external sulfate attack exposure and freeze and thaw cabinet are further explained in Section 4.7 and 4.8.

In addition to that, determined concrete combinations are produced replacing Portland cement with silica fume; fine aggregates with marble dust and crushed bricks to investigate mechanical properties and durability characteristics respectively. The determined concrete combinations produced, along with their replacement levels are illustrated in Table 3.8. The testing of these determined concrete specimens for

mechanical properties and durability characteristics investigated in this thesis are done at 28 days, 90 days, 180 days, 270 days and 365 days respectively.

Table 3.8. Determined concrete combinations.

Concrete combinations	Percentage content (%) in concrete mix				
	Cement	Silica fume	Marble dust	Crushed bricks	Fine aggregates
Control	100	-			100
C20SF	80	20	-	-	100
C20SF10MD	80	20	10	-	90
C20SF20MD	80	20	20	-	80
C20SF10CB	80	20	-	10	90
C20SF20CB	80	20	-	20	80

From the Table 3.8, it can be seen that Portland cement is 20% replaced by silica fume as a binder replacement. Furthermore, an addition of 10% and 20% marble dust and crushed bricks is done, which is used as a replacement of fine aggregates in the concrete matrix. These levels of replacement are chosen based on the recommendations provided in the literature review. Moreover, to investigate the suitability of using silica fume, marble dust and crushed bricks within the cementitious matrix, a pilot study has been conducted on cementitious mortars. The pilot study confirmed that the optimum level of 20% silica fume along with 10% and 20% of marble dust and crushed bricks is suitable for the development of sustainable concrete. Therefore, the concrete produced for this thesis has a maximum addition of 40% replacement materials compared to the conventional concrete.

Moreover, one of the major considerations for fresh concrete is the workability of concrete. To ensure good workability of concrete, since all concrete combinations are distinct to each other, the slump value is kept constant i.e. 75 – 100 mm for all concrete combinations. Therefore, water content i.e. water/binder ratio has been adjusted for each concrete combination respectively, as shown in the Table 3.9.

Table 3.9. Water content of determined concrete combinations.

Concrete combinations	Water/binder ratio (w/b ratio)
Control	0.54
C20SF	0.557
C20SF10MD	0.584
C20SF20MD	0.675
C20SF10CB	0.652
C20SF20CB	0.765

From the table 3.9, it can be seen that by the addition of supplementary cementitious materials and waste materials gradually increased the water content. It is well-known phenomenon that an increase in the fineness of binding materials as well as replacement materials, results in a gradual increase in water/binder ratio to achieve a good workable concrete. For instance, increase of w/b ratio between control concrete and 20SF concrete is reported to be 0.017. The increase in w/b ratio is normal, since silica fume has high fineness in comparison with Portland cement. Furthermore, by the addition of waste materials, w/b ratio increased significantly. For instance, crushed bricks has high absorption capacity compared to marble dust. Therefore, concrete containing crushed bricks does possess high w/b ratio, as observed by the values of w/b ratios in the Table 3.9. Increase in replacement level of waste materials also increased the w/b ratio.

3.4 Experimental procedures

3.4.1 Determination of Slump

Slump measurements are carried out on a freshly mixed concrete to determine the workability of these mixed using the standard slump test apparatus. This is also called as the indirect measurement of determining concrete consistency. The measured slump values indicate the amount of water used for the mix and flow characteristics of the freshly mixed concrete. The slump test works on the principle of inverted cone of concrete compacted under the action of gravity. The slump measurements are conducted according to the procedure given in ASTM C143-15a (2015). Slump cone,

scale for measurement and a tamping rod is used for this experiment. The concrete is filled in three consecutive layers. Each layer is tamped 25 times with the tamping rod. When the slump cone is completely filled with concrete, the top surface is levelled by rolling the tamping rod. Immediately after filling concrete, the cone is carefully lifted vertically in slow motion, making the concrete perform a slump. Slump cone is placed next to the concrete specimen under the test. The decrease in height of concrete with respect to the slump cone is determined as a measurement of slump value. To attain a constant workability, the slump value is maintained constant to 100 mm for all concrete mixes examined in this thesis. Figure 3.14 shows the determination of slump of freshly mixed concrete.



Figure 3.14. Determination of slump.

3.4.2 Determination of Compressive Strength Test

Compressive strength test for concrete cubes is performed using a standard compressive strength-testing equipment. Before the compressive strength test is performed, the specimens are cured with respect to their desired curing time and are then air-dried. BS EN 12390-3 (2002) is followed for the determination of compressive strength on standard cubes. The loading rate has been kept constant to 0.6 MPa/sec. An average compressive strength has been taken among all the values from each subsequent mixture of concrete produced. Figure 3.15 shows the compressive strength test machine, by which compressive strength of concrete cubic specimens is determined.



Figure 3.15. Compressive strength testing equipment for concrete samples.

3.4.3 Determination of Water Penetration Depth

Water penetration depth of standard concrete/mortar samples are determined according to BS EN 12390–8 (2009). Dry mass of the specimen is recorded prior to the experiment. This is recorded as the initial mass measurement of the concrete specimen. Initially, the specimen is tightly placed into the water permeability-testing machine. Careful adjustments must be done prior to the experiment to avoid any water leakage from the sides of the specimen during the test. The pressurized water is then applied from the bottom of the specimen for 72 hours. All the specimen are subjected to 1 atmospheric pressure (0.1 MPa). Following 72 hours of an exposure, each specimen is then removed from the water permeability-testing machine and final mass is measured using a top-loading balance. Split tensile test is then conducted to break the specimen into two equal halves. After the specimen is left to rest for few minutes, water penetration depth is marked with a board marker and the depth is measured by a ruler. Average depth is taken from four equidistant positions along the bottom of the specimen from where the pressurized water has been applied. Mass of absorbed water is calculated simply by subtracting initial mass from the final mass of the specimen. Figure 3.16 shows water permeability testing equipment, which is used to determine water penetration depth of concrete specimens.



Figure 3.16. Water permeability testing equipment.

3.4.4 Determination of Porosity by Mercury Intrusion Porosimetry

Determination of porosity of concrete samples is carried out using a mercury intrusion Porosimetry, as described in ASTM D4404-10 (2010). Under controlled pressure with progressive intrusion of mercury, the porosity of the concrete specimen is investigated. Mercury cannot penetrate through the pores of the concrete specimen by capillary action since the pressure required is inversely proportional to the diameter of the pore through which mercury must pass through. Therefore, external pressure is applied with respect to the diameter of the pores so that mercury can penetrate inside the pores of concrete specimen. Minimum pressure is applied to intrude mercury into larger pores present on the surface of concrete specimens. However, in case of smaller pores, high value of pressure is essential for proper intrusion of mercury into the pores of concrete specimen. The applied pressures versus mercury intrusion data is used to determine the pore volume and size distributions of concrete specimens.

3.4.5 Determination of Resistance to External Sulfate Attacks

Determination of resistance to external sulfate attacks on concrete samples is performed by measuring the volumetric change and compressive strength of concrete specimens. Sulfate solution is prepared using sodium sulfate (Na_2SO_4) in 1 liter of water, as reported in ASTM C1012/C1012M-15 (2015). Concrete specimens were water cured for 28 days before they were subjected to sulfate solution for further required specific testing time. Resistance to sulfate attack of concrete is assessed by

measuring the increase in expansion and loss in compressive strength. Expansion is measured using the length comparator as described in ASTM C490/C490M-17 (2017). Average length change is reported to nearest 0.01% in millimeters for each concrete specimen. The samples were dried before and after they were placed into the sulfate solution prior to length measurements. Therefore, initial mass and final mass measurements were also recorded. Mass loss can be recorded by subtracting the initial mass measurement from final mass measurement of each concrete specimen. Compressive strength test is also performed to examine the resistance of concrete specimens to external sulfate attack. Figure 3.17 shows the sulfate solution prepared for sulfate attack mechanism on concrete.



Figure 3.17. External sulfate attack curing condition.

3.4.6 Determination of Resistance to Freeze and Thaw Cycles

Resistance of concrete specimens to repeated freezing and thawing cycles is determined based on a standard procedure given in ASTM C666/C666M-15 (2015). The procedure involves a drastic temperature change within a closed chamber that allows to determine the resistance of concrete to freezing and thawing cycles for a specified period of time. In this experiment, freeze and thaw chamber with temperature and moisture control is used. The temperature control of the chamber is kept within the range from -30°C to 30°C along with the moisture control, which is kept in between the range from 75% to 85% moisture content. Standard cubic concrete samples are used for the determination of resistance to freezing and thawing cycles. Curing of the

concrete specimens is done for 28 days before placing them in the freeze and thaw chamber. After placing the concrete specimens inside the chamber, two continuous cycles of freezing and thawing are being set for each day for a required specific time. Dry mass measurements i.e. initial mass measurements are recorded prior to the placement of the specimens in the freeze and thaw chamber. After the required specific time is completed, specimens are taken off the freeze and thaw chamber and final mass measurements of the specimens are then recorded. Mass loss of the concrete specimens experienced during the freeze and thaw cycles are then calculated by subtracting initial mass from the final mass of specimen. The determination of the resistance to freeze and thaw cycles of concrete specimens is also performed by the compressive strength test. Compressive strength of concrete control sample, which is cured under water, is used for comparison. Hence, the resistance against rapidly freezing and thawing cycles is assessed by the compressive strength recorded for each concrete specimen. Freeze and thaw cabinet used for subjecting freeze and thaw cycles on concrete specimens is illustrated in Figure 3.18.



Figure 3.18. Freeze and thaw cabinet.

3.4.7 Scanning Electron Microscopy (SEM)

Scanning Electron Microscopy (SEM) is used to perform the microstructural analysis of the specimen. SEM is used to investigate the chemical and physical aspects of

cement hydration and setting. A thin layer of gold metal – platinum was sputtered onto the surface to reduce charging under electron beam. Hence, the development and ongoing process of cement hydration, pozzolanic reaction, as well as the influence of waste materials can be determined by microstructural analysis. Furthermore, SEM is also used to determine the composition and structure of concrete as well as the formation of microstructural cracks within the cementitious materials. During the image analysis, various magnifications are used to ensure significant microstructural characterization of cementitious materials. Furthermore, evaluation of concrete durability by influence of supplementary cementitious materials as a binding material and the effects of external influences such as resistance against freeze and thaw, external sulfate attacks and carbonation on the microstructure of cementitious materials can be investigated appropriately. (Nemati, 1997; Vlahovic, 2012). Scanning Electron Microscope is shown in Figure 3.19.



Figure 3.19. Scanning electron microscope.

3.4.8 X-Ray Florescence (XRF)

X-Ray florescence (XRF) spectrometry is used for the determination of an elemental and oxide composition of raw materials examined in this thesis. XRF works on the principle of the interaction of separated excited X-ray photons with atoms from an external source. X-ray photons emit an individual wavelength. Based on this principle, the desired elements are identified and determined in the specimen. Quantitative analysis of elements starting from sodium (Na) through uranium (U) can be done using XRF. For instance, in case of Portland cement, elements such as calcium, silica,

aluminum, iron are likely to be seen in major proportions. XRF apparatus can be seen in Figure 3.20.



Figure 3.20. XRF Apparatus.

3.4.9 Particle Size Distribution (PSD)

Malvern Mastersizer 2000 is used to determine the particle size distribution of the materials within the average particle size range from 1 to 300 μm equivalent spherical diameter. ASTM D4464-15 (2015) is followed as a standard procedure for determining particle size distribution using laser light scattering technique. Light scattering techniques are used; the angle and intensity of laser light scattered by the particles of the materials are selectively measured to determine the true grain size of the specimen. Laser beam is diffracted from the particles of the material present in an aqueous solution. Scattering information is analyzed the geometry of the particles of the specimen. The calculated particle sizes are presented in a graphical and tabular format in compliance with ASTM E11-17 (2017), where mesh provides a relative distribution of the particle sizes of the material.

CHAPTER 4

MECHANICAL PROPERTIES AND DURABILITY CHARACTERISTICS OF CONCRETE INCORPORATED WITH SILICA FUME AND MARBLE DUST

4.1 Introduction

This chapter discusses the mechanical properties and durability characteristics of concrete incorporated with silica fume and marble dust. To begin with, characterization of raw materials is discussed. Results associated with mechanical properties of concrete such as compressive strength are discussed to investigate the effect of incorporating silica fume and marble dust in concrete. In addition to that, results associated with durability characteristics of concrete such as water permeability, external sulfate attack, action to freeze and thaw and porosity measurements are then discussed to investigate the effect of incorporating silica fume and marble dust in concrete. Microstructural analysis carried out using Scanning Electron Microscope enlightened the microstructural developments as well as the physical and chemical reactions that take place in cementitious matrix incorporated with silica fume and marble dust.

4.2 Characterization of raw materials

Raw materials used in this section of thesis are Portland cement, silica fume, marble dust, fine aggregates and coarse aggregates. Elemental oxide composition of the raw materials, obtained from X-ray fluorescence spectroscopy, is illustrated in Table 4.1.

Table 4.1. Elemental oxide composition of Portland cement, silica fume, marble dust and fine aggregates determined by X-ray fluorescence spectroscopy.

Chemical composition	Portland cement (Wt. %)	Silica fume (Wt. %)	Marble dust (Wt. %)	Fine aggregates (Wt. %)
CaO	43.8	1.25	64.5	0.46
ZnO	0.01	0.02	0.01	-
SiO ₂	30.2	93.3	23.4	91.9
Al ₂ O ₃	11.4	0.73	43.2	3.91
Fe ₂ O ₃	5.11	1.82	2.83	0.65
SO ₃	3.29	0.22	0.47	0.04
MgO	2.61	0.89	1.73	0.14
K ₂ O	1.34	1.21	1.04	1.31
TiO ₂	0.74	-	0.48	0.83
Na ₂ O	0.51	0.28	0.79	0.49
MnO	0.43	0.09	0.07	0.04
Cl	0.03	0.04	0.07	0.01

All the major as well as minor compounds present in these raw materials are summarized in the Table 4.1 along with their weight expressed in percentage respectively. Elemental oxide composition of Portland cement shows cumulative content of CaO, SiO₂, Al₂O₃ and Fe₂O₃ to be 90%. Silica fume contains more than 90% of SiO₂ content and therefore, high pozzolanic activity can be observed during the pozzolanic reaction. Marble dust, described as a limestone powder in nature; more than 60% of CaO content is present in its elemental oxide composition. Hence, marble dust is suitable to be used as a filler replacement in this thesis. Fine aggregates, called quartz sand is used and the presence of high amounts of SiO₂ in the oxide composition is predictable.

In addition to the elemental oxide composition of these raw materials, particle size distribution analysis is also done, as shown in Figure 4.1.

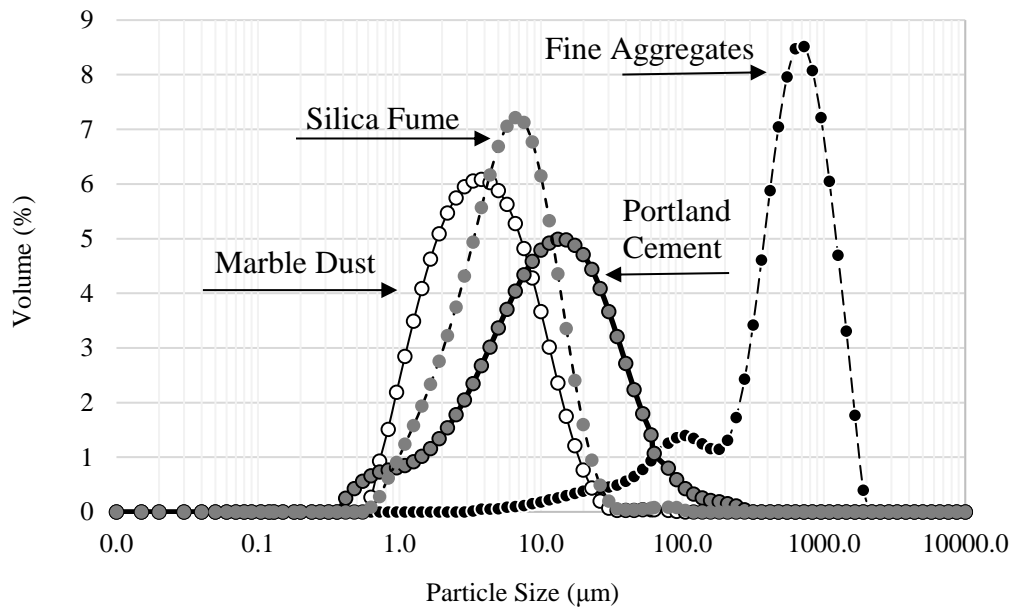


Figure 4.1. Particle size distribution of Portland cement, silica fume, marble dust and fine aggregates.

Figure 4.1 shows the particle size distribution of Portland cement, silica fume, marble dust and fine aggregates. Particle size of each material is expressed in microns. Comparison between particle size distributions of Portland cement with silica fume shows that silica fume particles have high fineness than Portland cement particles. The highest volume peak of silica fume particles is in the range of 1 to 10 microns, whereas for Portland cement, the range is in between 10 to 100 microns. Therefore, it must be emphasized that a coarser binding material i.e. Portland cement is partially replaced with a much finer particle size binding material i.e. silica fume in this section of the thesis.

Moreover, comparison between particle size distributions of fine aggregates with marble dust shows that marble dust particles show high degree of fineness. The highest volume peak of marble dust particles is in between 1 to 10 microns whereas fine aggregates are in between 100 and 1000 microns respectively. Therefore, it must be highlighted that a coarser filler material i.e. fine aggregates is partially replaced with a much finer particle size filler material i.e. marble dust in this section of the thesis.

4.3 Fresh properties

4.3.1 Water content

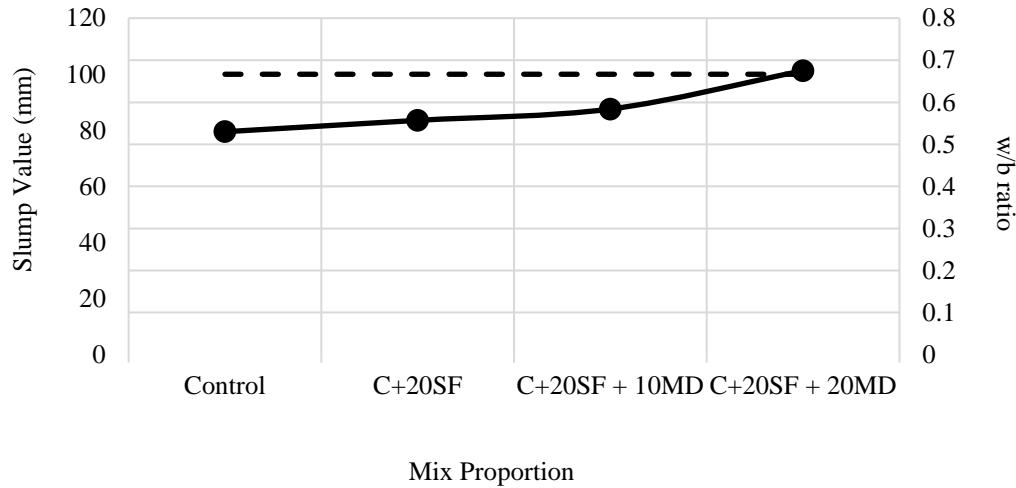


Figure 4.2. Slump (mm) and water/binder ratios for all the mix proportions of concrete incorporated with silica fume and marble dust. -----; slump values (mm), ●; water/binder ratio, plotted in a secondary axis.

Figure 4.2 shows that addition of 20% silica fume content as a partial binder replacement material to Portland cement resulted in an increase water/binder ratio from 0.54 to 0.557. Since, slump value of 100 mm is kept constant for all concrete combinations, 0.017 increase in water/binder ratio for 20% SF concrete specimen is necessary to achieve the same consistency of control concrete specimen. Furthermore, increase in the marble dust replacement levels resulted further increase in water/ binder ratio. For instance, w/b ratio of 20% SF + 10% MD and 20% SF + 20% MD were 0.584 and 0.675 respectively. When compared to the water/binder ratio of control concrete specimen, the addition of 10% and 20% marble dust content increase in w/b ratio of 0.044 and 0.135 is observed respectively. Such increase in the water demand of concrete by the addition of silica fume and marble dust is due to the fineness of these materials. Silica fume has high fineness in comparison with Portland cement whereas marble dust also has high fineness in comparison with fine aggregates. Since the density of concrete will increase by the addition of materials, which are finer than conventional concrete materials, the water/binder ratio is evident to increase to attain required consistency of 100 mm slump.

4.4 Mechanical properties

4.4.1 Compressive strength

Concrete specimens were prepared containing 20% silica fume as constant replacing Portland cement content. In addition to that, fine aggregates were replaced by marble dust with the replacement levels of 10 and 20 percent. Long-term compressive strength values of concrete specimens, all cured under normal curing conditions, are illustrated in Figure 4.3.

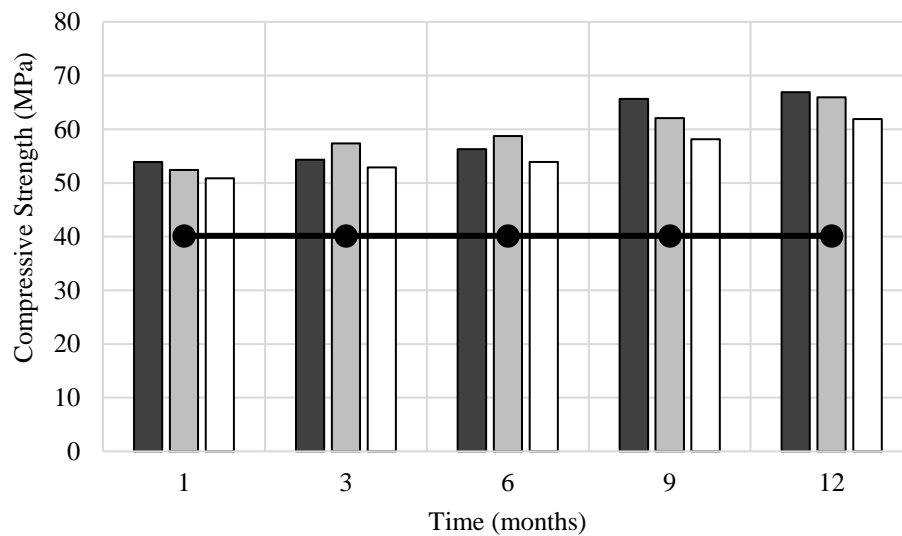


Figure 4.3. Compressive strength of silica fume – concrete incorporated with marble dust. ■; 20% SF, ▒; 20% SF with 10% MD, □; 20% SF with 20% MD, ●; concrete control at 28th days.

From Figure 4.3, results indicate an overall increase in compressive strength for all concrete mixes from 28 days to 1 year. For instance, concrete containing 20% SF had the compressive strength value of 53 MPa at 28 days, in comparison with control specimen, which had compressive strength of 40 MPa. Therefore, if 20% SF concrete specimen and control concrete specimen are compared, strength increase of 35% is already seen at 28 days. Furthermore, 20% SF concrete specimen shows 65% strength increase at 1 year in comparison with control concrete specimen at 28 days. Similarly, the compressive strength of 20% SF concrete specimen increased 25% at 1 year in comparison with 20% SF concrete specimen at 28 days. The major increase of compressive strength of 20% SF concrete specimen i.e. 17% increase in compressive strength can be seen in between 6 to 9 months. The overall increase in the 20% SF

concrete specimens from 28 days to 1 year, especially in between 6 to 9 months, is solely attributed to the pozzolanic activity of silica fume, which accelerates the formation of calcium-silicate-hydrate (C-S-H) gels in cementitious matrix. The formation of calcium-silicate-hydrate (C-S-H) gels is responsible from the development of strength of concrete. Since, pozzolanic reaction is slower than Portland cement hydration reaction, compressive strength values of 20% SF concrete specimen indicate that pozzolans such as silica fume require 6 to 9 months to attain its appreciable strength. Therefore, conducting a long-term study was vital to understand the actual influence of pozzolanic materials in concrete.

To further understand the influence of silica fume in concrete, microstructural images taken by scanning electron microscope, of concrete containing 100% Portland cement and 20% SF replacement specimens of 28 days and 1 year specimens are compared and analyzed. The microstructural images are illustrated from Figure 4.4 to Figure 4.7.

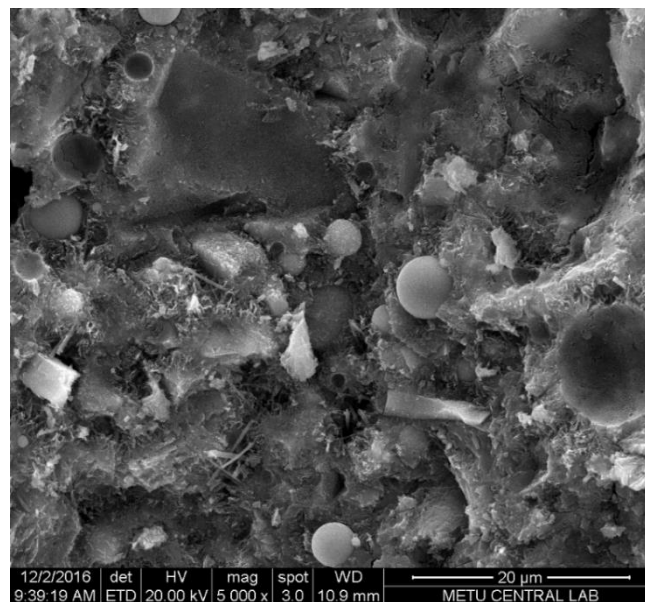


Figure 4.4. Concrete control at 28 days.

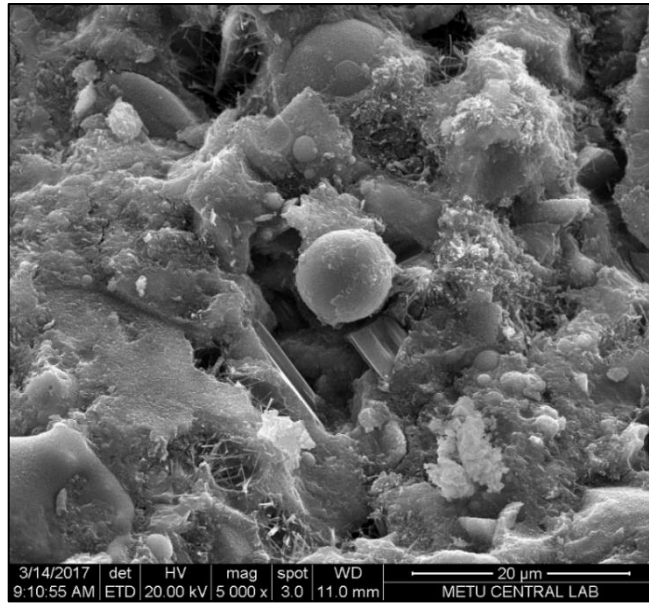


Figure 4.5. Concrete control at 1 year.

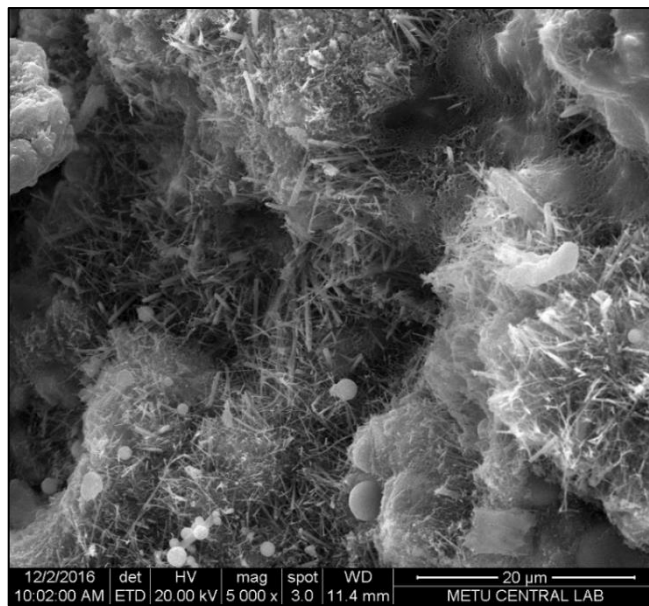


Figure 4.6. Concrete containing 20% SF at 28 days.

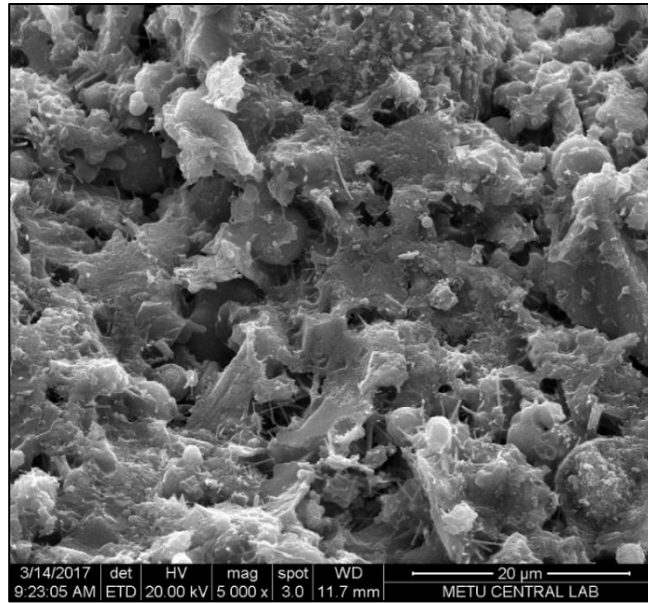


Figure 4.7. Concrete containing 20% SF at 1 year.

Figure 4.4 and Figure 4.5 show the microstructure of concrete containing 100% Portland cement. In Figure 4.4, the hexagonal crystalline structure represents the presence of CH compounds. The needle-like crystals represent the presence of C-S-H gels in Figure 4.4 and Figure 4.5. In addition to that, presence of clintonite can be seen under C-S-H gels in Figure 4.4, which shows the presence of gehlenite crystals (Al-rich formation). Hence, the evidence of hydration reaction at 28 days as well as at 1 year images can be seen due to the presence of C-S-H gels and CH compounds. However, after 1 year, denser microstructure can be seen due to the presence of evenly dispersed C-S-H gels.

Figure 4.6 and Figure 4.7 indicate the microstructure of concrete containing 20% SF as replacement material to Portland cement. In Figure 4.6, the image taken after 28 days clearly shows the presence of silicate compounds throughout the cementitious matrix. In Figure 4.6, solid round-shaped crystals surrounded by evenly dispersed C-S-H gels represents the presence of silica fume particles. Moreover, Figure 4.7 shows that after 1 year, the addition of silica fume increased the silica content in the cementitious matrix, hence, silicate compounds consume the CH compounds effectively, further contributing in the production of additional C-S-H gels. In addition to that, the microstructure of 20% SF concrete specimen is well consolidated. When compared to 1-year microstructural image of control concrete specimen, microstructure of 20% concrete specimen is denser. Though, it does resemble the

control concrete specimen microstructural image, however, due to production of further C-S-H gels by the availability of silica in cementitious matrix, the overall microstructure is more consolidated and denser compared to the microstructure of control concrete specimen.

Figure 4.3 also shows concrete specimens containing 20% SF replacement level of Portland cement with 10% and 20% marble dust replacement level of fine aggregates respectively. The results indicate a slight decrease in the compressive strength of concrete with increasing the replacement level of marble dust by 10% to 20% respectively, when compared to 20% SF concrete alone. However, 25% and 55% increase in compressive strength is seen at 28 days and at 1 year when compared to the compressive strength of control concrete specimen at 28 days. Therefore, such an increase in compressive strength of concrete by replacing 40% of the total content of concrete by supplementary cementitious materials and waste materials is remarkable for the sustainable use of concrete. Even though, the compressive strength of concrete containing marble dust is decreased when compared to concrete containing silica fume, it must be noted that compressive strength obtained at all combinations with marble dust are increasing with time. For instance, concrete incorporated with silica fume and marble dust has the compressive strength above 60 MPa at 1 year, which is viable for its use as structural concrete in construction industry. Concrete specimens of 20% SF with 10% MD and 20% MD also showed strength increase of 26% and 23% at 1 year respectively in comparison with the compressive strength of these combinations at 28 days. Hence, the compressive strengths of concrete containing silica fume and marble dust, at all the ages, do possess higher mechanical properties, in comparison with control concrete specimen. Hence, 40% replacement of concrete content by waste materials such as silica fume and marble dust not only reduces the burden on natural resources but also significantly enhances the compressive strength, making it viable to be used as structural concrete for the construction industry.

4.5 Durability

4.5.1 Water permeability

Permeability of concrete is regarded as a considerable measure to investigate durability of concrete and resistance against adverse external and internal conditions. In this

thesis, water penetration depth is used to assess the permeability of concrete specimens. Concrete specimens incorporated with 20% silica fume as constant replacement material to Portland cement content; 10% and 20% marble dust as a replacement material to fine aggregates are used to investigate the water penetration depth. Long-term water penetration depths of concrete specimens, along with mass of absorbed water during the experiment are illustrated in Figure 4.8.

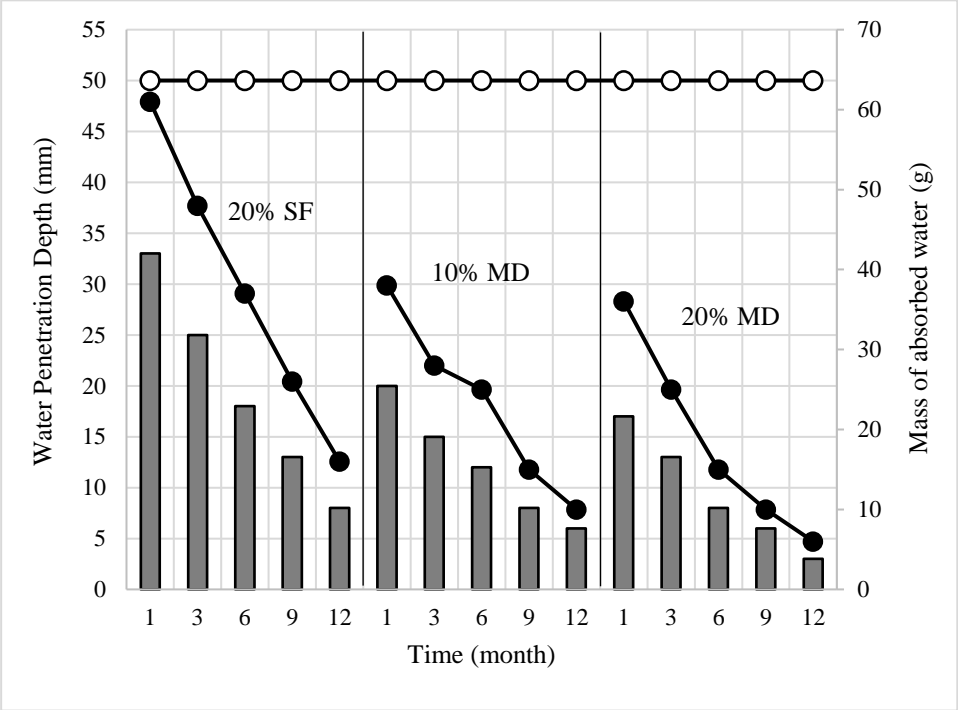


Figure 4.8. Water penetration depth of concrete incorporated with 20% SF and with 10 and 20% MD. ○; water penetration depth of concrete control specimen at 28th days, ●; Mass of absorbed water through the application of pressurized water during the experiment, plotted in a secondary axis.

The results shown in Figure 4.8 indicate an overall decrease of water penetration depth in all the combinations of concrete with time. For instance, water penetration depth of control concrete specimen is noted to be 50 mm at 28 days. In comparison to that, water penetration depths of 20% SF, 20% SF + 10% MD and 20% SF + 20% MD are 32 mm, 20 mm and 18 mm respectively. Therefore, it can be seen that the addition of silica fume as well as marble dust resulted in a decrease in water penetration depth, even at short-term durations. Furthermore, water permeability of 20% SF concrete specimen is decreased 73% from 28 days to 1 year respectively. As for concrete specimens containing 10% marble dust and 20% marble dust, water penetration depth is decreased 65% and 88% from 28 days to 1 year. Therefore, increase in the

replacement level of marble dust led to an even more substantial decrease in the water penetration depth of concrete. The reason for such decrease is due to the advancement of pozzolanic reaction in the cementitious matrix and the filler effect of marble dust. Pozzolanic reaction caused the CH compounds to react with silicate compounds, present by the addition of silica fume to produce additional C-S-H gels. Additional C-S-H gels reduced the availability of pores present in the cementitious matrix, thus, reducing the permeability of concrete. In addition to that, when coarser particles of fine aggregates are partially replaced with marble dust, decrease in free volume within the cementitious matrix takes place. Free volume present in the cementitious matrix occupied by the addition of marble dust drastically reduces the permeability of concrete. To further illustrate the role of addition of marble dust, microstructural images of concrete specimens containing 20% silica fume along with 20% marble dust are taken from scanning electron microscope at 28 days and 1 year respectively. The associated Figure 4.9 and Figure 4.10 are illustrated below.

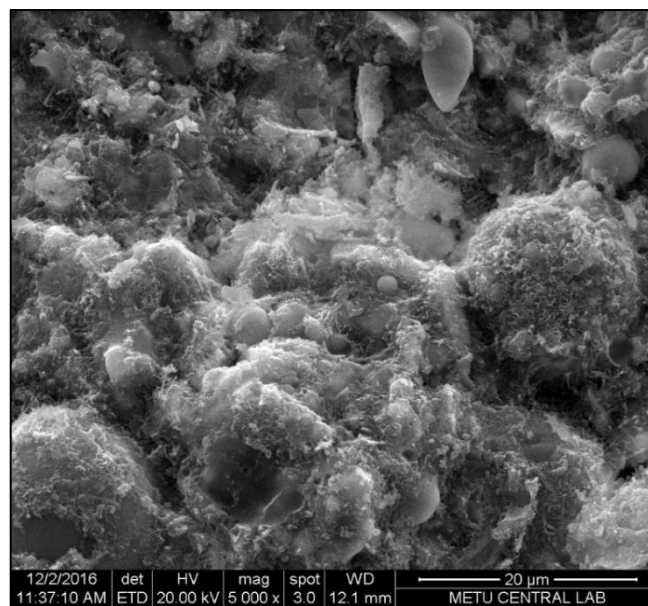


Figure 4.9. Concrete containing 20% SF + 20% MD at 28 days.

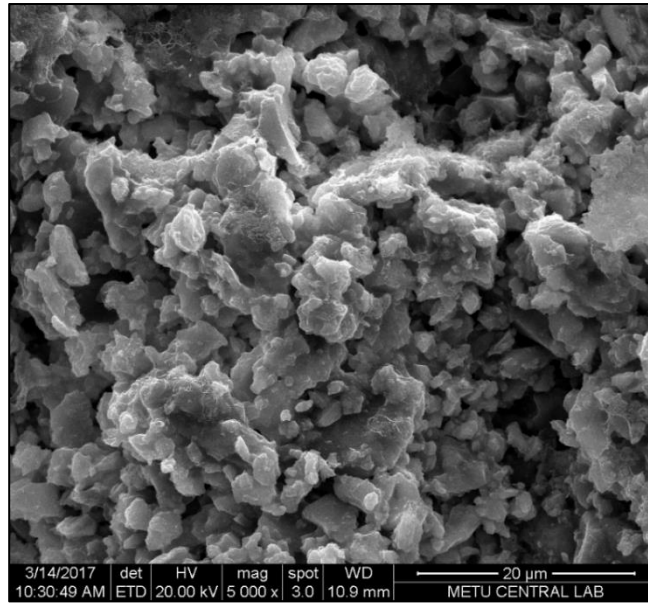


Figure 4.10. Concrete containing 20% SF + 20% MD at 1 year.

Figure 4.9 and Figure 4.10 show the microstructure of 20% SF + 20% MD at 28 days and at 1 year respectively. Excess fibrous formation can be observed in Figure 4.9 due to the presence of marble dust along with silica fume. Evenly dispersed particles all over the microstructure, as illustrated in Figure 4.9, proves that the addition of marble dust seems to provide an overall affect towards microstructural development.

In addition to that, when the microstructural images of 20% SF + 20% MD concrete specimens are compared to Figure 4.4 and Figure 4.5 i.e. control concrete specimens and Figures 4.6 and 4.7 i.e. 20% SF concrete specimens, it can be seen that a substantial decrease in capillary pore volume of the concrete is observed. For instance, Figure 4.9 illustrating the microstructural image of 20% SF and 20% MD concrete specimen at 28 days shows higher amount of finely divided silicate crystals on the surface of the specimen, due to the presence of silica fume in the cementitious matrix. In addition to that, filler effect induced by marble dust is clearly visible that decreases the free volume within the cementitious matrix. However, after 1 year, the microstructure of 20% SF + 20% MD, shown in Figure 4.10, is more consolidated and possesses more uniform structure consisting small particles which are closely bound together. Therefore, the continuous pores present in the cementitious matrix are reduced by the addition of silica fume and marble dust. Hence, the water permeability of concrete

incorporated with silica fume and marble dust is significantly minimized at long-term durations.

Moreover, the mass of absorbed water through the application of pressurized water during the experiment is also plotted on the secondary axis, as shown in Figure 4.8. The results show that concrete specimen containing 20% SF had a decrease in mass loss of water of approximately 70% from 28 days to 1 year. Similarly, mass of absorbed water of concrete specimens incorporated with 20% SF + 10% MD and 20% SF + 20% MD had decrease of approximately 73% and 81% from 28 days to 1 year respectively. Furthermore, at 28 days, the percentage difference between the mass of absorbed water is 40% only by the addition of 20% marble dust, when compared to 20% SF concrete specimen only. In addition to that, at long-term durations, the use of silica fume along with the incorporation of marble dust results in a systematic decrease in the mass of absorbed water during the experiment. Since, the permeability of concrete is reduced significantly by the addition of silica fume and marble dust, especially at long-term durations; therefore, it is evident that the systematic decrease in water penetration depth is supported with the systematic decrease in the mass of absorbed water.

4.5.2 External sulfate attack

Resistance against external sulfate attack of concrete incorporated with 20% silica fume as partial binder replacement of Portland cement along with 10% and 20% marble dust as partial filler replacement of fine aggregates is investigated. Prior to sulfate attack exposure, all the concrete specimens were cured under normal curing conditions for 28 days so that, all the concrete must attain substantial hydration of concrete. Long-term external sulfate attack measurements of concrete specimens are carried out based on compressive strength loss and expansion of concrete specimens as shown in Figure 4.11.

The results illustrated in Figure 4.11 indicate that compressive strength loss of concrete is decreased with the incorporation of both silica fume and marble dust. Compressive strength loss is expressed in percentage and can be defined as percentage loss in compressive strength compared to compressive strength of concrete cured under

normal curing conditions. Therefore, the compressive strength loss mentioned in this section is due to the action of external sulfate attack on concrete.

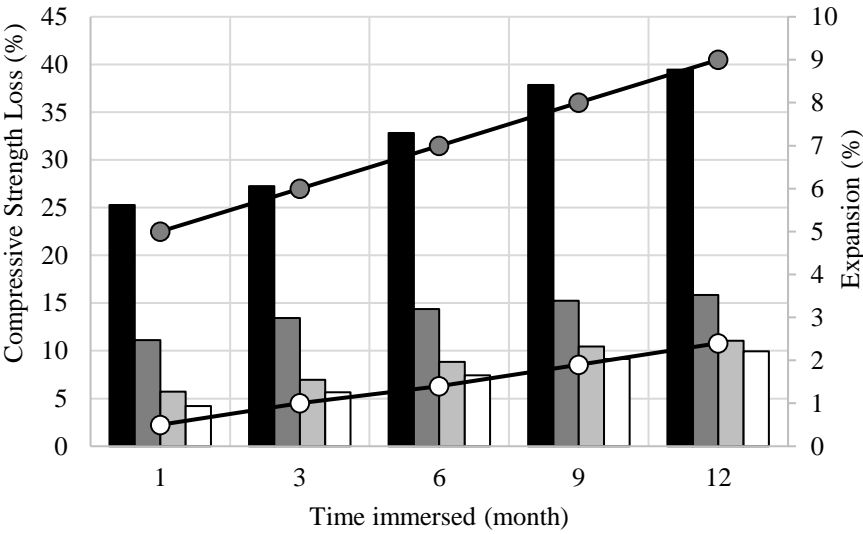


Figure 4.11. Compressive strength loss of concrete subjected to sulfate attack versus immersed time. ■; concrete control, ■; concrete with 20% SF, ■; concrete with 20% SF and 10% MD, □; concrete with 20% SF and 20% MD. Expansion of concrete subjected to sulfate attack is plotted in a secondary axis, ●; concrete control, ○; concrete incorporated with 20% SF and 20% MD.

For instance, at 28 days, control concrete specimen had an overall compressive strength loss of approximately 25% whereas 20% SF concrete specimen had only approximately 11% compressive strength loss. Similarly, 20% SF + 10% MD and 20% SF + 20% MD concrete specimens had an overall compressive strength loss of approximately 6% and 4% respectively. Similar trend can be seen at long-term durations, hence by increasing the replacement levels of marble dust with time resulted in a systematic decrease in the compressive strength loss of concrete. At 1 year, difference in the compressive strength loss among control concrete and 20% SF + 20% MD concrete specimens is almost 30%, which is considerably high. The addition of silica fume and marble dust, considerably, increased the resistance of concrete against external sulfate attacks. Since, CH compounds are used up effectively by the availability of silica compounds from silica fume, additional C-S-H gels were formed, which made the microstructure of pozzolanic concrete denser than the microstructure of control concrete. CH compounds are normally used as a reactant in the sulfate reaction, mentioned in Section 2.3.3 and 2.5.3 respectively. The development of external sulfate attack is mitigated by the addition of silica fume due to less available

CH compounds in the cementitious matrix. Moreover, marble dust, being finer material than fine aggregates, can increase the density of concrete by reducing the free volume present within the cementitious matrix of concrete. The permeability of concrete is reduced, hence, the ingress of sulfate ions into the cementitious matrix is mitigated significantly. Therefore, reduced compressive strength loss of concrete specimens containing silica fume and marble dust, in comparison with control concrete specimen, is evident.

Concrete specimens exposed to external sulfate attack are then subjected to the measurement of expansion, as shown previously in Figure 4.11 on the secondary axis. Expansion of control concrete and 20% SF + 20% MD concrete specimen is investigated for a period of 1 year. Expansion of control concrete is significantly higher, in comparison with 20% SF + 20% MD concrete. For instance, at 28 days, the expansion of control concrete specimen is measured to be approximately 5%, whereas for 20% SF + 20% MD concrete specimen, the expansion is only approximately 0.5%. Hence, even at 28 days, the difference of expansion is 4.5%, which is considerably high. Overall trend is increasing with time that shows that expansion of concrete is inevitable; however, the difference among the expansion values is significant. Moreover, the difference in expansion among control concrete and 20% SF + 20% MD concrete specimens increases from 4.5% to 7% at 1 year. Hence, control concrete specimen subjected to external sulfate attack exhibited much higher expansion in comparison with 20% SF + 20% MD concrete specimen.

The reason of higher expansion in control concrete specimen is due to the formation of ettringite and gypsum by the action of sulfate attack in the cementitious matrix. As mentioned previously in Section 2.2.4, when excess gypsum reacts with water in the presence of C_3A within the hydration reaction of Portland cement, ettringite is produced. Formation of ettringite and gypsum cause volume increase, thus expansion and subsequent cracking of concrete is inevitable. Tian and Cohen (2000) reported that the phenomenon of formation of ettringite and gypsum during sulfate attack results in volume expansion that may further cause subsequent cracking. In case of 20% SF + 20% MD concrete specimen, the increase in expansion of concrete was only 2% from 28 days to 1 year respectively. Compared with control concrete specimen, the addition of silica fume and marble dust reduced the expansion of concrete by 74% at 1 year.

Thus, concrete containing silica fume and marble dust showed appropriate resistance to the action of external sulfate attack since reduced volume expansion is observed during the experiment.

To further investigate the influence of silica fume and marble dust under the exposure of external sulfate attack in concrete, microstructural images of these concrete combinations are taken by scanning electron microscopy. Concrete specimens containing 100% Portland cement, 20% SF replacement and 20% SF + 20% MD replacement at 28 days and 1 year are compared and analyzed. The microstructural images are illustrated from Figure 4.12 to Figure 4.17.

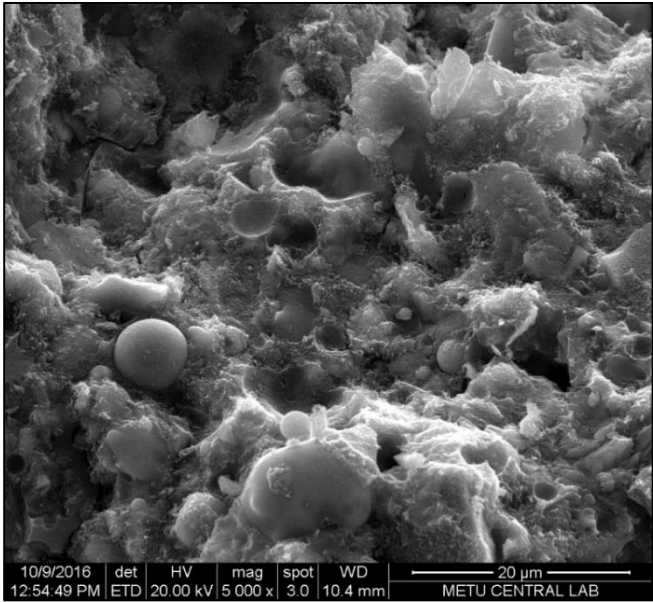


Figure 4.12. Concrete control under sulfate attack at 28 days.

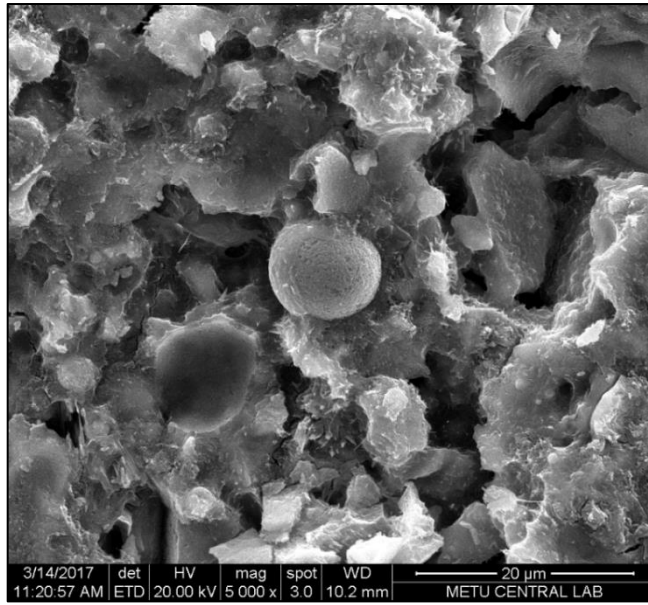


Figure 4.13. Concrete control under sulfate attack at 1 year.

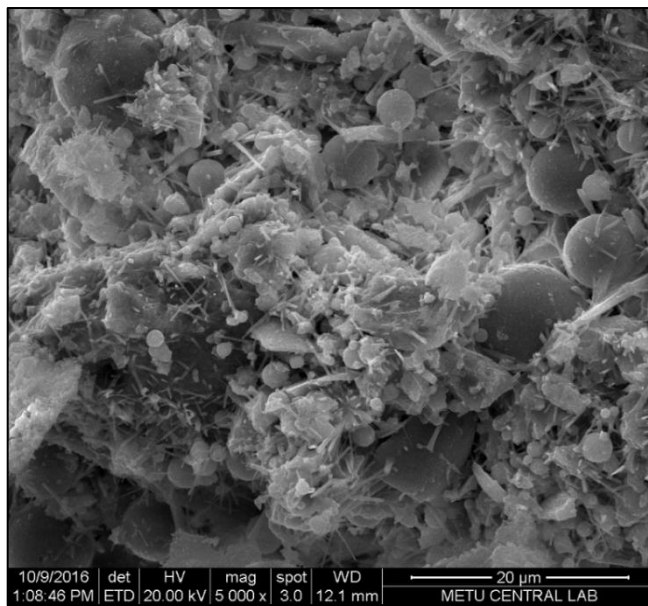


Figure 4.14. Concrete containing 20% SF under sulfate attack at 28 days.

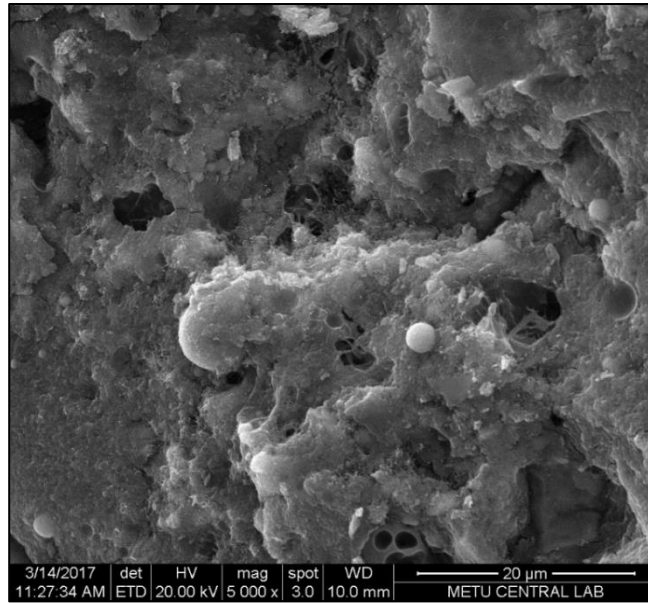


Figure 4.15. Concrete containing 20% SF under sulfate attack at 1 year.

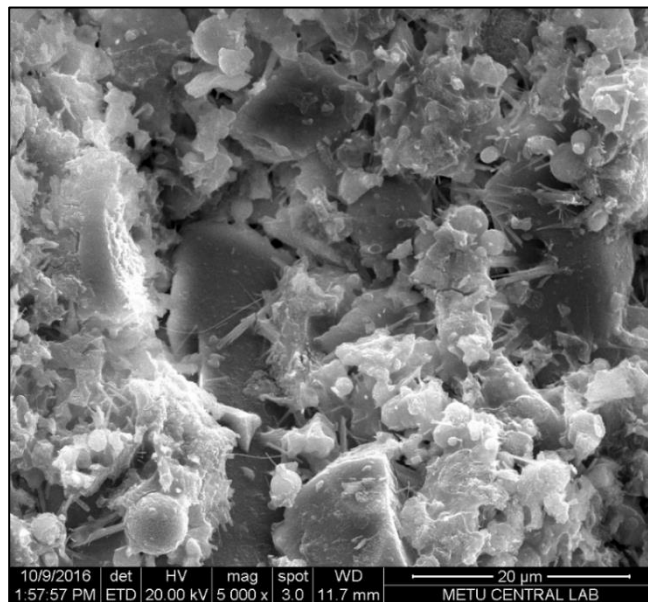


Figure 4.16. Concrete containing 20% SF + 20% MD under sulfate attack at 28 days.

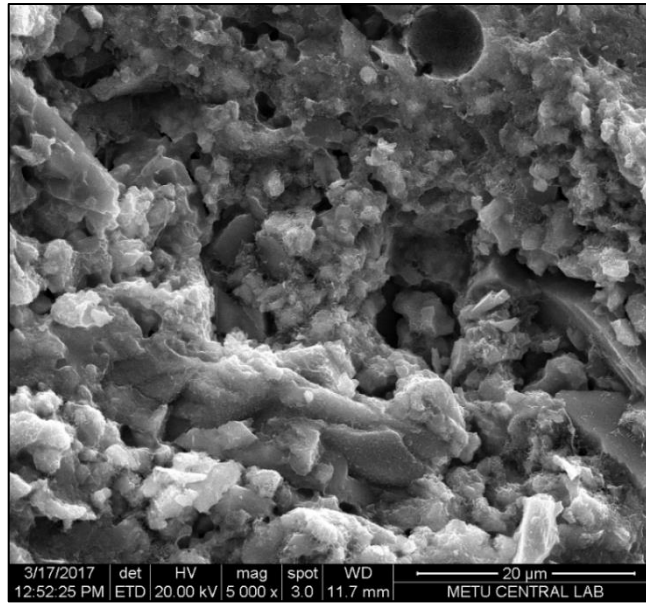


Figure 4.17. Concrete containing 20% SF + 20% MD under sulfate attack at 1 year.

Figure 4.12 and Figure 4.13 show the microstructures of 100% Portland cement concrete exposed to external sulfate attack for 28 days and 1 year respectively. CH compounds, formed in the cementitious matrix have reacted the sulfates, hence the formation of ettringite around C-S-H gels is evident within the microstructure at 28 days. Presence of gehlenite crystals can be seen in Figure 4.12. However, after 1 year, the microstructure of control concrete specimen is fairly consolidated, however the abundant presence for ettringite causes volume expansion resulting internal cracking of concrete. Hence, the compressive strength loss is evident as well as higher expansion of concrete. The results shown in Figure 4.11 for control concrete specimen are coherent with its microstructure, thus highlighting the reasons of compressive strength loss as well as increased volume expansion.

In addition to that, Figure 4.14 and Figure 4.15 show the microstructure of 20% SF concrete specimens exposed to external sulfate attack for 28 days and 1 year respectively. Compared to control concrete specimen, it can be seen that large quantities of silicate compounds are present in the cementitious matrix at 28 days. Thus, these silicate compounds have reacted with CH compounds to further produce additional C-S-H gels. Hence, CH compounds are much less available for the reaction with the sulfate ions, since the reaction takes place between silicate compounds and CH compounds. Microstructurally, amount of C-S-H gels present in cementitious matrix is the key parameter to assess the strength of concrete. Therefore, by the

production of additional C-S-H gels in the cementitious matrix, the compressive strength loss is fairly reduced, even at 28 days in comparison with control concrete specimen. However, at 1 year, silicate compounds are less visible as well as CH compounds. The microstructure is well consolidated and silicate compounds are completely surrounded by C-S-H gels. Thus, the loss of compressive strength is minimized by the presence of additional C-S-H gels available in the cementitious matrix of 20% SF concrete specimen.

Moreover, Figure 4.16 and Figure 4.17 show the microstructure for 20% SF + 20% MD concrete specimens exposed to external sulfate attack for 28 days and 1 year respectively. Presence of gehlenite crystals can be observed in Figure 4.16 however, it is partially modified due to the presence of silica fume and marble dust particles. Compared to the control and 20% SF concrete specimens at 28 days, it can be seen that marble dust particles are surrounded by the C-S-H gels. The presence of both, marble dust particles and silicate compounds significantly consolidated the cementitious matrix. Furthermore, silicate compounds are less visible as well as the CH compounds in the cementitious matrix at long-term duration. The absence of gehlenite crystals also provides an evidence of reduced expansion at 1-year. Hence, more compact and consolidated microstructure is observed at 1-year concrete specimen. Thus, further reduction of compressive strength loss and expansion of concrete in comparison with 20% SF concrete specimen is done not only by the presence of additional C-S-H gels but also filler effect of marble dust particles induced in the 20% SF + 20% MD concrete specimen respectively.

4.5.3 Freeze and thaw resistance

Resistance against freeze and thaw of concrete incorporated with 20% silica fume as partial binder replacement to Portland cement along with 10% and 20% marble dust as partial filler replacement to fine aggregates is investigated. Prior to freeze and thaw exposure, all the concrete specimens were cured under normal curing conditions for 28 days so that, all the concrete must attain substantial hydration of concrete. Long-term freezing and thawing measurements of concrete specimens are carried out based on compressive strength loss and mass loss of concrete specimens, as illustrated in Figure 4.18.

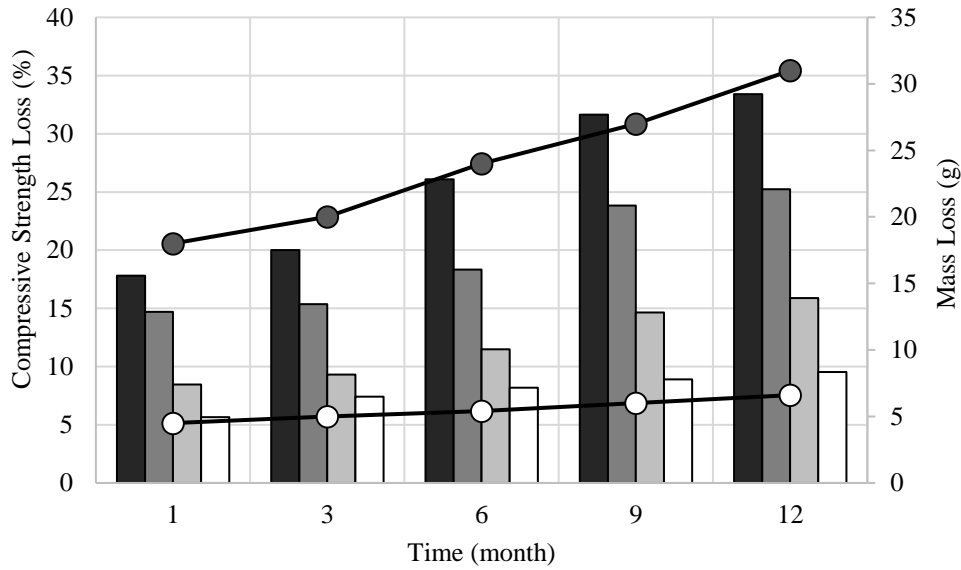


Figure 4.18. Compressive strength loss of concrete subjected to freeze and thaw versus time. ■; concrete control, ■; concrete with 20% SF, ■; concrete with 20% SF and 10% MD, □; concrete with 20% SF and 20% MD. Mass loss of concrete subjected to freeze and thaw is plotted on in secondary axis, ●; concrete control, ○; concrete incorporated with 20% SF and 20% MD.

The results illustrated in Figure 4.18 indicate that the presence of silica fume and marble dust resulted decrease in compressive strength loss of concrete. Hence, the resistance to freeze and thaw is increased significantly by the presence of silica fume and increasing percentage replacement of marble dust. For instance, at 28 days, control concrete specimen had an overall compressive strength loss of 18% whereas 20% SF concrete specimen had only 15% compressive strength loss. Similarly, 20% SF + 10% MD and 20% SF + 20% MD concrete specimens had an overall compressive strength loss of 8% and 5% respectively, when compared to compressive strength loss of control concrete specimen. Similar trend can be seen at long-term durations, hence by increasing the replacement levels of marble dust with time resulted in a systematic decrease in the compressive strength loss of concrete. At 1 year, the compressive strength loss difference among control concrete and 20% SF + 20% MD concrete specimens is almost 24%, which is considerably high. The addition of silica fume and marble dust, considerably, increased the resistance of concrete against freeze and thaw cycles.

Mass loss of concrete due to the exposure of freeze and thaw cycles is also determined as it is associated with the compressive strength loss of concrete. As the number of

freeze and thaw cycles are increasing, the subsequent hydraulic pressure in the cementitious matrix system is increasing. Hence, progressive development of micro-cracks result in greater mass loss of concrete specimen, which further results in compressive strength loss of concrete. For instance, at 28 days, the difference in mass loss between control concrete specimen and 20% SF + 20% MD concrete specimen is 75%, which is considerably high. Overall trend is increasing with time, which shows that increase in mass loss as the number of freeze, and thaw cycles are increasing. However, the difference among the mass loss of control concrete and 20% SF + 20% MD concrete specimens is significant. The mass loss of control concrete specimen increased 41% from 28 days to 1 year, whereas for 20% SF + 20% MD concrete specimen, the mass loss increased 31% from 28 days to 1 year. It must be noted that there is a rapid increase of mass loss in control concrete specimen compared to 20% SF + 20% MD concrete specimen. Hence, control concrete specimen subjected to freezing and thawing exhibited much higher mass loss since the hydraulic pressure caused by the freeze and thaw cycles was higher which caused increased development of micro-cracking in comparison with 20% SF + 20% MD concrete specimen.

The values of mass loss of these concrete specimens are in good agreement with the compressive strength loss as well. The density of concrete incorporated with silica fume and marble dust has been increased which reduced the availability of pores. Hence, concrete containing silica fume and marble dust became less permeable. Increase in the mass loss was attributed to the increase in the hydraulic pressure and hence subsequent cracking that results increase in loss of compressive strength. Similarly, higher compressive strength loss in control concrete specimen is due to the presence of additional cracks, which caused the mass loss during the action of freeze and thaw. However, concrete containing silica fume and marble dust had less compressive strength loss, hence, less cracks are developed that caused reduction in mass loss under the action of freeze and thaw. Therefore, it is evident that compressive strength loss and mass loss of concrete under the action of freeze and thaw are coherent with each other. Thus, the addition of silica fume and marble dust in concrete enhanced the resistance to withstand compressive strength loss as well as micro cracking caused by the action of freeze and thaw.

To further investigate the influence of silica fume and marble dust under the action of freeze and thaw in concrete, microstructural images of these concrete combinations are taken by scanning electron microscope. Concrete specimens containing 100% Portland cement, 20% SF replacement and 20% SF + 20% MD replacement at 28 days and 1 year are compared and analyzed. The microstructural images are illustrated from Figure 4.19 to Figure 4.24.

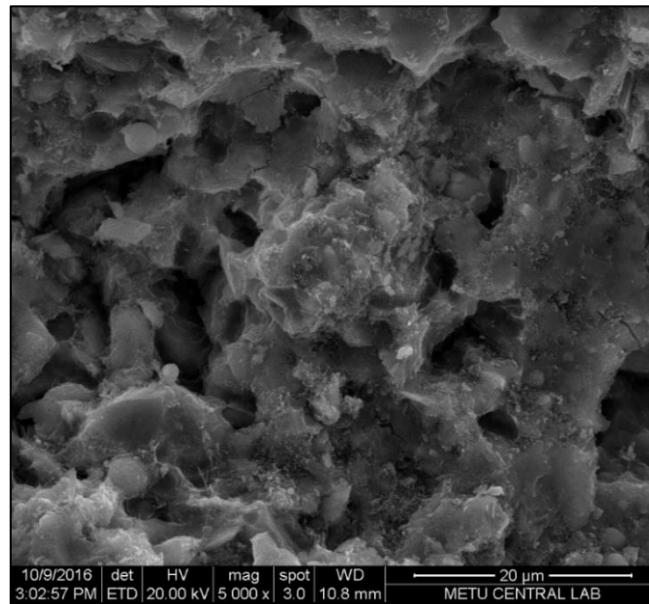


Figure 4.19. Concrete control under freeze and thaw at 28 days.

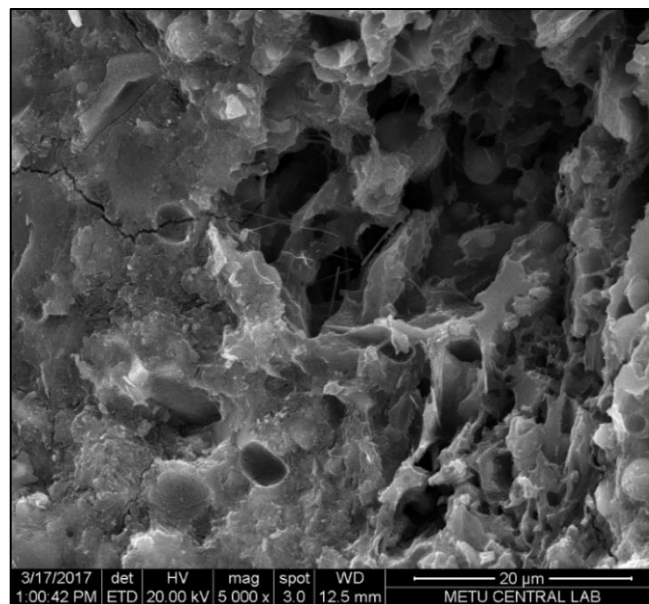


Figure 4.20. Concrete control under freeze and thaw at 1 year.

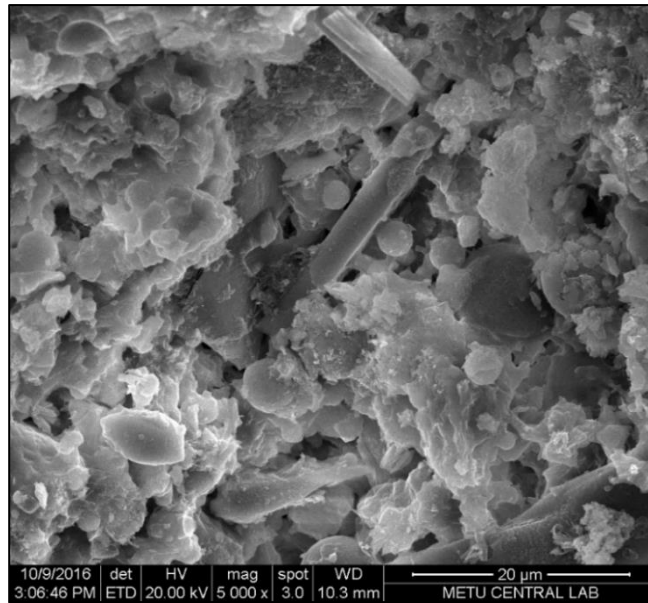


Figure 4.21. Concrete containing 20% SF under freeze and thaw at 28 days.

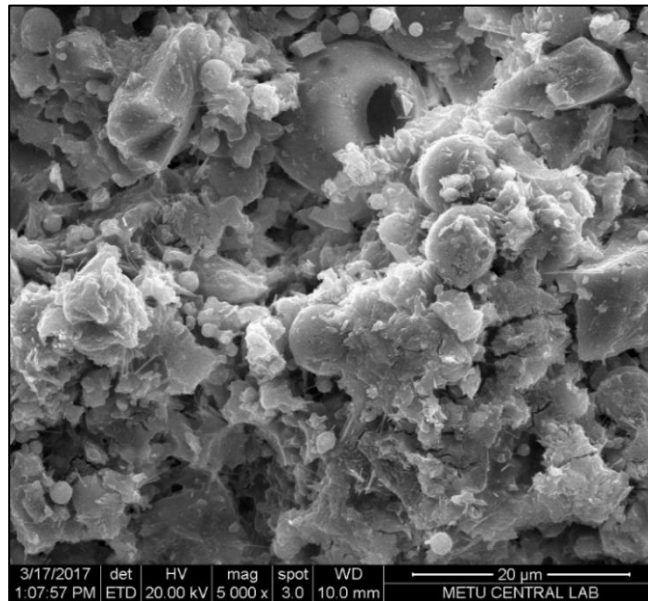


Figure 4.22. Concrete containing 20% SF under freeze and thaw at 1 year.

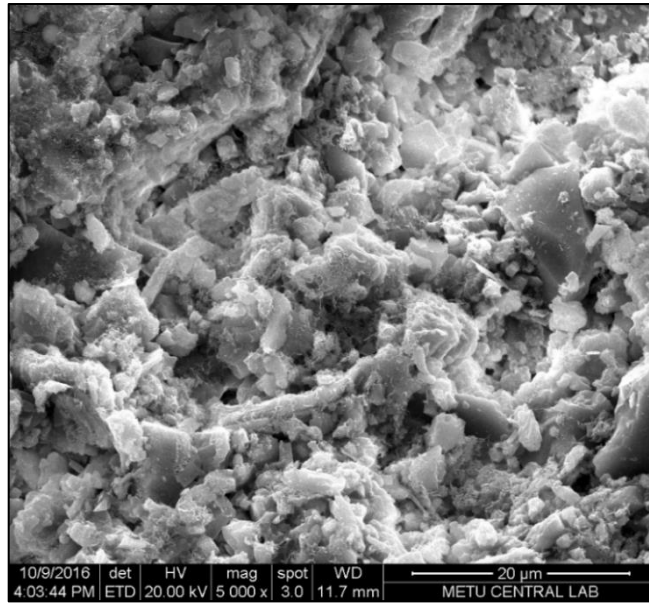


Figure 4.23. Concrete containing 20% SF + 20% MD under freeze and thaw at 28 days.

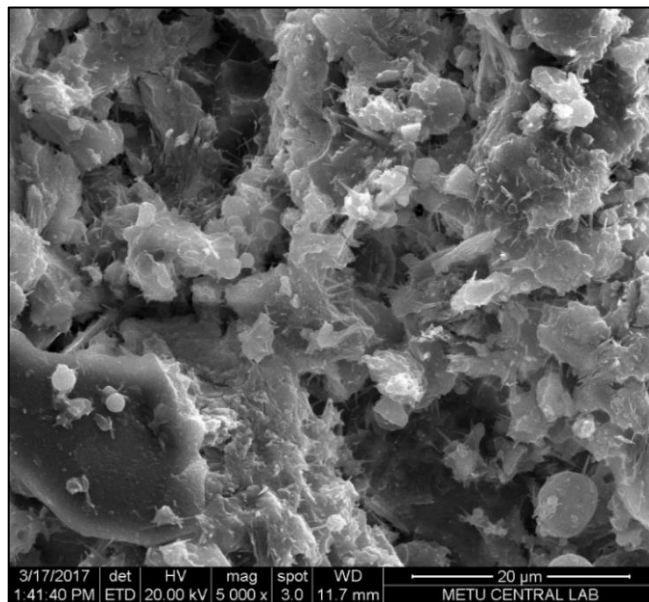


Figure 4.24. Concrete containing 20% SF + 20% MD freeze and thaw attack at 1 year.

Figure 4.19 and Figure 4.20 show the microstructures of 100% Portland cement concrete under the action of freeze and thaw for 28 days and 1 year respectively. Development of cracks is evident in the microstructure of control concrete specimen being under the action of freeze and thaw for long-term duration. It can be seen in Figure 4.20 that a crack has been propagated in the roughly horizontal direction on the top left hand side of the microstructural image. Since, the action of freeze and thaw is repeatedly continued, volume of water present in the pores of cementitious matrix tends to expand and hence, development of cracks is apparent. Hence, the results

shown in Figure 4.18 are coherent with the microstructures of control concrete specimens at 28 days and 1 year under the action of freeze and thaw. Mass loss, resulted by cracking of concrete, which further increased compressive strength loss, is evident from the microstructure. Furthermore, the permeability of control concrete specimen can influence the resistance to freeze and thaw. Water penetration depth of control concrete specimen at short as well as long-term durations, as shown in Figure 4.8, shows that control concrete specimen has high water penetration depth in comparison with other concrete combinations. Therefore, more water can imbibe in wet conditions under the action of freeze and thaw, which caused greater mass loss and resulted in more compressive strength loss of control concrete specimen.

In addition to that, Figure 4.21 and Figure 4.22 show the microstructure of 20% SF concrete specimens under the action of freeze and thaw for 28 days and 1 year respectively. Compared with control concrete specimen, it can be seen that less cracks are present in the microstructure. Reduced development of cracks might be due to the presence of silicate compounds, which have reacted with CH compounds to further produce additional C-S-H gels. Similar observations can be seen in Figure 4.23 and Figure 4.24 that show the microstructure for 20% SF + 20% MD concrete specimens under the action of freeze and thaw for 28 days and 1 year respectively. It can be seen that marble dust particles are surrounded by the C-S-H gels. Therefore, addition of silica fume increased the resistance against freeze and thaw action of concrete that mainly attributed to the formation of additional C-S-H gels as the result of the pozzolanic reaction among silica and CH compounds. Further addition of marble dust in concrete that is already incorporated with silica fume caused significant reduction of pores present in the cementitious matrix. The hydraulic pressure that results in micro-cracking are reduced by the addition of silica fume and marble dust as number of pores and the size of pores are decreased in the cementitious matrix. In addition to that, significant reduction of pores is also associated with the permeability of these concrete specimens. As shown in Figure 4.8, water penetration depth of concrete incorporated with silica fume and marble dust is considerably lower in comparison with control concrete. Therefore, less water can imbibe in wet conditions under the action of freeze and thaw, which caused lower mass loss and resulted in less compressive strength loss of control concrete specimen.

4.5.4 Porosity

Porosity measurements of concrete are done to investigate the effects of using silica fume and marble dust as partial replacement materials of Portland cement and fine aggregates under various cure conditions. Control concrete, 20% SF, 20% SF + 10% MD and 20% SF + 20% MD concrete specimens cured under normal curing conditions are investigated for porosity measurement after 1 year. Porosity in percentage values as well as pore volume in cm^3 is reported in Table 4.2.

Table 4.2. Porosity measurements of concrete incorporated with silica fume and marble dust under normal curing conditions.

Concrete combinations	Cure condition	Porosity (%)	Pore volume (cm^3)
Cement	Water Cured	39.2	0.2814
Cement + 20% SF	Water Cured	30.8	0.2207
Cement + 20% SF + 10% MD	Water Cured	28.4	0.2123
Cement + 20% SF + 20% MD	Water Cured	25.3	0.1659

Table 4.2 summarizes the porosity and pore volume of concrete specimens incorporated with silica fume and marble dust under normal curing condition. It can be seen that addition of silica fume resulted in a significant decrease in both the porosity and pore volume at long-term duration i.e. 1 year respectively. For instance, control concrete specimen, cured under normal curing condition has the porosity and pore volume of 39.2% and 0.2814 cm^3 , whereas 20% SF concrete specimen has the porosity and pore volume of 30.8 % and 0.2207 cm^3 respectively. Since, silica fume is a pozzolanic binding material and possesses higher fineness in comparison with Portland cement, silica particles reacted with CH compound present in the cementitious matrix, producing additional C-S-H gels. More consolidated and uniform cementitious matrix has been made; hence, the pores are significantly reduced. Thus, 9% decrease in porosity and 22% decrease in pore volume by the addition of 20% silica fume is evident in long-term durations.

Moreover, addition of silica fume along with an increase in the replacement level of marble dust resulted in further decrease in both the porosity and pore volume at long-

duration for the concrete specimens cured under normal curing conditions respectively. For instance, compared with 20% SF concrete specimen, by the addition of 10% and 20% marble dust, further 2% and 5% decrease in porosity is observed. Pore volume also decreased from 0.2207 cm³ to 0.2123 cm³ and 0.1659 cm³ by partially replacing fine aggregates with 10% and 20% marble dust content respectively. Compared to control concrete specimen, by the addition of 20% silica fume content and 20% marble dust content, 14% decrease in porosity as well as 41% decrease in pore volume is observed. The addition of marble dust decreased the free volume of pores present within the cementitious matrix, which made the microstructure well consolidated and uniformly distributed as shown previously in Figure 4.10. The pores present in the cementitious matrix were reduced by the addition of silica fume. Further reduction of pores was done by the addition of marble dust. Therefore, the porosity and pore volume decreased considerably at long-term durations.

Similarly, control concrete, 20% SF, and 20% SF + 20% MD concrete specimens cured under sulfate solution are investigated for porosity measurement after 1 year. Porosity in percentage values as well as pore volume in cm³ is reported in Table 4.3.

Table 4.3. Porosity measurements of concrete incorporated with silica fume and marble dust under sulfate solution.

Concrete combinations	Cure condition	Porosity (%)	Pore volume (cm³)
Cement	Sulfate solution	47.1	0.4365
Cement + 20% SF	Sulfate solution	34.5	0.2571
Cement + 20% SF + 20% MD	Sulfate solution	28.7	0.2145

Table 4.3 summarizes the porosity and pore volume of concrete specimens incorporated with silica fume and marble dust under sulfate solution. In comparison with the concrete under normal curing conditions, irrespective of concrete combinations, the porosity and pore volume of concrete increased substantially under sulfate solution. Sulfate ions, present in the sulfate solution, will react with C₃A and gypsum present in the cementitious matrix to produce ettringite that will cause volume expansion. Hence, porosity and pore volume is evident to increase. However, addition

of silica fume resulted in a significant decrease in both the porosity and pore volume cured under sulfate solution at long-term duration. For instance, control concrete specimen, cured under sulfate solution has the porosity and pore volume of 47.1% and 0.4365 cm^3 , whereas 20% SF concrete specimen has the porosity and pore volume of 34.5% and 0.2571 cm^3 respectively.

Silicate compounds are present in the cementitious matrix by the addition of silica fume. Silicate compounds reacted with CH compounds present in the cementitious matrix, producing additional C-S-H gels. Due to this reaction, the CH compounds are less available to react with the sulfate ions present in the sulfate solution. The expansion of concrete is reduced due to the production of additional C-S-H gels, hence more consolidated and uniform cementitious matrix has been made, as seen in Figure 4.15. Hence, the capillary pores are significantly reduced in the cementitious matrix of 20% SF concrete specimen. Thus, 13% decrease in porosity and 41% decrease in pore volume by the addition of 20% silica fume is evident in long-term durations.

Moreover, addition of silica fume along with an increase in the replacement level of marble dust resulted in further decrease in both the porosity and pore volume at long-duration for the concrete specimens cured under sulfate solution respectively. For instance, by the addition of 20% marble dust, further 6% decrease in porosity is seen, in comparison with 20% SF concrete specimen. Pore volume also decreased from 0.2571 cm^3 to 0.2145 cm^3 , only by partially replacing fine aggregates with 20% marble dust content. In comparison with control concrete specimen, by the addition of 20% silica fume content and 20% marble dust content, 18% decrease in porosity as well as 51% decrease in pore volume is observed. Marble dust, being finer filler material in comparison with fine aggregates, increased the density of concrete by filling the pores present within the cementitious matrix of concrete. It also reduces the permeability of concrete. Hence, the microstructure of 20% SF + 20% MD is well consolidated and uniformly distributed at long-term duration, as shown previously in Figure 4.17. To summarize, additional C-S-H gel production caused by the addition of silica fume resulted a uniform microstructure. Hence, the pores present in the cementitious matrix were reduced. In addition to that, further reduction of pores was done by the addition of marble dust, which made the microstructure denser and well consolidated. Therefore, the porosity and pore volume of concrete incorporated with silica fume and

marble dust, even under sulfate solution, decreased considerably at long-term durations.

Moreover, control concrete, 20% SF, and 20% SF + 20% MD concrete specimens under the action of freeze and thaw are investigated for porosity measurement after 1 year. Porosity in percentage values as well as pore volume in cm^3 is reported in Table 4.4.

Table 4.4. Porosity measurements of concrete incorporated with silica fume and marble dust under action of freeze and thaw.

Concrete combinations	Cure Condition	Porosity (%)	Pore Volume (cm^3)
Cement	Freeze and thaw	49.3	0.4584
Cement + 20% SF	Freeze and thaw	36.6	0.2612
Cement + 20% SF + 20% MD	Freeze and thaw	30.4	0.2194

Table 4.4 summarizes the porosity and pore volume of concrete specimens incorporated with silica fume and marble dust under action of freeze and thaw respectively. In comparison with the concrete under normal curing conditions, irrespective of concrete combinations, the porosity and pore volume of concrete increased substantially under action of freeze and thaw. Moreover, addition of silica fume resulted in a significant decrease in both the porosity and pore volume cured under action of freeze and thaw at long-term duration. For instance, control concrete specimen under the action of freeze and thaw has the porosity and pore volume of 49.3% and 0.4584 cm^3 , whereas 20% SF concrete specimen has the porosity and pore volume of 36.6 % and 0.2612 cm^3 respectively. Hence, 13% decrease in porosity and 43% decrease in pore volume by the addition of 20% silica fume is evident in long-term durations.

Moreover, addition of silica fume along with an increase in the replacement level of marble dust resulted in further decrease in both the porosity and pore volume at long-duration for the concrete specimens under action of freeze and thaw respectively. For instance, by the addition of 20% marble dust, further 6% decrease in porosity is observed, compared to 20% SF concrete specimen. Pore volume also decreased from 0.2612 cm^3 to 0.2194 cm^3 , only by partially replacing fine aggregates with 20% marble

dust content. In comparison with control concrete specimen, by the addition of 20% silica fume content and 20% marble dust content, 19% decrease in porosity as well as 52% decrease in pore volume is observed.

Subsequent hydraulic pressure in the cementitious matrix system increases by the repeatedly freezing and thawing cycles which results in progressive development of micro-cracks in concrete. Incorporation of silica fume and marble dust resulted in reduction of number of pores and size of pores present in the cementitious matrix. Thus, increase in the density in cementitious matrix made concrete less permeable.

Microstructurally, it can be seen in Figure 4.22 and Figure 4.24 that silicate compounds are present in the cementitious matrix. Hence, silicate compounds reacted with CH compounds to further produce additional C-S-H gels, which significantly makes the microstructure well consolidated and uniform. Moreover, marble dust particles are also surrounded by the C-S-H gels. Thus, addition of marble dust in concrete incorporated with silica fume resulted significant reduction of pores present in the cementitious matrix. As significant reduction of pores is coherent with the water penetration depth of concrete, water penetration depth of concrete incorporated with silica fume and marble dust is significantly low. Limited amount of water can imbibe in wet conditions under the action of freeze and thaw, in comparison with control concrete specimen. Therefore, the porosity and pore volume of concrete incorporated with silica fume and marble dust, even under action of freeze and thaw, decreased considerably at long-term durations.

4.6 Conclusions

In this chapter, the effect of marble dust used as a replacement material to fine aggregate on the long-term mechanical properties and durability characteristics of concrete incorporated with fixed proportion of silica fume is investigated.

The results reported in this chapter indicate that an increase in the replacement level of marble dust with the fixed proportion of silica fume resulted in a slight decrease in compressive strength of concrete, when compared to concrete incorporated with silica fume only. However, the strength values of the pozzolanic concrete obtained at all

volume fractions of marble dust were increasing with time and were higher compared to the control concrete specimen at all times.

Furthermore, the use of silica fume and marble dust resulted in a significant decrease in the water penetration depth and porosity of the concrete. Based on the microstructural investigations, significant reduction in the volume of the capillary pores of concrete incorporated with silica fume and marble dust is observed. The increase in the replacement level of marble dust resulted in further substantial reduction in the water penetration depth and porosity of the concrete due to the filler effect of marble dust that led to a decrease in free volume of the cement matrix.

In addition to that, the resistance to external sulfate attack and action of freeze and thaw of concrete incorporating silica fume and marble dust are examined by measuring compressive strength loss of concrete specimens, which were subjected to external sulfate attack and action of freeze and thaw respectively. The results indicate that incorporation of both silica fume and marble dust resulted in a decrease in the compressive strength loss and hence led to an increased resistance to external sulfate attack and action of freeze and thaw of the concrete. Microstructural analyses support the enhanced resistance to external sulfate attack and action of freeze and thaw of concrete. The formation of additional C-S-H gels, due to the result of the pozzolanic reaction between silica fume and CH compounds, and the filler effect of marble dust played a key role in enhancing the resistance to sulfate attack and action of freeze and thaw of concrete.

CHAPTER 5

MECHANICAL PROPERTIES AND DURABILITY CHARACTERISTICS OF CONCRETE INCORPORATED WITH SILICA FUME AND CRUSHED BRICKS

5.1 Introduction

This chapter discusses the mechanical properties and durability characteristics of concrete incorporated with silica fume and crushed bricks. To begin with, characterization of raw materials is discussed. Results associated with mechanical properties of concrete such as compressive strength are discussed to investigate the effect of incorporating silica fume and crushed bricks in concrete. Moreover, results associated with durability characteristics of concrete such as water permeability, external sulfate attack, action to freeze and thaw and porosity measurements are then discussed to investigate the effect of incorporating silica fume and crushed bricks in concrete. Microstructural analysis carried out using Scanning Electron Microscope enlightened the microstructural developments as well as the physical and chemical reactions that take place in cementitious matrix incorporated with silica fume and crushed bricks.

5.2 Characterization of raw materials

Raw materials used in this section of thesis are Portland cement, silica fume, crushed bricks, fine aggregates and coarse aggregates. Elemental oxide composition of the raw materials, obtained from X-ray fluorescence spectroscopy, is illustrated in Table 5.1.

Table 5.1. Elemental oxide composition of Portland cement, silica fume, crushed bricks and fine aggregates determined by X-ray fluorescence spectroscopy.

Chemical composition	Portland cement (Wt. %)	Silica fume (Wt. %)	Crushed bricks (Wt. %)	Fine aggregates (Wt. %)
CaO	43.8	1.25	21.6	0.46
ZnO	0.01	0.02	0.02	-
SiO ₂	30.2	93.3	41.0	91.9
Al ₂ O ₃	11.4	0.73	13.4	3.91
Fe ₂ O ₃	5.11	1.82	10.2	0.65
SO ₃	3.29	0.22	3.02	0.04
MgO	2.61	0.89	6.03	0.14
K ₂ O	1.34	1.21	1.91	1.31
TiO ₂	0.74	-	0.93	0.83
Na ₂ O	0.51	0.28	1.06	0.49
MnO	0.43	0.09	0.29	0.04
Cl	0.03	0.04	0.07	0.01

All the major as well as minor compounds present in these raw materials are summarized in the Table 5.1 along with their weight expressed in percentage respectively. Elemental oxide composition of Portland cement shows cumulative content of CaO, SiO₂, Al₂O₃ and Fe₂O₃ to be 90%. Silica fume contains more than 90% of SiO₂ content and therefore, high pozzolanic activity can be observed during the pozzolanic reaction. Crushed bricks, can be described as clayey material in nature; 41% of SiO₂, 13.4% of Al₂O₃ and 10.2% of Fe₂O₃ content is present in its elemental oxide composition. The presence of Si and Al content may conform semi – pozzolanic properties, however, crushed bricks used in this thesis are microstructurally crystalline in nature. Furthermore, the particle size distribution of crushed bricks also shows that the material is not finely powdered. Hence, crushed bricks are suitable to be used as a filler replacement in this thesis. Moreover, fine aggregates, called as quartz sand is used and the presence of high amounts of SiO₂ present in the oxide composition is predictable.

In addition to the elemental oxide composition of these raw materials, particle size distribution analysis is also done, as shown in Figure 5.1.

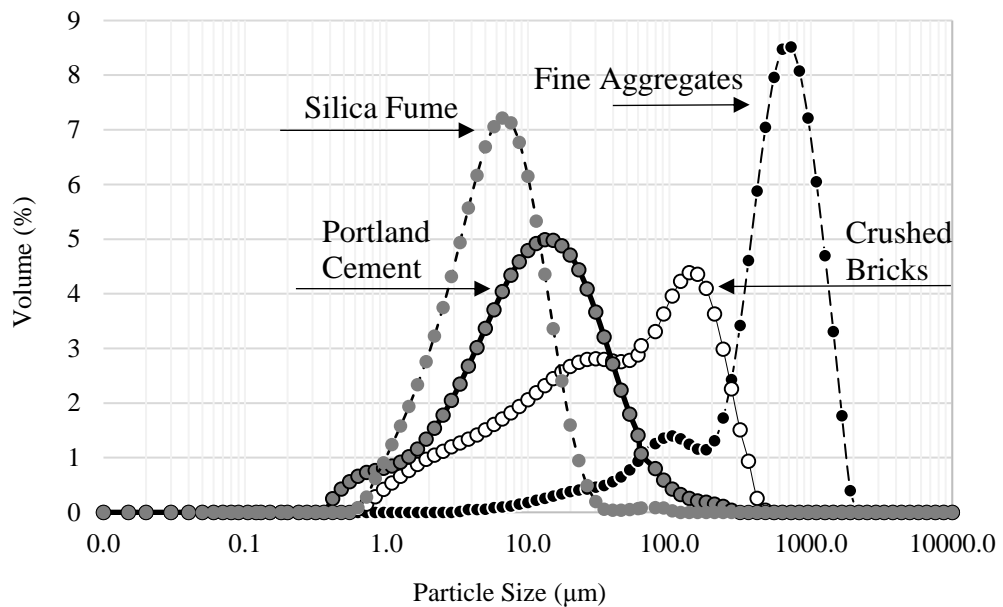


Figure 5.1. Particle size distribution of Portland cement, silica fume, crushed bricks and fine aggregates

Figure 5.1 shows the particle size distribution of Portland cement, silica fume, crushed bricks and fine aggregates. Particle size of each material is expressed in microns. Comparison between particle size distributions of Portland cement with silica fume shows that silica fume particles have high fineness than Portland cement particles. The highest volume peak of silica fume particles is in the range of 1 to 10 microns, whereas for Portland cement, the range is in between 10 to 100 microns respectively. Therefore, it must be emphasized that a coarser binding material i.e. Portland cement is partially replaced with a much finer particle size binding material i.e. silica fume in this section of the thesis.

Moreover, comparison between particle size distributions of fine aggregates with crushed bricks shows that crushed bricks particles show high degree of fineness. The highest volume peak of crushed bricks particles is in between 50 to 500 microns whereas fine aggregates are in between 100 and 1000 microns. Therefore, it must be highlighted that a coarser filler material i.e. fine aggregates is partially replaced with a much finer particle size filler material i.e. crushed bricks in this section of the thesis.

5.3 Fresh properties

5.3.1 Water content

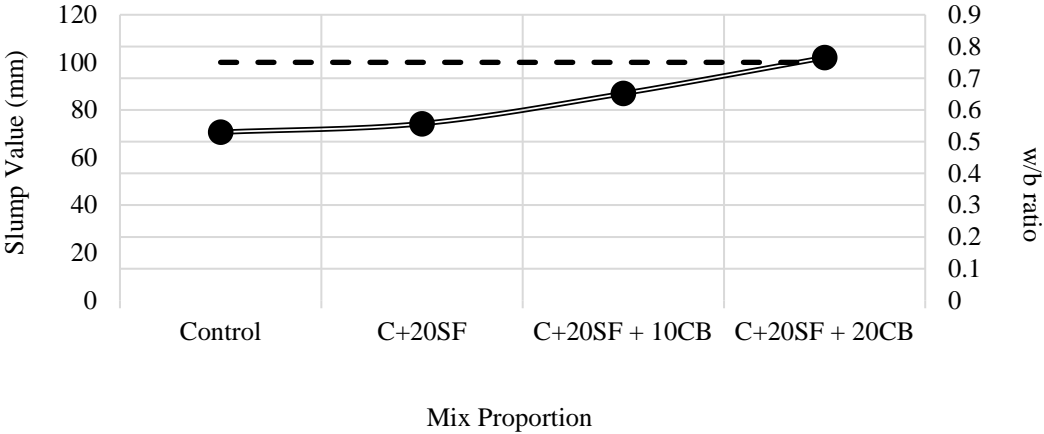


Figure 5.2. Slump (mm) and water/binder ratios for all the mix proportions of concrete incorporated with silica fume and crushed bricks. -----; slump values (mm), ●; water/binder ratio, plotted in a secondary axis.

Figure 5.2 shows that addition of 20% silica fume content as a partial binder replacement material to Portland cement resulted in an increase water/binder ratio from 0.54 to 0.557. Since, slump value of 100 mm is kept constant for all concrete combinations, 0.017 increase in water/binder ratio for 20% SF concrete specimen is necessary to achieve the same consistency of control concrete specimen. Furthermore, increase in the crushed bricks replacement levels resulted further increase in water/ binder ratio. For instance, w/b ratio of 20% SF + 10% CB and 20% SF + 20% CB were 0.652 and 0.765 respectively. When compared to the water/binder ratio of control concrete specimen, the addition of 10% and 20% crushed bricks content increase in w/b ratio of 0.112 and 0.225 is observed respectively. Such increase in the water demand of concrete by the addition of silica fume and crushed bricks is due to the fineness of these materials. Silica fume has high fineness in comparison with Portland cement whereas crushed bricks also has high fineness in comparison with fine aggregates. Furthermore, crushed bricks particles possess high absorption capacity, as mentioned in Section 2.9.1.2. Therefore, the water/binder ratio is evident to increase. Furthermore, the density of concrete will increase by the addition of materials that are finer than conventional

concrete materials, the water/binder ratio is also evident to increase to attain required consistency of 100 mm slump.

5.4 Mechanical properties

5.4.1 Compressive strength

Concrete specimens were prepared containing 20% silica fume as constant replacing Portland cement content. In addition to that, crushed bricks with the replacement levels of 10% and 20% are replaced from fine aggregates. Long-term compressive strength values of concrete specimens, all cured under normal curing conditions, are illustrated in Figure 5.3.

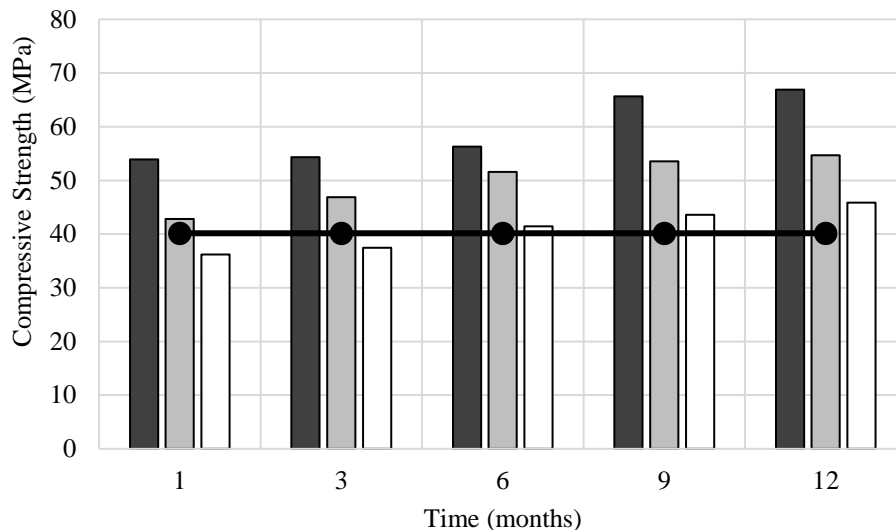


Figure 5.3. Compressive strength of silica fume – concrete incorporated with crushed bricks. ■; 20% SF, ▒; 20% SF with 10% CB, □; 20% SF with 20% CB, ●; concrete control at 28th days.

From Figure 5.3, results indicate an overall increase in compressive strength for all concrete mixes from 28 days to 1 year. Compressive strength results of control concrete and 20% SF concrete have already been discussed in Section 5.4.1. Concrete specimens containing 20% SF as a replacement level of Portland cement with 10% and 20% crushed bricks as a replacement level of fine aggregates are discussed in this section. The results indicate a decrease in the compressive strength, especially at early ages, by the addition of crushed bricks, when compared to cement control and 20% SF concrete specimens. At 28 days, the compressive strength of 20% SF + 10% CB is

almost equal to cement control specimen whereas, the compressive strength of 20% SF + 20% CB is decreased by 10%. However, at 6 months, the compressive strength of 20% SF + 20% CB is equal to the compressive strength of cement control specimen at 28 days. Furthermore, after 1 year, the compressive strength has been increased 38% and 13% for 20% SF + 10% CB and 20% SF + 20% CB respectively. The increase in compressive strength of concrete incorporated with silica fume and crushed bricks, especially after 6 months is attributed to the pozzolanic reaction in the cementitious matrix. Since, pozzolanic reaction is slower compared to hydration of Portland cement, time required to react with CH compounds for the additional production of C-S-H gels can be varied, especially by the presence of crushed bricks in the cementitious matrix. However, it must be noted that such an increase in compressive strength of concrete by replacing 40% of the total content of concrete by supplementary cementitious materials and waste materials is remarkable for the sustainable use of concrete. When compared to concrete incorporated with SF alone, a decrease in compressive strength of 13% and 31% is observed at 1 year with the addition of 10% and 20% CB. Even though, the compressive strength of concrete containing crushed bricks decreased when compared with concrete containing silica fume, it must be noted that compressive strength obtained at all combinations with crushed bricks are increasing with time. For instance, compressive strength of concrete incorporated with silica fume and crushed bricks is less than the compressive strength compared to concrete incorporated with silica fume and marble dust. However, it must be noted that concrete containing silica fume and crushed bricks is viable for its use as structural concrete in construction industry. Utilization of waste materials such as crushed bricks reduces the burden of relying on natural resources only. Furthermore, durability characteristics of concrete are also important to be considered. Concrete specimens of 20% SF with 10% CB and 20% CB also showed strength increase of 30% and 25% at 1 year respectively in comparison with the compressive strength of these combinations at 28 days. Hence, the compressive strengths of concrete containing silica fume and crushed bricks, especially at long-term, do possess better mechanical properties, compared to control concrete specimen at 28 days. Therefore, conducting a long-term study was important to understand the influence of crushed bricks along with pozzolanic addition in concrete.

5.5 Durability

5.5.1 Water permeability

Concrete specimens incorporated with 20% silica fume as constant material replacing Portland cement content; 10% and 20% crushed bricks replacing fine aggregates are investigated for water penetration depth. Long-term water penetration depths of concrete specimens, along with mass of absorbed water during the experiment are illustrated in Figure 5.4.

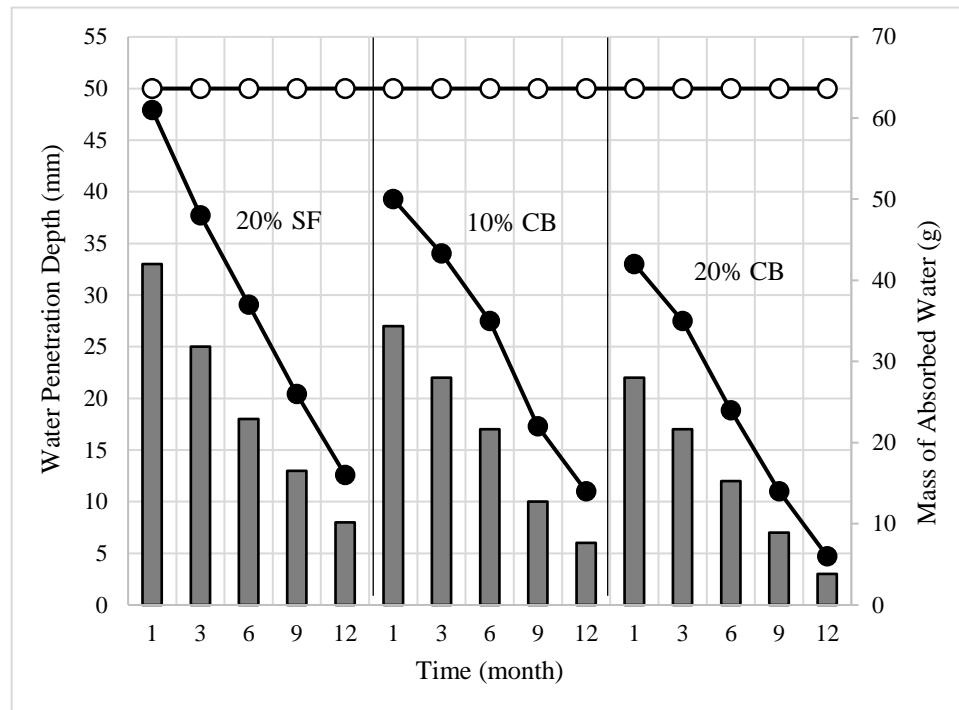


Figure 5.4. Water penetration depth of concrete incorporated with 20% SF and with 10% CB and 20% CB. \circ ; water penetration depth of concrete control specimen at 28th days, \bullet ; Mass of absorbed water through the application of pressurized water during the experiment, plotted in a secondary axis.

The results shown in Figure 5.4 indicate an overall decrease of water penetration depth in all the combinations of concrete with time. For instance, water penetration depth of control concrete specimen is noted to be 50 mm at 28 days. In comparison to that, water penetration depths of 20% SF, 20% SF + 10% CB and 20% SF + 20% CB are 32 mm, 27 mm and 22 mm respectively. Therefore, it can be seen that the addition of silica fume and crushed bricks reduced water penetration depth, even at short-term durations. Furthermore, concrete specimens containing 10% crushed bricks and 20% crushed bricks, water penetration depth is decreased 77% and 86% from 28 days to 1

year. The reason for such decrease is due to the advancement of pozzolanic reaction in the cementitious matrix and the filler effect of crushed bricks. Pozzolanic reaction caused the CH compounds to react with silicate compounds, present by the addition of silica fume to produce additional C-S-H gels. In addition to that, when coarser particles of fine aggregates are partially replaced with crushed bricks, decrease in free volume within the cementitious matrix takes place. Free volume present in the cementitious matrix occupied by the addition of crushed bricks drastically reduces the permeability of concrete. To further illustrate the role of addition of crushed bricks, microstructural images of concrete specimens containing 20% silica fume along with 20% crushed bricks are taken from scanning electron microscope at 28 days and 1 year respectively. The associated Figure 5.5 and 5.6 are illustrated as below.

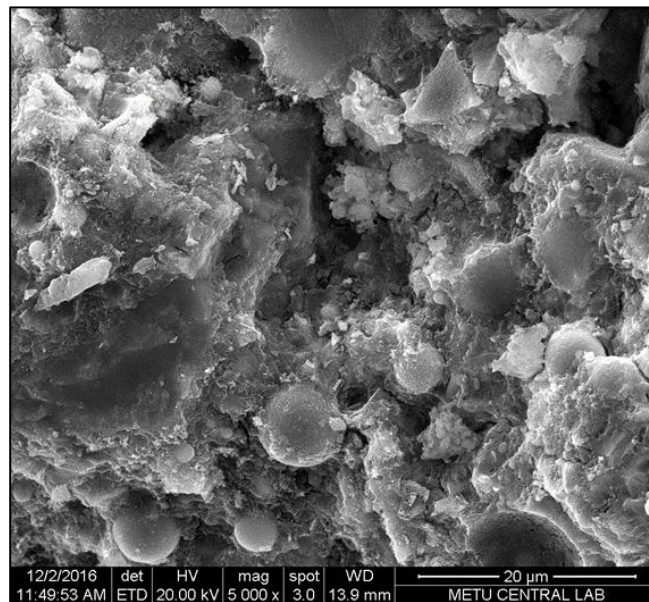


Figure 5.5. Concrete containing 20% SF + 20% CB at 28 days.

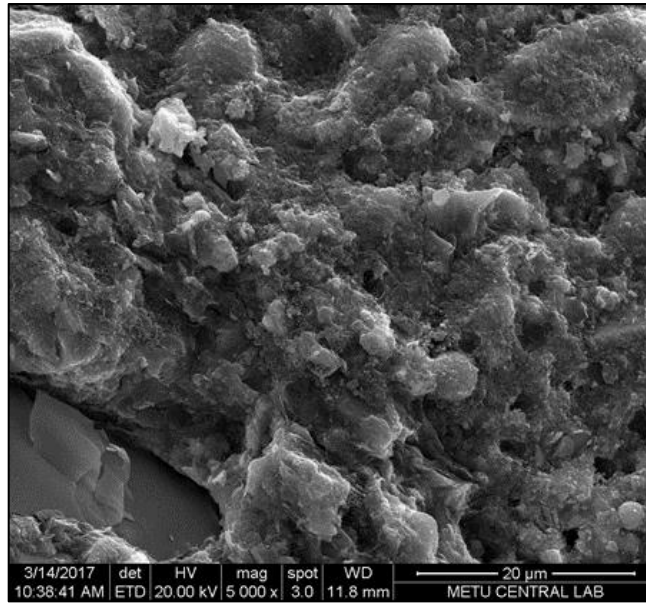


Figure 5.6. Concrete containing 20% SF + 20% CB at 1 year.

Figure 5.5 and Figure 5.6 show the microstructure of 20% SF + 20% CB at 28 days and at 1 year respectively. Presence of crushed bricks particles can be seen in figure 5.5. These figures show a decrease in capillary pore volume of the concrete that is associated with the reduction of water penetration depth of concrete incorporation of silica fume and crushed bricks. For instance, Figure 5.5 illustrating the microstructural image of 20% SF and 20% CB concrete specimen at 28 days shows higher amount of finely divided silicate crystals on the surface of the specimen, due to the presence of silica fume in the cementitious matrix. In addition to that, filler effect induced by crushed bricks is clearly visible which decreases the free volume within the cementitious matrix. However, after 1 year, the microstructure of 20% SF + 20% CB, shown in Figure 5.6, is more consolidated and possesses more uniform structure consisting small particles which are closely bound together. Therefore, the continuous pores present in the cementitious matrix are reduced by the addition of silica fume and crushed bricks. Hence, the permeability is significantly minimized at long-term durations.

Moreover, the mass of absorbed water through the application of pressurized water during the experiment is also plotted on the secondary axis, as shown in Figure 5.4. The results show that mass of absorbed water of concrete specimens incorporated with 20% SF + 10% CB and 20% SF + 20% CB had decrease of 75% and 88% from 28 days to 1 year. However, if the comparison is done among combinations containing

20% SF only and 20% SF + 20% CB at 28 days, difference between the mass of absorbed water is 28% of water, which is quite crucial, especially at short-term durations. However, at long-term durations, the use of silica fume along with the incorporation of crushed bricks results in a systematic decrease in the mass of absorbed water during the experiment. Since, the permeability of concrete is significantly reduced by the addition of silica fume and crushed bricks, especially at long-term durations; therefore, it is evident that the systematic decrease in water penetration depth is supported with the systematic decrease in the mass of absorbed water.

5.5.2 External sulfate attack

Resistance against external sulfate attack of concrete incorporated with 20% silica fume as partial binder replacement of Portland cement along with 10% and 20% crushed bricks as partial filler replacement of fine aggregates is investigated. Prior to sulfate attack exposure, all the concrete specimens were cured under normal curing conditions for 28 days so that, all the concrete must attain substantial hydration of concrete. Long-term external sulfate attack measurements of concrete specimens are carried out based on compressive strength loss and expansion of concrete specimens, shown in Figure 5.7.

The results illustrated in Figure 5.7 indicate that compressive strength loss of concrete is decreased with the incorporation of both silica fume and crushed bricks. Compressive strength loss is expressed in percentage and can be defined as percentage loss in compressive strength compared to compressive strength of concrete cured under normal curing conditions. Therefore, the compressive strength loss mentioned in this section is due to the action of external sulfate attack on concrete. For instance, at 28 days, 20% SF + 10% CB and 20% SF + 20% CB concrete specimens had an overall compressive strength loss of 8% and 6% respectively, when compared with compressive strength loss of control concrete specimen. Similar trend is observed at long-term durations, hence by increasing the replacement levels of crushed bricks with time resulted in a systematic decrease in the compressive strength loss of concrete. At 1 year, the compressive strength loss difference among control concrete and 20% SF + 20% CB concrete specimens is almost 30%, which is considerably high.

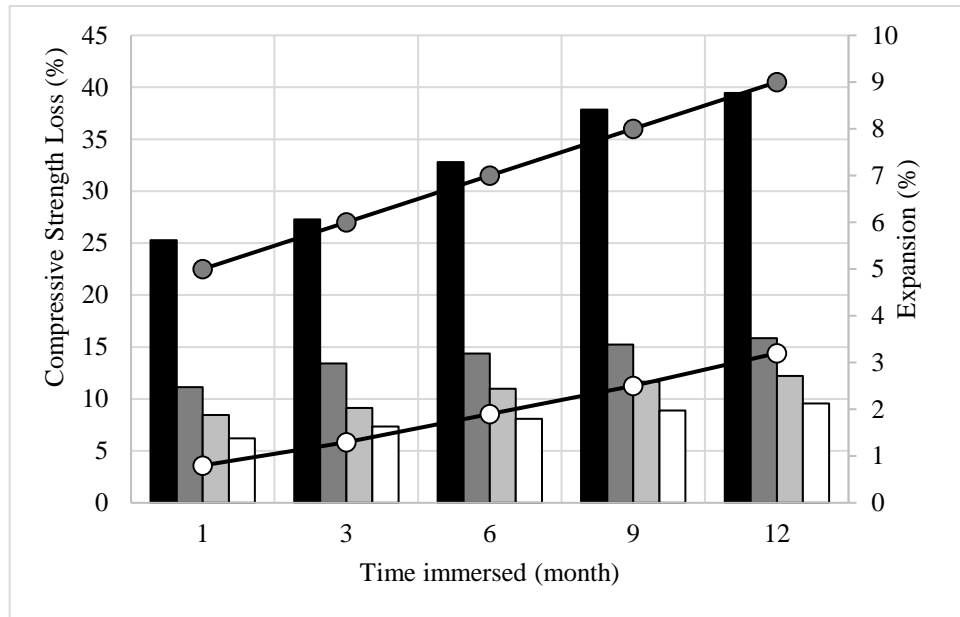


Figure 5.7. Compressive strength loss of concrete subjected to sulfate attack versus immersed time. ■; concrete control, ▒; concrete with 20% SF, ▓; concrete with 20% SF and 10% CB, □; concrete with 20% SF and 20% CB. Expansion of concrete subjected to sulfate attack is plotted in a secondary axis, ●; concrete control, ○; concrete incorporated with 20% SF and 20% CB.

The addition of silica fume and crushed bricks significantly increased the resistance of concrete against external sulfate attacks. Since, CH compounds are used up effectively by the availability of silica compounds from silica fume, additional C-S-H gels were formed that made the microstructure of pozzolanic concrete denser than the microstructure of control concrete. CH compounds are normally used as a reactant in the sulfate reaction, mentioned in Section 2.3.3 and 2.5.3 respectively. Therefore, less availability of CH compounds mostly mitigated the development of external sulfate attack by the addition of silica fume. Moreover, crushed bricks, being finer material than fine aggregates, can increase the density of concrete by reducing the free volume present within the cementitious matrix of concrete. The permeability of concrete decreased since the ingress of sulfate ions into the cementitious matrix reduced significantly. Hence, reduced compressive strength loss of concrete specimens containing silica fume and crushed bricks, compared to control concrete specimen, is evident.

Concrete specimens exposed to external sulfate attack are then subjected to a measurement of expansion as this is shown on the secondary axis in Figure 5.7. Expansion of control concrete and 20% SF + 20% CB concrete specimen is

investigated for a period of 1 year. Expansion of control concrete is significantly higher, in comparison with 20% SF + 20% CB concrete. For instance, at 28 days, the expansion of control concrete specimen is measured to be approximately 5%, whereas for 20% SF + 20% CB concrete specimen, the expansion is only close to 0.8%. Hence, even at 28 days, the difference of expansion is approximately 4.2%, which is considerably high. Overall trend is increasing with time that shows that expansion of concrete is inevitable; however, the difference among the expansion values is considerable. Moreover, the difference in expansion among control concrete and 20% SF + 20% CB concrete specimens increases from 4.2% to 5.8% at 1 year. Hence, control concrete specimen subjected to external sulfate attack exhibited much higher expansion in comparison with 20% SF + 20% CB concrete specimen. The reason of higher expansion in control concrete specimen is due to the formation of ettringite and gypsum by the action of sulfate attack in the cementitious matrix. Formation of ettringite and gypsum cause volume increase, thus expansion and subsequent cracking of concrete is inevitable. In case of 20% SF + 20% CB concrete specimen, the increase in expansion of concrete was 2.4% from 28 days to 1 year respectively. Compared to control concrete specimen, the addition of silica fume and crushed bricks reduced the expansion of concrete by 64% at 1 year. Thus, concrete containing silica fume and crushed bricks showed appropriate resistance to the action of external sulfate attack since reduced volume expansion is observed during the experiment.

To further investigate the influence of silica fume and crushed bricks under the exposure of external sulfate attack microstructurally in concrete, microstructural images of concrete combinations are taken by scanning electron microscopy. Figure 5.8 and Figure 5.9 illustrate the microstructural images of concrete specimen containing 20% SF + 20% CB replacement at 28 days and 1 year.

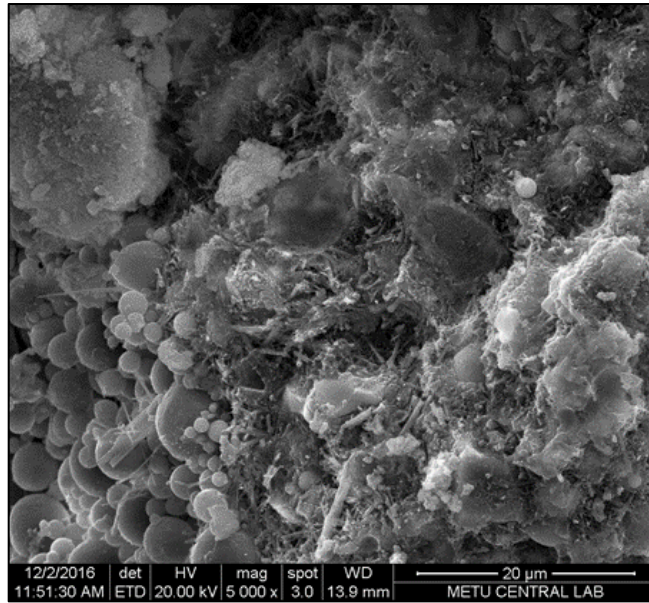


Figure 5.8. Concrete containing 20% SF + 20% CB under sulfate attack at 28 days.

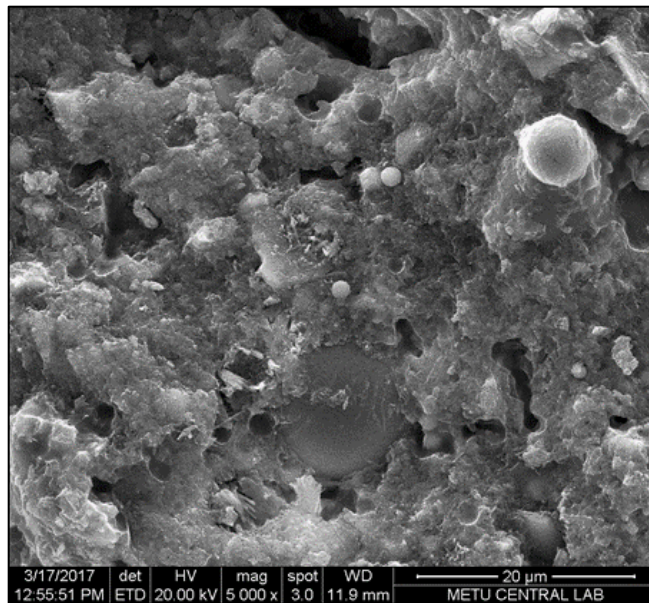


Figure 5.9. Concrete containing 20% SF + 20% CB under sulfate attack at 1 year.

Figure 5.8 and Figure 5.9 show the microstructure for 20% SF + 20% CB concrete specimens exposed to external sulfate attack for 28 days and 1 year respectively. Compared to the microstructural images of control and 20% SF concrete specimens at 28 days seen in Section 5.5.2, it can be observed in Figure 5.8 that crushed bricks particles are surrounded by the C-S-H gels. The presence of both, crushed bricks particles and silicate compounds significantly consolidated the cementitious matrix. Furthermore, silicate compounds are less visible as well as the CH compounds in the

cementitious matrix at long-term duration, illustrated in Figure 5.9. Moreover, the absence of gehlenite crystals also provides an evidence of reduced expansion at 1-year. Hence, more compact and consolidated microstructure is observed at 1-year concrete specimen. Thus, further reduction of compressive strength loss and expansion of concrete, compared with 20% SF concrete specimen, is done not only by the presence of additional C-S-H gels but also the filler effect of crushed bricks particles induced in the 20% SF + 20% CB concrete specimen respectively.

5.5.3 Freeze and thaw resistance

Resistance against freeze and thaw of concrete incorporated with 20% silica fume as partial binder replacement of Portland cement along with 10% and 20% crushed bricks as partial filler replacement of fine aggregates is investigated. Prior to freeze and thaw exposure, all the concrete specimens were cured under normal curing conditions for 28 days so that, all the concrete must attain substantial hydration of concrete. Long-term freezing and thawing measurements of concrete specimens are carried out based on compressive strength loss and mass loss of concrete specimens, as illustrated in Figure 5.10.

The results illustrated in Figure 5.10 indicate compressive strength loss of concrete, hence, the resistance to freeze and thaw is increased significantly by the presence of silica fume and increasing percentage replacement of crushed bricks. For instance, at 28 days, 20% SF + 10% CB and 20% SF + 20% CB concrete specimens had an overall compressive strength loss of 11% and 7% respectively, when compared to compressive strength loss of control concrete specimen. Similar trend can be seen at long-term durations, hence by increasing the replacement levels of crushed bricks with time resulted in a systematic decrease in the compressive strength loss of concrete. At 1 year, the compressive strength loss difference among control concrete and 20% SF + 20% CB concrete specimens is almost 20%, which is considerably high. The addition of silica fume and crushed bricks, considerably, increased the resistance of concrete against freeze and thaw cycles.

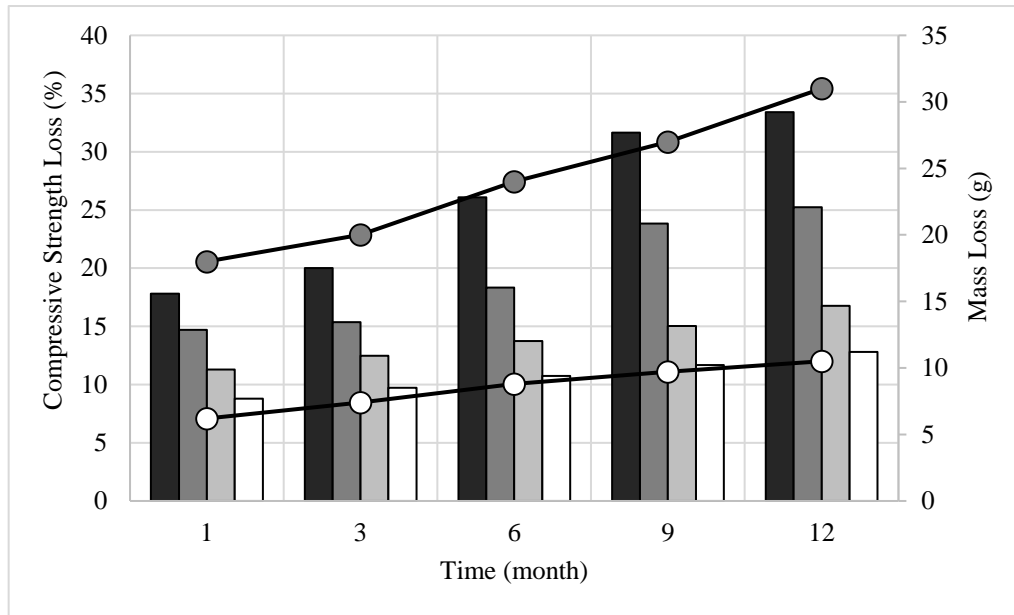


Figure 5.10. Compressive strength loss of concrete subjected to freeze and thaw versus time. ■; concrete control, ▒; concrete with 20% SF, ▓; concrete with 20% SF and 10% CB, □; concrete with 20% SF and 20% CB. Mass loss of concrete subjected to freeze and thaw is plotted on in secondary axis, ●; concrete control, ○; concrete incorporated with 20% SF and 20% CB.

Mass loss of concrete due to the exposure of freeze and thaw cycles are also determined since it is associated with the compressive strength loss of concrete. It has been mentioned in Section 5.5.3 that as the number of freeze and thaw cycles are increasing, the subsequent hydraulic pressure in the cementitious matrix system is increasing. Hence, progressive development of micro-cracks result in greater mass loss of concrete specimen, which further results in compressive strength loss of concrete. At 28 days, the difference in mass loss between control concrete specimen and 20% SF + 20% CB concrete specimen is 63%, which is considerably high. Overall trend is increasing with time, which shows that increase in mass loss as the number of freeze, and thaw cycles are increasing. However, the difference among the mass loss of control concrete and 20% SF + 20% CB concrete specimens is significant. The mass loss of control concrete specimen increased 39% from 28 days to 1 year, whereas for 20% SF + 20% CB concrete specimen, the mass loss increased 30% from 28 days to 1 year. It must be noted that there is a rapid increase of mass loss in control concrete specimen compared to 20% SF + 20% CB concrete specimen. Hence, control concrete specimen subjected to freezing and thawing, compared to 20% SF + 20% CB concrete specimen, exhibited much higher mass loss since the hydraulic pressure caused by the freeze and thaw

cycles was higher which caused increased development of micro cracking. Moreover, the values of mass loss of these concrete specimens are in a good agreement with the compressive strength loss as well. The density of concrete incorporated with silica fume and crushed bricks has been increased which reduced the availability of pores. Hence, concrete containing silica fume and crushed bricks became less permeable. In addition to that, higher mass loss led to greater loss of compressive strength. Higher compressive strength loss in control concrete specimen is due to the presence of additional cracks that caused the mass loss during the action of freeze and thaw. However, concrete containing silica fume and crushed bricks had less compressive strength loss, hence, less cracks are developed which caused reduction in mass loss under the action of freeze and thaw. Therefore, it is evident that compressive strength loss and mass loss of concrete under the action of freeze and thaw are coherent with each other. Thus, the addition of silica fume and crushed bricks in concrete enhanced the resistance to withstand compressive strength loss as well as micro cracking caused by the action of freeze and thaw.

To further investigate the influence of silica fume and crushed bricks under the action of freeze and thaw microstructurally in concrete, microstructural images of concrete combinations are taken by scanning electron microscope. Figure 5.11 and Figure 5.12 analyze concrete specimen containing 20% SF + 20% CB replacement at 28 days and 1 year, as the microstructural images are illustrated.

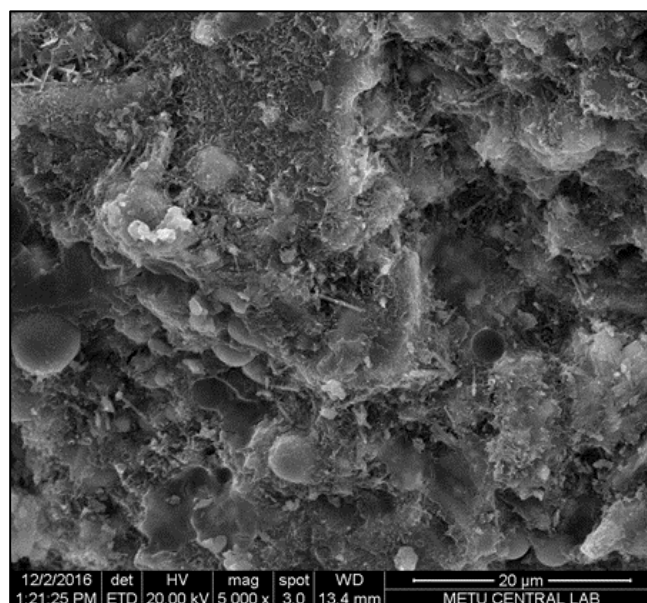


Figure 5.11. Concrete containing 20% SF + 20% CB under freeze and thaw at 28 days.

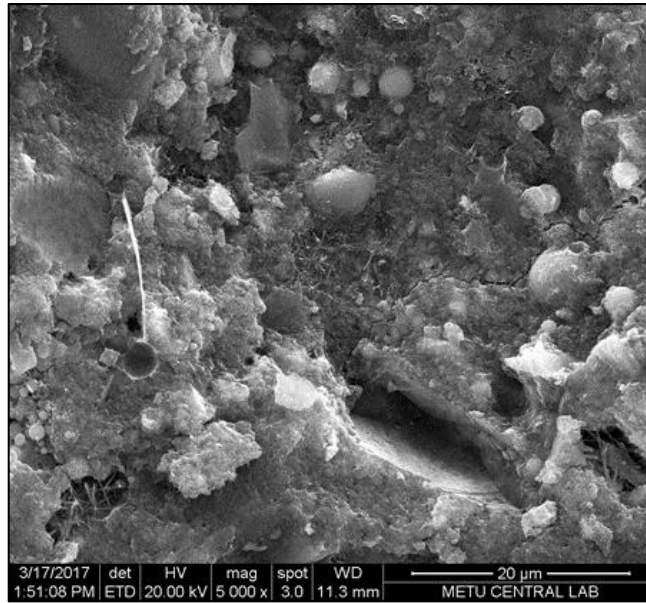


Figure 5.12. Concrete containing 20% SF + 20% CB freeze and thaw attack at 1 year.

Figure 5.11 and Figure 5.12 show the microstructure for 20% SF + 20% CB concrete specimens under the action of freeze and thaw for 28 days and 1 year respectively. At 28 days, it can be seen that crushed bricks particles are surrounded by the C-S-H gels. Furthermore, at 1 year, it can be seen in Figure 5.12 that a crack has been propagated in the roughly diagonal direction on the middle right hand side of the microstructural image. Since, the action of freeze and thaw is repeatedly continued, volume of water present in the pores of cementitious matrix tends to expand and hence, development of cracks is apparent. However, compared to control concrete specimen, it can be observed that less cracks are present in the microstructure. Reduced development of cracks might be due to the presence of silicate compounds. Therefore, addition of silica fume increased the resistance against freeze and thaw action of concrete that mainly attributed to the formation of additional C-S-H gels as the result of the pozzolanic reaction among silica and CH compounds. Further addition of crushed bricks in concrete that is already incorporated with silica fume caused significant reduction of pores present in the cementitious matrix. The hydraulic pressure that results in micro-cracking are reduced by the addition of silica fume and crushed bricks. In addition to that, significant reduction of pores can also be linked with the permeability of these concrete specimens. Since the water penetration depth of concrete incorporated with silica fume and crushed bricks is considerably lower in comparison with control concrete as shown in Figure 5.4. Therefore, less water can imbibe in wet conditions

under the action of freeze and thaw, which caused lower mass loss and resulted in less compressive strength loss of control concrete specimen.

5.5.4 Porosity

Porosity measurements of concrete are done to investigate the effects of using silica fume and crushed bricks as partial replacement materials of Portland cement and fine aggregates under various cure conditions. Control concrete, 20% SF, 20% SF + 10% CB and 20% SF + 20% CB concrete specimens cured under normal curing conditions are investigated for porosity measurement after 1 year. Porosity in percentage values as well as pore volume in cm^3 is reported in Table 5.2.

Table 5.2. Porosity measurements of concrete incorporated with silica fume and crushed bricks under normal curing conditions.

Concrete combinations	Cure condition	Porosity (%)	Pore volume (cm^3)
Cement	Water Cured	39.2	0.2814
Cement + 20% SF	Water Cured	30.8	0.2207
Cement + 20% SF + 10% CB	Water Cured	27.6	0.2085
Cement + 20% SF + 20% CB	Water Cured	25.1	0.1609

Table 5.2 summarizes the porosity and pore volume of concrete specimens incorporated with silica fume and crushed bricks under normal curing condition respectively. It can be seen that addition of silica fume indicated a significant decrease in both the porosity and pore volume at long-term duration. For instance, control concrete specimen, cured under normal curing condition has the porosity and pore volume of 39.2% and 0.2814 cm^3 , whereas 20% SF concrete specimen has the porosity and pore volume of 30.8% and 0.2207 cm^3 respectively. Moreover, it can be seen that addition of silica fume along with an increase in the replacement level of crushed bricks resulted in further decrease in both the porosity and pore volume at long-duration for the concrete specimens cured under normal curing conditions. For instance, compared to 20% SF concrete specimen, by the addition of 10% and 20% crushed bricks, further 3% and 5% decrease in porosity is seen. Pore volume also decreased from 0.2207 cm^3 to 0.2085 cm^3 in case of 10% crushed bricks and 0.1659 cm^3 in case of 20% crushed bricks respectively. Compared to control concrete

specimen, by the addition of 20% silica fume content and 20% crushed bricks content, 15% decrease in porosity as well as 42% decrease in pore volume is seen. The addition of crushed bricks decreased the free volume of pores present within the cementitious matrix, which made the microstructure well consolidated and uniformly distributed as shown previously in Figure 5.6. The pores present in the cementitious matrix were reduced by the addition of silica fume. Further reduction of pores was done by the addition of crushed bricks. Therefore, the porosity and pore volume decreased considerably at long-term durations.

Similarly, control concrete, 20% SF, and 20% SF + 20% CB concrete specimens cured under sulfate solution are investigated for porosity measurement after 1 year. Porosity in percentage values as well as pore volume in cm^3 is reported in Table 5.3.

Table 5.3. Porosity measurements of concrete incorporated with silica fume and crushed bricks under sulfate solution.

Concrete combinations	Cure condition	Porosity (%)	Pore volume (cm^3)
Cement	Sulfate solution	47.1	0.4365
Cement + 20% SF	Sulfate solution	34.5	0.2571
Cement + 20% SF + 20% CB	Sulfate solution	29.2	0.2179

Table 5.3 summarizes the porosity and pore volume of concrete specimens incorporated with silica fume and crushed bricks under sulfate solution respectively. In comparison with the concrete under normal curing conditions, irrespective of concrete combinations, the porosity and pore volume of concrete increased substantially under sulfate solution. Sulfate ions, present in the sulfate solution, will react with C_3A and gypsum present in the cementitious matrix to produce ettringite that will cause volume expansion. Hence, porosity and pore volume is evident to increase. Addition of silica fume and crushed bricks resulted in a significant decrease in both the porosity and pore volume cured under sulfate solution at long-term duration. For instance, compared to 20% SF concrete specimen, by the addition of 20% crushed bricks, 5% decrease in porosity is observed. Pore volume also decreased from 0.2571 cm^3 to 0.2179 cm^3 , only by partially replacing fine aggregates with 20% crushed bricks content. Compared to control concrete specimen, by the addition of

20% silica fume content and 20% crushed bricks content, 18% decrease in porosity as well as 51% decrease in pore volume is seen. Crushed bricks, being finer filler material in comparison with fine aggregates, increased the density of concrete by filling the pores present within the cementitious matrix of concrete. It also reduces the permeability of concrete. Hence, the microstructure of 20% SF + 20% CB is well consolidated and uniformly distributed at long-term duration and is previously shown in Figure 5.9. Additional C-S-H gel production caused by the addition of silica fume resulted a uniform microstructure. The pores present in the cementitious matrix were also reduced. However, further reduction of pores was done by the addition of crushed bricks, which made the microstructure denser and well consolidated. Therefore, the porosity and pore volume of concrete incorporated with silica fume and crushed bricks, even under sulfate solution, decreased considerably at long-term durations.

Moreover, control concrete, 20% SF, and 20% SF + 20% CB concrete specimens under the action of freeze and thaw are investigated for porosity measurement after 1 year. Porosity in percentage values as well as pore volume in cm^3 is reported in Table 5.4.

Table 5.4. Porosity measurements of concrete incorporated with silica fume and crushed bricks under action of freeze and thaw.

Concrete combinations	Cure condition	Porosity (%)	Pore volume (cm^3)
Cement	Freeze and thaw	49.3	0.4584
Cement + 20% SF	Freeze and thaw	36.6	0.2612
Cement + 20% SF + 20% CB	Freeze and thaw	32.5	0.2236

Table 5.4 summarizes the porosity and pore volume of concrete specimens incorporated with silica fume and crushed bricks under action of freeze and thaw respectively. In comparison with the concrete under normal curing conditions, irrespective of concrete combinations, the porosity and pore volume of concrete increased substantially under action of freeze and thaw. Addition of silica fume and crushed bricks resulted in a significant decrease in both the porosity and pore volume cured under action of freeze and thaw at long-term duration. For instance, compared to 20% SF concrete specimen, by the addition of 20% crushed bricks, further 4% decrease in porosity is seen. Pore volume also decreased from 0.2612 cm^3 to 0.2236

cm³, only by partially replacing fine aggregates with 20% crushed bricks content. In comparison with control concrete specimen, by the addition of 20% silica fume content and 20% crushed bricks content, 17% decrease in porosity as well as 52% decrease in pore volume is seen.

Subsequent hydraulic pressure in the cementitious matrix system increases by the repeatedly freezing and thawing cycles which results in progressive development of micro-cracks in concrete. Concrete specimens incorporated with silica fume and crushed bricks, the density of concrete has been increased which made concrete less permeable. Microstructurally, the presence of silicate compounds and the crushed bricks surrounded by the C-S-H gels can be seen in Figure 5.12. Silicate compounds reacted with CH compounds to further produce additional C-S-H gels, which significantly makes the microstructure well consolidated and uniform. Addition of crushed bricks in concrete resulted significant reduction of pores present in the cementitious matrix. Significant reduction of pores is coherent with the water penetration depth of concrete specimens incorporated with silica fume and crushed bricks. Water penetration depth of concrete incorporated with silica fume and crushed bricks is significantly low. Limited amount of water can imbibe in wet conditions under the action of freeze and thaw, in comparison with control concrete specimen. Therefore, the porosity and pore volume of concrete incorporated with silica fume and crushed bricks, even under action of freeze and thaw, decreased considerably at long-term durations.

5.6 Conclusions

In this chapter, the effect of crushed bricks used as a replacement material to fine aggregate on the long-term mechanical properties and durability characteristics of concrete incorporated with fixed proportion of silica fume is investigated.

The results reported in this chapter indicate that an increase in the replacement level of crushed bricks with the fixed proportion of silica fume resulted in a slight decrease in compressive strength of concrete, when compared to concrete incorporated with silica fume only. However, the strength values of the pozzolanic concrete obtained at all volume fractions of crushed bricks were increasing with time and were higher compared to the control concrete specimen at all times.

Furthermore, the use of silica fume and crushed bricks resulted in a significant decrease in the water penetration depth and porosity of the concrete. Based on the microstructural analysis carried out using SEM, significant reduction in the volume of the capillary pores of concrete incorporated with silica fume and crushed bricks is observed. However, increase in the replacement level of crushed bricks resulted in further substantial reduction in the water penetration depth and porosity of the concrete due to the filler effect of crushed bricks that led to a decrease in free volume of the cement matrix.

In addition to that, the resistance to external sulfate attack and action of freeze and thaw of concrete incorporating silica fume and crushed bricks are inspected by measuring compressive strength loss of concrete specimens that were subjected to external sulfate attack and action of freeze and thaw respectively. The results indicate that incorporation of both silica fume and crushed bricks resulted in a decrease in the compressive strength loss and hence led to an increased resistance to external sulfate attack and action of freeze and thaw of concrete. Microstructural analyses enlightened the actual mechanism for the enhanced resistance to external sulfate attack and action of freeze and thaw of concrete. The formation of additional C-S-H, due to the result of the pozzolanic reaction between silica fume and CH compounds, and the filler effect of crushed bricks played a significant role in advancing the resistance to sulfate attack and action of freeze and thaw of concrete.

CHAPTER 6

CONCLUSIONS AND RECOMMENDATIONS

6.1 Conclusions

In this thesis, mechanical properties and durability characteristics of concrete incorporated with silica fume as partial binder replacement to Portland cement and marble dust and crushed bricks as partial filler replacement material to fine aggregates are investigated.

Along with the mechanical properties and durability characteristics, it was evident that a long-term study and microstructural analyses are necessary to comprehend the development of sustainable concrete. Hence, to ensure qualitative development of sustainable concrete, each parameter investigated in this thesis contains specific findings and conclusions.

Water demand had increased for concrete incorporated with SCMs and waste materials due to the fineness of these materials. Particle size distributions of SCMs and waste materials confirm that these materials are finer compared to Portland cement and fine aggregates, respectively. Density of concrete increased by the addition of these materials. Hence, it was evident that water demand was likely to increase to attain required consistency among all the concrete mixes.

Mechanical properties have enhanced significantly by the addition of SCMs and waste materials at long-term. At short-term, the overall increase by the addition of SCMs and waste materials was approximately 35%. However, at long-term, further increment of 25% was observed which ensures that the development of sustainable concrete by the use of SCMs and waste materials. Microstructural analyses confirmed the additive role of SCMs and waste materials towards short and long-term development of sustainable concrete.

Water permeability reduced significantly up to 80% by the addition of SCMs and waste materials in concrete. Advancement of pozzolanic reaction due to the presence of SCMs and the filler effect induced by the waste materials reduced the amount of

pores available in the concrete. Thus, the structure of concrete incorporated with SCMs and waste materials became more consolidated and free volume present in the cementitious matrix decreased significantly. Mass loss associated with the water permeability drastically reduced due to the less availability of capillary pores in cementitious matrix by the addition of SCMs and waste materials. Microstructural analyses showed the reduction in availability of capillary pores at short and long-term, thus, developing the sustainable concrete to be less permeable.

Compressive strength loss of concrete incorporated with SCMs and waste materials reduced remarkably from approximately 25% to 4% at short-term and approximately 40% to 10% at long-term under the subject of external sulfate attack. Comparatively, expansion of concrete incorporated with SCMs and waste materials reduced up to approximately 70% at long-term. Since formation of ettringite and gypsum cause volume increase, hence, expansion and subsequent cracking of concrete is inevitable. However, concrete incorporated with SCMs and waste materials show less compressive strength loss and low expansion of concrete under the action of external sulfate attack. More consolidated structure and significant reduction in free volume, illustrated by microstructural analyses, was observed for concrete incorporated with SCMs and waste materials. Thus, addition of SCMs and waste materials in concrete resulted in higher resistance to external sulfate attack compared to conventional concrete.

Compressive strength loss of concrete incorporated with SCMs and waste materials reduced significantly from approximately 17% to 6% at short-term and approximately 33% to 11% at long-term under the subject of freezing and thawing cycles. Furthermore, mass loss reduced up to 70% by the addition of SCMs and waste materials. Since, the subsequent hydraulic pressure in the cementitious matrix system and occurring frequency of freeze and thaw cycles possess a direct relationship. Progressive development of micro-cracks result in greater mass loss of concrete specimen, which further results in compressive strength loss of concrete. However, concrete incorporated with SCMs and waste materials show less compressive strength loss and reduced mass loss of concrete under the action of freeze and thaw. Density of concrete increased by the addition of SCMs and waste materials, illustrated by microstructural analyses. Thus, addition of SCMs and waste materials in concrete

resulted in higher resistance to freeze and thaw cycles compared to conventional concrete.

Porosity determined by mercury intrusion porosimetry at long-term shows a remarkable reduction in porosity as well as pore volume for the concrete incorporated with SCMs and waste materials, particularly cured under sulfate solution and freeze and thaw cycles. In general, 20% decrease in porosity along with 50% decrease in pore volume was observed in all the curing conditions by the incorporation of SCMs and waste materials. Microstructure analyses of concrete incorporated with SCMs and waste materials confirmed that more consolidated and denser structure of cementitious matrix was observed. Hence, reduction in porosity and pore volume, by the addition of SCMs and waste materials at long-term, is evident.

Moreover, the use of SCMs and waste materials in production of concrete showed a reduction in energy consumption as well as mitigation of CO₂ emissions; resulting an overall environmental impact of using SCMs and waste materials during the production of concrete. As a general notion mentioned earlier in Section 1.1, that “for one ton of manufactured Portland cement, one ton of CO₂ emissions are released in the atmosphere”. Hence, by 40% partial replacement of conventional concrete constituents with SCMs and waste materials provide significant evidence of reduction in energy consumption as well as CO₂ emissions. This reduction shows the sustainable effectiveness of using SCMs and waste materials in the development of concrete. Since SCMs and waste materials are by-products of various industrial and agricultural processes, the recycling potential of these materials has been proved by observing significant advancements in mechanical properties and durability characteristics of concrete.

Therefore, by replacing 40% of the constituents of conventional concrete by SCMs and waste materials confirms the enhancement in the quality of concrete as the mechanical properties and durability characteristics are remarkably improved over long-term. Furthermore, dependence of utilizing Portland cement and natural resources for producing concrete can be reduced comparatively if further utilization of SCMs and waste materials begins to develop in the construction industry. Hence, the development of sustainable concrete by the incorporation of SCMs and waste materials

truly provides a benchmark to ensure the effective role of sustainability in construction materials.

6.2 Recommendations

Various recommendations proposed as future work are as follows:

- Concrete combinations of various supplementary cementitious materials (SCMs) and waste materials might be incorporated as binder and filler replacement material for concrete manufacture. Furthermore, the level of replacement might also change to see the effect of SCMs and waste materials in concrete under various replacement levels. Tertiary concrete mixes might also be produced incorporating two or three types of SCMs along with different waste materials to observe the role of various additions of SCMs and waste materials respectively.
- Other suitable waste material might be used to assess the role of partially replacing coarse aggregates along with partially replacing Portland cement and fine aggregates.
- Mechanical properties might further be investigated by determining stress-strain relationship, flexural and shear strength of concrete. Similarly, durability characteristics such as sorptivity, chloride ion penetration, carbonation and acid attacks might also investigate to understand other durability characteristics of concrete.
- Economic assessment of the production of concrete incorporating SCMs and waste materials must be carried out. For instance, producing unit m^3 of sustainable concrete might provide substantial consideration of the economic feasibility of sustainable concrete.

REFERENCES

- ACI Committee 211.1., (2009) Standard practice for selecting proportions for normal, heavyweight, and mass concrete. Proportioning Concrete Mixtures (ACI 211.1-91 R2009), American Concrete Institute, Farmington Hills.
- Adamson, M., Razmjoo, A., & Poursaee, A. (2015). Durability of concrete incorporating crushed brick as coarse aggregate. *Construction and Building Materials*, 94, 426-432.
- Aimin, X., & Sarkar, S. L. (1991). Microstructural study of gypsum activated fly ash hydration in cement paste. *Cement and Concrete Research*, 21(6), 1137-1147.
- Aiqin, W., Chengzhi, Z., Mingshu, T., & Ningsheng, Z. (1999). ASR in mortar bars containing silica glass in combination with high alkali and high fly ash contents. *Cement and Concrete Composites*, 21(5), 375-381.
- Akhtaruzzaman, A. A., & Hasnat, A. (1983). Properties of concrete using crushed brick as aggregate. *Concrete International*, 5(02), 58-63.
- Al-Ani, M., & Hughes, B. (1989). Pulverized-fuel ash and its uses in concrete. *Mag. Concr. Res*, 41(147), 55-63.
- Aldahdooh, M. A. A., Bunnori, N. M., & Johari, M. M. (2013). Evaluation of ultra-high-performance-fiber reinforced concrete binder content using the response surface method. *Materials & Design*, 52, 957-965.
- Aliabdo, A. A., Elmoaty, A. E. M. A., & Auda, E. M. (2014). Re-use of waste marble dust in the production of cement and concrete. *Construction and building materials*, 50, 28-41.
- Alyamaç, K. E., & Ince, R. (2009). A preliminary concrete mix design for SCC with marble powders. *Construction and Building Materials*, 23(3), 1201-1210.
- Aprianti, E. (2017). A huge number of artificial waste material can be supplementary cementitious material (SCM) for concrete production—a review part II. *Journal of Cleaner Production*, 142, 4178-4194.
- Aruntaş, H. Y., Gürü, M., Dayı, M., & Tekin, I. (2010). Utilization of waste marble dust as an additive in cement production. *Materials & Design*, 31(8), 4039-4042.
- ASTM C1012 / C1012M-15, (2015). Standard Test Method for Length Change of Hydraulic-Cement Mortars Exposed to a Sulfate Solution, ASTM International, West Conshohocken, PA.
- ASTM C1240-15. (2015). Standard Specification for Silica Fume Used in Cementitious Mixtures, ASTM International, West Conshohocken, PA.

ASTM C127-15. (2015). Standard Test Method for Relative Density (Specific Gravity) and Absorption of Coarse Aggregate, ASTM International, West Conshohocken, PA.

ASTM C128-15. (2015). Standard Test Method for Relative Density (Specific Gravity) and Absorption of Fine Aggregate, ASTM International, West Conshohocken, PA.

ASTM C143/C143M-15a. (2015). Standard Test Method for Slump of Hydraulic-Cement Concrete, ASTM International, West Conshohocken, PA.

ASTM C150/C150M-16e1. (2016). Standard Specification for Portland Cement, ASTM International, West Conshohocken, PA.

ASTM C1602/C1602M-12. (2012). Standard Specification for Mixing Water Used in the Production of Hydraulic Cement Concrete, ASTM International, West Conshohocken, PA.

ASTM C191-13. (2013). Standard Test Methods for Time of Setting of Hydraulic Cement by Vicat Needle, ASTM International, West Conshohocken, PA.

ASTM C192/C192M-16a. (2016). Standard Practice for Making and Curing Concrete Test Specimens in the Laboratory, ASTM International, West Conshohocken, PA.

ASTM C33/C33M-16e1. (2016). Standard Specification for Concrete Aggregates, ASTM International, West Conshohocken, PA.

ASTM C490/C490M-17. (2017). Standard Practice for Use of Apparatus for the Determination of Length Change of Hardened Cement Paste, Mortar, and Concrete, ASTM International, West Conshohocken, PA.

ASTM C595/C595M-17. (2017). Standard Specification for Blended Hydraulic Cements, ASTM International, West Conshohocken, PA, 2017.

ASTM C618-15. (2015). Standard Specification for Coal Fly Ash and Raw or Calcined Natural Pozzolan for Use in Concrete, ASTM International, West Conshohocken, PA.

ASTM C666/C666M-15. (2015). Standard Test Method for Resistance of Concrete to Rapid Freezing and Thawing, ASTM International, West Conshohocken, PA.

ASTM C94/C94M-17a. (2017). Standard Specification for Ready-Mixed Concrete, ASTM International, West Conshohocken, PA.

ASTM C989/C989M-16e1. (2016). Standard Specification for Slag Cement for Use in Concrete and Mortars, ASTM International, West Conshohocken, PA.

ASTM D4404-10. (2010). Standard Test Method for Determination of Pore Volume and Pore Volume Distribution of Soil and Rock by Mercury Intrusion Porosimetry, ASTM International, West Conshohocken, PA.

ASTM D4464-15. (2015). Standard Test Method for Particle Size Distribution of Catalytic Materials by Laser Light Scattering, ASTM International, West Conshohocken, PA.

ASTM E11-17. (2017). Standard Specification for Woven Wire Test Sieve Cloth and Test Sieves, ASTM International, West Conshohocken, PA.

Bapat, J. D. (2012). *Mineral admixtures in cement and concrete*. CRC Press.

Barbhuiya, S. A., Gbagbo, J. K., Russell, M. I., & Basheer, P. A. M. (2009). Properties of fly ash concrete modified with hydrated lime and silica fume. *Construction and Building Materials*, 23(10), 3233-3239.

Bektas, F., Wang, K., & Ceylan, H. (2009). Effects of crushed clay brick aggregate on mortar durability. *Construction and Building Materials*, 23(5), 1909-1914.

Belaidi, A. S. E., Azzouz, L., Kadri, E., & Kenai, S. (2012). Effect of natural pozzolana and marble powder on the properties of self-compacting concrete. *Construction and Building Materials*, 31, 251-257.

Berry, E. E., Hemmings, R. T., & Cornelius, B. J. (1990). Mechanisms of hydration reactions in high volume fly ash pastes and mortars. *Cement and Concrete Composites*, 12(4), 253-261.

Binici, H., Kaplan, H., & Yilmaz, S. (2007). Influence of marble and limestone dusts as additives on some mechanical properties of concrete. *Scientific Research and Essays*, 2(9), 372-379.

Binici, H., Shah, T., Aksogan, O., & Kaplan, H. (2008). Durability of concrete made with granite and marble as recycle aggregates. *Journal of materials processing technology*, 208(1), 299-308.

BS EN 12390 – 3. (2002). Testing hardened concrete. Compressive strength of test specimens. London: BSI.

BS EN 12390 – 8. (2009). Testing hardened concrete. Depth of penetration of water under pressure. London: BSI.

Cachim, P. B. (2009). Mechanical properties of brick aggregate concrete. *Construction and Building Materials*, 23(3), 1292-1297.

Chang, P. K. (2004). An approach to optimizing mix design for properties of high-performance concrete. *Cement and Concrete Research*, 34(4), 623-629.

Corinaldesi, V., Moriconi, G., & Naik, T. R. (2010). Characterization of marble powder for its use in mortar and concrete. *Construction and building materials*, 24(1), 113-117.

Correia, J. R., De Brito, J., & Pereira, A. S. (2006). Effects on concrete durability of using recycled ceramic aggregates. *Materials and Structures*, 39(2), 169-177.

- De Sensale, G. R. (2010). Effect of rice-husk ash on durability of cementitious materials. *Cement and Concrete Composites*, 32(9), 718-725.
- Debieb, F., & Kenai, S. (2008). The use of coarse and fine crushed bricks as aggregate in concrete. *Construction and building materials*, 22(5), 886-893.
- Demirel, B. (2010). The effect of the using waste marble dust as fine sand on the mechanical properties of the concrete. *International journal of physical sciences*, 5(9), 1372-1380.
- Devenny, A., & Khalaf, F. M. (1999). Use of crushed brick as coarse aggregate in concrete. *Masonry International*, 12(3), 81-84.
- Duan, P., Shui, Z., Chen, W., & Shen, C. (2013). Effects of metakaolin, silica fume and slag on pore structure, interfacial transition zone and compressive strength of concrete. *Construction and Building Materials*, 44, 1-6.
- Elahi, A., Basheer, P. A. M., Nanukuttan, S. V., & Khan, Q. U. Z. (2010). Mechanical and durability properties of high performance concretes containing supplementary cementitious materials. *Construction and Building Materials*, 24(3), 292-299.
- Erdem, T. K., & Kırca, Ö. (2008). Use of binary and ternary blends in high strength concrete. *Construction and Building Materials*, 22(7), 1477-1483.
- Ergün, A. (2011). Effects of the usage of diatomite and waste marble powder as partial replacement of cement on the mechanical properties of concrete. *Construction and Building Materials*, 25(2), 806-812.
- Gartner, E., & Hirao, H. (2015). A review of alternative approaches to the reduction of CO₂ emissions associated with the manufacture of the binder phase in concrete. *Cement and Concrete research*, 78, 126-142.
- Gesoğlu, M., Güneyisi, E., Kocabağ, M. E., Bayram, V., & Mermerdaş, K. (2012). Fresh and hardened characteristics of self-compacting concretes made with combined use of marble powder, limestone filler, and fly ash. *Construction and Building Materials*, 37, 160-170.
- Ghrici M, Kenai S, Meziane E. (2006). Mechanical and durability properties of cement mortar with Algerian natural pozzolana. *Mater Sci*; 41:6965–72.
- Ghrici M, Kenai S, Said-Mansour M. (2007). Mechanical properties and durability of mortar and concrete containing natural pozzolana and limestone blended cements. *Cem Concr Comp*; 29:542–9.
- Grist, E. R., Paine, K. A., Heath, A., Norman, J., & Pinder, H. (2015). The environmental credentials of hydraulic lime-pozzolan concretes. *Journal of Cleaner Production*, 93, 26-37.
- Han, S. H., Kim, J. K., & Park, Y. D. (2003). Prediction of compressive strength of fly ash concrete by new apparent activation energy function. *Cement and Concrete Research*, 33(7), 965-971.
- Hansen, T. C. (Ed.). (2004). *Recycling of demolished concrete and masonry* (Vol. 6). CRC Press.

- Harrison, A. J. W. (2013). Low Carbon Cements and Concretes in Modern Construction. *The Masterbuilder*.
- Hebhoub, H., Aoun, H., Belachia, M., Houari, H., & Ghorbel, E. (2011). Use of waste marble aggregates in concrete. *Construction and Building Materials*, 25(3), 1167-1171.
- Hooton, R. D., & Bickley, J. A. (2014). Design for durability: the key to improving concrete sustainability. *Construction and Building Materials*, 67, 422-430.
- Ismail, Z. Z., & AL-Hashmi, E. A. (2008). Reuse of waste iron as a partial replacement of sand in concrete. *Waste Management*, 28(11), 2048-2053.
- Ismail, Z. Z., & Al-Hashmi, E. A. (2008). Use of waste plastic in concrete mixture as aggregate replacement. *Waste Management*, 28(11), 2041-2047.
- Juenger, M. C. G., Winnefeld, F., Provis, J. L., & Ideker, J. H. (2011). Advances in alternative cementitious binders. *Cement and concrete research*, 41(12), 1232-1243.
- Juenger, M. C., & Siddique, R. (2015). Recent advances in understanding the role of supplementary cementitious materials in concrete. *Cement and Concrete Research*, 78, 71-80.
- Khalaf, F. M. (2006). Using crushed clay brick as coarse aggregate in concrete. *Journal of Materials in Civil Engineering*, 18(4), 518-526.
- Khalaf, F. M., & DeVenny, A. S. (2005). Properties of new and recycled clay brick aggregates for use in concrete. *Journal of materials in civil engineering*, 17(4), 456-464.
- Khaloo, A. R., Dehestani, M., & Rahmatabadi, P. (2008). Mechanical properties of concrete containing a high volume of tire-rubber particles. *Waste Management*, 28(12), 2472-2482.
- Khatib, J. M. (2005). Properties of concrete incorporating fine recycled aggregate. *Cement and Concrete Research*, 35(4), 763-769.
- Kosmatka, S. H., Kerkhoff, B., & Panarese, W. C. (2011). Design and control of concrete mixtures. Portland Cement Association.
- Lam, L., Wong, Y. L., & Poon, C. S. (1998). Effect of fly ash and silica fume on compressive and fracture behaviors of concrete. *Cement and Concrete Research*, 28(2), 271-283.
- Li, H., Xiao, H. G., Yuan, J., & Ou, J. (2004). Microstructure of cement mortar with nano-particles. *Composites Part B: Engineering*, 35(2), 185-189.
- Liu, S., Sun, W., Lin, W., & Lai, J. (2003). Preparation and durability of a high performance concrete with natural ultra-fine particles. *Guisuanyan Xuebao (Journal of the Chinese Ceramic Society) (China)*, 31, 1080-1085.
- Long, G., Gao, Y., & Xie, Y. (2015). Designing more sustainable and greener self-compacting concrete. *Construction and Building Materials*, 84, 301-306.

- Ltifi, M., Guefrech, A., Mounanga, P., & Khelidj, A. (2011). Experimental study of the effect of addition of nano-silica on the behaviour of cement mortars. *Procedia Engineering*, 10, 900-905.
- Malhotra, V. M. (2006). Reducing CO₂ emissions. *Concrete international*, 28(09), 42-45.
- Malhotra, V. M. (2010). Global warming and role of supplementary cementing materials and superplasticizers in reducing greenhouse gas emissions from the manufacturing of Portland cement. *International Journal of Structural Engineering*, 1(2), 116-130.
- Malhotra, V. M., Zhang, M. H., Read, P. H., & Ryell, J. (2000). Long-term mechanical properties and durability characteristics of high-strength/high-performance concrete incorporating supplementary cementing materials under outdoor exposure conditions. *Materials Journal*, 97(5), 518-525.
- Mansur, M. A., Wee, T. H., & Lee, S. C. (1999). Crushed bricks as coarse aggregate for concrete. *Materials Journal*, 96(4), 478-484.
- Massazza, F. (2001). Pozzolana and pozzolanic cements. *Lea's chemistry of cement and concrete*, 4, 471-635.
- Mazloom, M., Ramezani pour, A. A., & Brooks, J. J. (2004). Effect of silica fume on mechanical properties of high-strength concrete. *Cement and Concrete Composites*, 26(4), 347-357.
- Mehta, P. K. (1999). Advancements in concrete technology. *Concrete International*, 21(6), 69-76.
- Mehta, P. K., & Monteiro, P. J. (2006). *Concrete: microstructure, properties, and materials*. 2006.
- Menéndez, G. V. B. B., Bonavetti, V., & Irassar, E. F. (2003). Strength development of ternary blended cement with limestone filler and blast-furnace slag. *Cement and Concrete Composites*, 25(1), 61-67.
- Miličević, I., Bjegović, D., & Siddique, R. (2015). Experimental research of concrete floor blocks with crushed bricks and tiles aggregate. *Construction and Building materials*, 94, 775-783.
- Miura, N., Takeda, N., Chikamatsu, R., & Sogo, S. (1993). Application of super workable concrete to reinforced concreted structures with difficult construction conditions. *Special Publication*, 140, 163-186.
- Mohamadien, H. A. (2012). The Effect of marble powder and silica fume as partial replacement for cement on mortar. *International journal of civil and structural engineering*, 3(2), 418.
- Nazari, A., & Riahi, S. (2011). The effects of SiO₂ nanoparticles on physical and mechanical properties of high strength compacting concrete. *Composites Part B: Engineering*, 42(3), 570-578.

- Nemati, K. M. (1997). Fracture analysis of concrete using scanning electron microscopy. *Scanning*, 19(6), 426-430.
- Neville, A. M. (1995). *Properties of concrete* (Vol. 4). London: Longman.
- Omar, O. M., Elhameed, G. D. A., Sherif, M. A., & Mohamadien, H. A. (2012). Influence of limestone waste as partial replacement material for sand and marble powder in concrete properties. *HBRC Journal*, 8(3), 193-203.
- Oner, A., & Akyuz, S. (2007). An experimental study on optimum usage of GGBS for the compressive strength of concrete. *Cement and Concrete Composites*, 29(6), 505-514.
- Oner, A., Akyuz, S., & Yildiz, R. (2005). An experimental study on strength development of concrete containing fly ash and optimum usage of fly ash in concrete. *Cement and Concrete Research*, 35(6), 1165-1171
- Papadakis, V. G., & Tsimas, S. (2002). Supplementary cementing materials in concrete: Part I: efficiency and design. *Cement and Concrete Research*, 32(10), 1525-1532.
- Paya, J., Monzo, J., Borrachero, M. V., & Peris-Mora, E. (1995). Mechanical treatment of fly ashes. Part I: Physico-chemical characterization of ground fly ashes. *Cement and Concrete Research*, 25(7), 1469-1479.
- Paya, J., Monzo, J., Borrachero, M. V., Peris, E., & Gonzalez-Lopez, E. (1997). Mechanical treatments of fly ashes. Part III: studies on strength development of ground fly ashes (GFA)—cement mortars. *Cement and concrete research*, 27(9), 1365-1377.
- Paya, J., Monzo, J., Borrachero, M. V., Peris-Mora, E., & González-López, E. (1996). Mechanical treatment of fly ashes part II: particle morphologies in ground fly ashes (GFA) and workability of GFA-cement mortars. *Cement and Concrete Research*, 26(2), 225-235.
- Poon, C. S., & Chan, D. (2007). The use of recycled aggregate in concrete in Hong Kong. *Resources, Conservation and Recycling*, 50(3), 293-305.
- Raman, S. N., Ngo, T., Mendis, P., & Mahmud, H. B. (2011). High-strength rice husk ash concrete incorporating quarry dust as a partial substitute for sand. *Construction and Building Materials*, 25(7), 3123-3130.
- Rodrigues, R., de Brito, J., & Sardinha, M. (2015). Mechanical properties of structural concrete containing very fine aggregates from marble cutting sludge. *Construction and Building Materials*, 77, 349-356.
- Rodríguez, E. D., Bernal, S. A., Provis, J. L., Payá, J., Monzó, J. M., & Borrachero, M. V. (2012). Structure of portland cement pastes blended with sonicated silica fume. *Journal of Materials in Civil Engineering*, 24(10), 1295-1304.

Rößler, C., Bui, D. D., & Ludwig, H. M. (2014). Rice husk ash as both pozzolanic admixture and internal curing agent in ultra-high performance concrete. *Cement and Concrete Composites*, 53, 270-278.

Sharma, N., & Kumar, R. (2015, April). Review on Use of Waste Marble Powder as Partial Replacement in Concrete Mix. In *EFES-2015 National Conference on Emerging Fields in Engineering and Science ISSN* (pp. 2349-0918).

Shehata, M. H., & Thomas, M. D. (2002). Use of ternary blends containing silica fume and fly ash to suppress expansion due to alkali–silica reaction in concrete. *Cement and Concrete Research*, 32(3), 341-349.

Shi, C., Jiménez, A. F., & Palomo, A. (2011). New cements for the 21st century: the pursuit of an alternative to Portland cement. *Cement and concrete research*, 41(7), 750-763.

Siddique, R., & Kadri, E. H. (2011). Effect of metakaolin and foundry sand on the near surface characteristics of concrete. *Construction and Building Materials*, 25(8), 3257-3266.

Snellings, R., Mertens, G., & Elsen, J. (2012). Supplementary cementitious materials. *Reviews in Mineralogy and Geochemistry*, 74(1), 211-278.

Tagnit-Hamou A, Pertove N, Luke K. Properties of concrete containing diatomaceous earth. *ACI Mater J* 2003; 100(1):73–8.

Thomas, M. D. A., Shehata, M. H., Shashiprakash, S. G., Hopkins, D. S., & Cail, K. (1999). Use of ternary cementitious systems containing silica fume and fly ash in concrete. *Cement and concrete research*, 29(8), 1207-1214.

Tian B and Cohen MD. (2000). Does gypsum formation during sulfate attack on concrete lead to expansion? *Cement and Concrete Research* 30:117–123.

Topcu, I. B., Bilir, T., & Uygunoğlu, T. (2009). Effect of waste marble dust content as filler on properties of self-compacting concrete. *Construction and Building Materials*, 23(5), 1947-1953.

Toutanji, H., Delatte, N., Aggoun, S., Duval, R., & Danson, A. (2004). Effect of supplementary cementitious materials on the compressive strength and durability of short-term cured concrete. *Cement and Concrete Research*, 34(2), 311-319

Türker, P., Erdogan, B., & Erdogdu, K. (2007). Influence of marble powder on microstructure and hydration of cements. *Cem Concr World*, 38, 2378-83.

Türkmen, İ. (2003). Influence of different curing conditions on the physical and mechanical properties of concretes with admixtures of silica fume and blast furnace slag. *Materials Letters*, 57(29), 4560-4569.

- Van den Heede, P., & De Belie, N. (2012). Environmental impact and life cycle assessment (LCA) of traditional and 'green' concretes: literature review and theoretical calculations. *Cement and Concrete Composites*, 34(4), 431-442.
- Van Tuan, N., Ye, G., Van Breugel, K., & Copuroglu, O. (2011). Hydration and microstructure of ultra-high performance concrete incorporating rice husk ash. *Cement and Concrete Research*, 41(11), 1104-1111.
- Van Tuan, N., Ye, G., Van Breugel, K., Fraaij, A. L., & Dai Bui, D. (2011). The study of using rice husk ash to produce ultra-high performance concrete. *Construction and Building Materials*, 25(4), 2030-2035.
- Vlahović, M. M., & Jovanić, P. B. (2012). Scanning electron microscopy analysis of sulfur-polymer composite subjected to induced destruction.
- Walker, R., & Pavía, S. (2011). Physical properties and reactivity of pozzolans, and their influence on the properties of lime–pozzolan pastes. *Materials and Structures*, 44(6), 1139-1150.
- Wu, K. R., Chen, B., Yao, W., & Zhang, D. (2001). Effect of coarse aggregate type on mechanical properties of high-performance concrete. *Cement and Concrete Research*, 31(10), 1421-1425.
- Yazıcı, H. (2008). The effect of silica fume and high-volume Class C fly ash on mechanical properties, chloride penetration and freeze–thaw resistance of self-compacting concrete. *Construction and Building Materials*, 22(4), 456-462.
- Yu, R., Spiesz, P., & Brouwers, H. J. H. (2014). Effect of nano-silica on the hydration and microstructure development of Ultra-High Performance Concrete (UHPC) with a low binder amount. *Construction and Building Materials*, 65, 140-150.
- Yu, R., Spiesz, P., & Brouwers, H. J. H. (2015). Development of an eco-friendly Ultra-High Performance Concrete (UHPC) with efficient cement and mineral admixtures uses. *Cement and Concrete Composites*, 55, 383-394.
- Zelić, J., Krstulović, R., Tkalčec, E., & Krolo, P. (1999). Durability of the hydrated limestone-silica fume Portland cement mortars under sulphate attack. *Cement and concrete research*, 29(6), 819-826.
- Zhang, T., Yu, Q., Wei, J., & Zhang, P. (2012). Efficient utilization of cementitious materials to produce sustainable blended cement. *Cement and Concrete Composites*, 34(5), 692-699.